A computer model for a seven storey timber building constructed with X-lam panels and an experiment on the Kerto-Q Laminated Veneer Lumber connection

Student:

Jelmer Boukes
Delft University of Technology
Faculty of Civil Engineering

Graduation committee:

Prof.ir. F.S.K. Bijlaard
Dr.ir. J.W.G. van de Kuilen
Dr.ir. P.C.J. Hoogenboom
Msc. C. Sandhaas
Ir. S. Janssen

A computer model for a seven storey timber building constructed with X-lam panels and an experiment on the Kerto-Q Laminated Veneer Lumber connection

Delft University of Technology

Summary

The world of timber nowadays has to deal with two goals: firstly convincing the world of the qualities of the new products and secondly the negative image of a natural, hence an unpredictable material.

One of the projects to reduce these limitations is the SOFIE project. Within this project there are many experiments and research objects. On of them is a full-scale earthquake test on a seven-storey building, which forms the basis for this report.

Good results were obtained in the full scale test on the seven storey building. These results pointed out that the X-lam structures seems to be a promising building method. The goal of this thesis is to write a three dimensional (3D) computer model for the earthquake response of the seven-storey timber building. In addition to the modelling of the building, an experiment is done on the shear wall-to-wall X-lam connection. Both subjects are treated in this report.

The experiment on the shear wall-to-wall X-lam connection is done at Delft University of Technology. The experiment consists of two ramp tests and six cyclic tests on a downscaled connection according to European standard EN12512. Experiments are done on three layered X-lam specimens and five layered X-lam specimens.

The software for the 3D modelling is DRAIN 3D. The program originally was developed at the Berkeley University, California, USA. Within the program elements modelling timber hysteresis behaviour are present. These are added and developed by the Florence University, Italy, Europe.

In the experiment three and five layered specimens are tested within the same test setup. Results indicate a negligible difference in the specimen response to cyclic loading, so three or five layered specimens have equal mechanical properties in this configuration.
The failure of the wall-to-wall connection can be explained by plastic deformation of the screws. The properties of the screw and the timber allow very large embedment displacement and the formation of plastic hinges in the fasteners. Fastener bending angles are around 25°.
The amount of energy dissipated in the connection with a total of 12 screws lies between 3 and 4 kNm. A double connection is tested, so between 1.5 and 2 kNm per joint tested, with 3 fasteners per shear plane and 6 fasteners per wall-to-wall connection.

The final model results are compared with the results from the full scale experiment mentioned above. A difference of approximately 10-40% in horizontal directions is found in the results form the model and the experiment. The influence of the experimented wall-to-wall connection on the total building behaviour is investigated by doubling the spring's stiffness and strength in the model. It is concluded that doubling these properties has an influence on the building behaviour of 50% until 70%. The accuracy of the model is investigated by halving the time-step used for calculation. For the horizontal directions and error of 10% is found.

1 SOFIE project and thesis motivation

1.1 Introduction

For a long time modern materials such as steel and concrete dominated the market for (complex) structural systems. At the moment timber is discovered again as a good alternative for these materials due to newly developed products and its esthetical value. However for these products produced with new techniques, there are problems in convincing the public opinion of the suitability of timber as building material. This is the case for almost every new technique in the world. But the problem of timber is that it has to deal with an old and wrong image. For example the fire resistance of timber is thought of being bad, but with the new products is considerably improved. Another thought is based on timber being a natural product. Timber as a natural product has to deal with decrease in for example strength due to natural errors in the material. With this decrease it is not possible to construct the large spans and heights that are common in today's complex structural systems. Again this problem is anticipated for by the new developed (laminated) timber products. The world of timber nowadays has to deal with two goals: firstly convincing the world of the qualities of the new products and secondly deal with the negative image of a natural, hence a weak and unpredictable, material.

Many projects are present at the moment to fulfil these two goals. The number of projects is too large to refer to all in this introduction. One of the projects is called the SOFIE project initiated by IVALSA, an Italian institute. The SOFIE project is used as the basis for this report.

The SOFIE project is an extensive investigation that aims at defining the performance and capabilities of the construction system with cross-laminated panels (X-Lam). X-lam panels are massive cross-laminated wooden panels with a thickness varying from 50 millimetres up to 300 millimetres. The complete project consists of experiments on fire resistance desirability and energy performance towards earthquake tests. [www.progettosofie.it]

Seismic performance of multi storey buildings is a sensitive issue. This is due to the complexity of the seismic response of real structures and the lack of proper modelling and test data. Timber X-lam structures possess some inherent characteristics that make them particularly suited for the use in regions with earthquake activity. Both due to material properties (lightness and load bearing capacity) and to system properties (ductility and capacity of energy dissipation), timber structures perform well under earthquake loading. [Cecotti et all, 2006]

The good behaviour in (earthquake) dynamic loading is an argument to choose for timber construction for single as well as multi-storey buildings. Therefore earthquake engineering for multi-storey buildings can be used to gain more trust in timber construction and to deal with the negative image mentioned above. This report is using the seismic research part of the SOFIE project.

The earthquake part of the SOFIE project consists out of two different main parts. One part is the experiments on the X-lam material and its applications. The other part is computer modelling of the structure. The completed tests (at the moment of writing) can be found chronologically in Figure 1-1. The computer modelling runs almost simultaneously to the experiments. In practise this means that the successful experiment on the wall diaphragm is modelled first in a working model before the next step in the project is started. Modelling before experimenting is done also. At the moment of writing this report, the project has reached the phase where the experiment on the seven storey structure is completed (in October 2007). After the test, the next step was to create a mathematical model of the structure, which will be done in this report. Another conclusion from the experiment was that more insight is needed in the shear wall to wall connection. This connection is therefore experimented and modelled within the scope of this thesis.

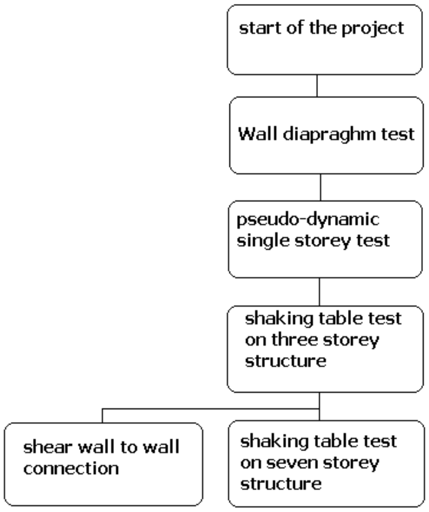

Figure 1-1, project path within SOFIE

1.2 Formulation of the objective of the thesis

Good results were obtained in the full scale test on the seven storey building. The results of the experiments within the SOFIE project point out that the confidence in the earthquake resistance of X-lam structures is correct.

Full scale tests are expensive and time consuming. These are two reasons why it is desirable to develop a computer model for preliminary design of X-lam structures.

The goal for the Master Thesis is to write a three dimensional (3D) computer model for the earthquake response on the seven-storey timber building which was tested within the scope of the SOFIE project in October 2007 in Japan. Next to the modelling of the building, an experiment is completed on the shear wall-to-wall connection.

1.3 Layout of the report

In chapter 0 the problem of earthquake engineering is treated. Subjects that are discussed are the earthquake phenomenon and the engineering tools to resist the earthquake forces. Chapter 3 is describing the preliminary experiments in the SOFIE structure and the full scale experiment on the building. In chapter 4 the seven-storey SOFIE building is checked with the design codes. Chapter 5 is describing an experiment done on the wall-to-wall connection. In chapter 6 the modelling steps of the SOFIE structure is treated. Chapter 7 contains the results of the model after which in chapter 8 and 9 conclusions and recommendations are formulated.

1.4 Acknowledgements

Special thanks are given to IVALSA for delivering the test results of the seven-storey full-scale test.

The experiment within the scope of this thesis was possible due to different parties. Rothoblaas is thanked for supplying the screws for the connection. Finnforest delivered the kerto-Q LVL strips and the X-lam panels for the experiment.

2 Background

2.1 Introduction

An earthquake is a vibration of the earth produced by a rapid release of energy. Earthquakes have a great impact on economical, structural and mental issues. Earthquakes occur for a short period, aftershocks can continue for weeks, but the damage can continue for years. With a well developed earth science and earthquake engineering, the economic as well as the human damage can be minimized. This chapter is written to give some background information on the phenomenon of earthquakes and how it is dealt with in engineering practise. The chapter starts with some background information on the origin of earthquakes and some seismic theories in section 2.2.1. Measuring of earthquakes and forecasting them is very valuable in earthquake engineering and other social aspects. How this is done is explained in section 2.2.3. Finally, the earthquake engineering principles in Europe are explained with regard of the European standard (Eurocode 8) in section 2.3. In this section, a short description of the SOFIE structure can be found also. This is done to evaluate whether the SOFIE structure meets with the European standard for earthquake engineering.

2.2 Earthquake background and theories

[C. Brunious and A. Warner]

Earthquakes occur by the displacement on faults, when there is a build-up of stress in the crust caused by plate movement at a subduction zone or other fault lines (see Figure 2-1 upper left). The subduction zone of an earthquake is the area of intense activity caused by the movement of two plates where one plate ducts beneath the other. There are three types of plate boundaries where this subduction occurs: ocean to ocean, ocean to continent and continent to continent (Figure 2-1). In an ocean to ocean mechanism, the plates are pulled apart. In an ocean to continent subduction, one plate is thrust under the other. In a continent to continent mechanism, the plates collide.

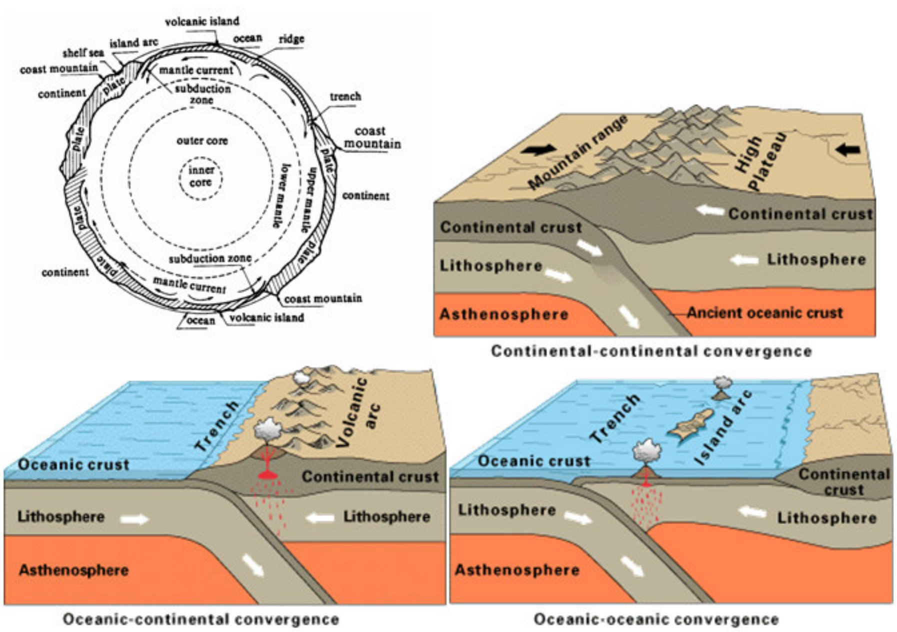

Figure 2-1, cross section of the earth and three locations subduction zones[1]

Earthquakes can be classified in two classes: interplate (95%) and intraplate (5%). In interplate earthquakes energy is released at plate boundaries. The theory of intraplate earthquakes states that the plates are assumed not to be rigid or free from internal rupture.

The Earth's crust is a collection plates that move with unequal speed and direction. Within the theory of plate tectonics these plates are explained from the idea that the outmost part of the earth (lithosphere) was once concentrated in a single continent. After breaking loose, large and stable slabs arise, called tectonic plates (see Figure 2-2). These slabs, with a thickness around 80 kilometres, have a different horizontal movement relative to the neighbouring slabs. The disruption produced at the boundaries between plates results in earthquakes.

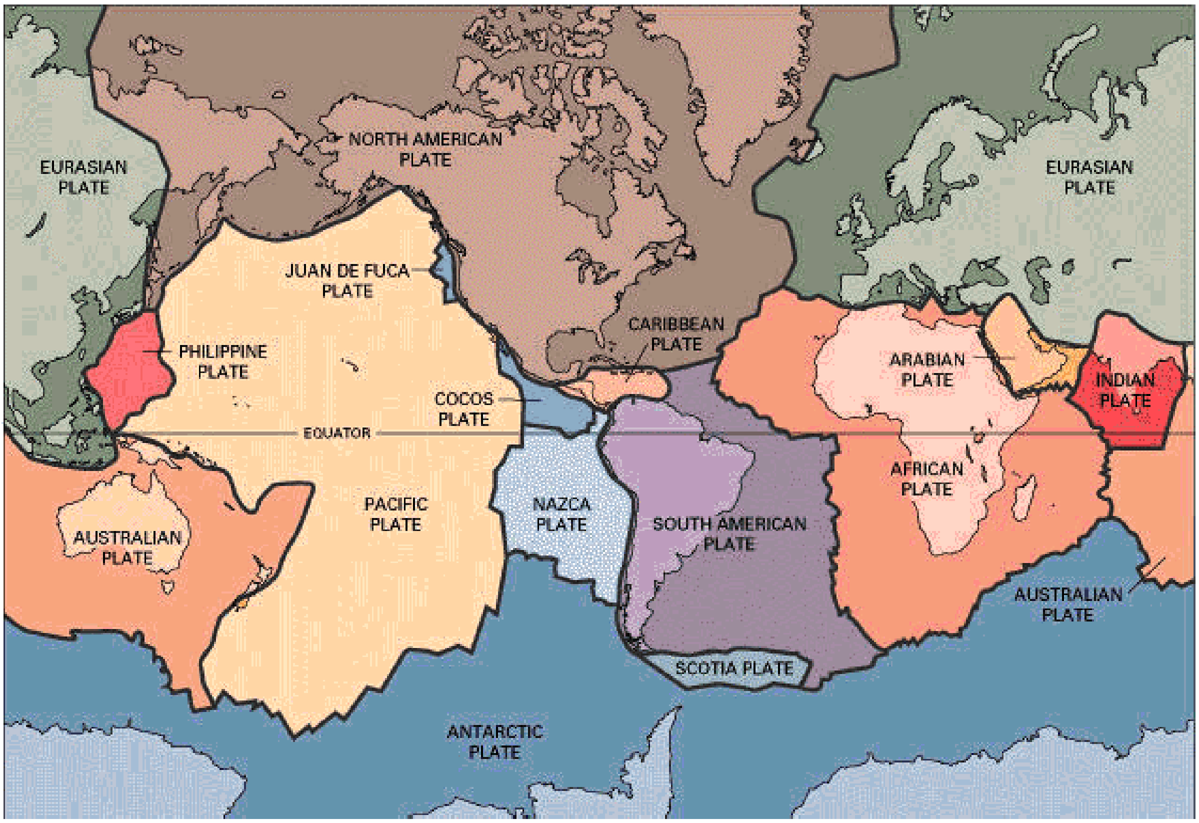

Figure 2-2, map of the world with tectonic plates[1]

2.2.1 Locating, measuring and predicting earthquakes

Seismographs (Figure 2-3) record the ground shaking that result from earthquakes and help to locate the epicentre of an earthquake. Seismographs have a mass that is freely suspended from a support. This support is attached directly to the ground. When the vibration of the ground reaches the instrument, the movement of earth in relation to the stationary mass is recorded.

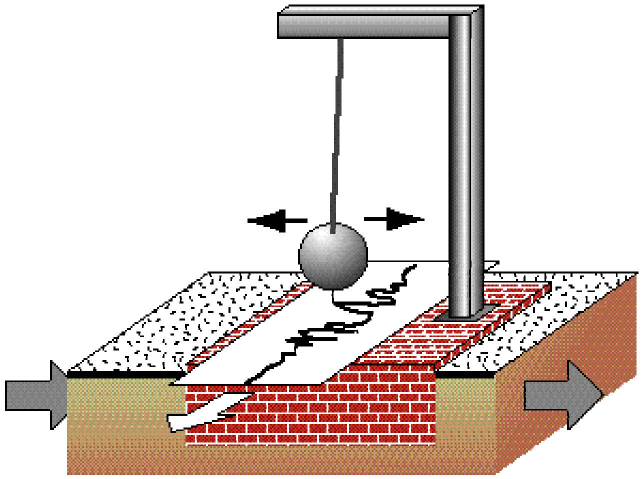

Figure 2-3, drawing of a seismograph[1]

When the ground shakes due to earthquakes, the base and frame of the instrument move with it, but inertia keeps the pendulum in place. It will then move relatively to the shaking of the ground. As it moves it records the pendulum displacements. This is called a seismogram. A seismogram is a representation of the relative movement of the ground. A seismogram generally is presented in three directions, north-south, east-west and vertical.

In earthquake engineering, representation of the earthquake in terms of acceleration (called accelerogram) is more valuable. The maximum acceleration causes the most severe damage. Accelerograms are recorded by an accelerometer. Its appearance is similar to a seismograph. As an example the accelerogram for the Kobe 1995 earthquake is given in Figure 2-4. The accelerogram is presenting the north-south horizontal acceleration versus time.

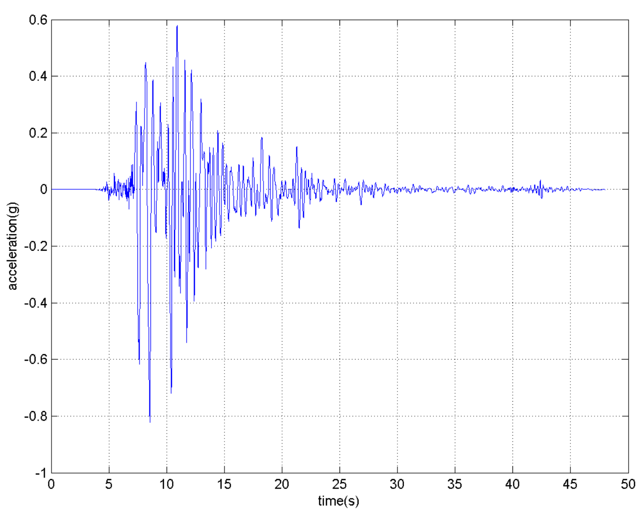

Figure 2-4, accelerogram Kobe 1995, north-south direction

2.2.2 Classification of earthquakes

The magnitude of an earthquake can be expressed on a logarithmic scale introduced by Charles Richter in 1935. The magnitude is estimated by measuring the ground amplitudes. The energy range of earthquake is classified by Richter's scale into 8 classes (see Table 2-1).
Earthquake intensity, on the other hand, is an estimate of the violence of an earthquake shaking at a given site. This reflects the size of the seismic wave, the distance from the epicentre, geological structures and social factors. Earthquake intensity is measured with the Modified Mercalli Intensity Scale (MMI). MMI (see Table 2-2) is classifying the amount of shaking and damage during an earthquake. Earthquakes can have only one magnitude but a larger amount of intensities. This is because magnitude is a defined calculation, whereas intensity varies with location, calculating the amount of damage done to structures, the degree to which the earthquake was felt by individuals and the presence of secondary effects.

Richter Magnitudes	Effects Near Epicentre	Estimated Number per Year
<2.0	Generally not felt, but recorded	600,000
2.0-2.9	Potentially Perceptible	300,000
3.0-3.9	Felt by some	49,000
4.0-4.9	Felt by most	6200
5.0-5.9	Damaging shocks	800
6.0-6.9	Destructive in populous regions	266
7.0-7.9	Major earthquakes; inflict serious damage	18
>8.0	Great earthquakes; cause extensive destruction near epicentre	1.4

Table 2-1, Richter scale [Tarbuck et all]

I. Not felt except by a very few under especially favorable circumstances.
II. Felt only by a few persons at rest, especially on upper floors of buildings.
III. Felt quite noticeably indoors, especially on upper floors of buildings, but many people do not recognize it as an earthquake.
IV. During the day felt indoors by many, outdoors by few. Sensation like heavy truck strinking building.
V. Felt by nearly everyone, many awakened. Disturbances of trees, poles and other tall objects sometimes noticed.
VI. Felt by all; many frightened and run outdoors. Some heavy furniture moved; few instances of fallen plaster or damaged chimneys. Damage slight.
VII. Everybody runs outdoors. Damage negligible in buildings of good design and construction; slight to moderate in well-built ordinary structures; considerable in poorly built or badly designed structures.
VIII. Damage slight in specially designed structures; considerable in ordinary substantial buildings with partial collapse; great in poorly built structures. (Fall of chimneys, factory stacks, columns, monuments, walls.)
IX. Damage considerable in specially designed structures. Buildings shifted off foundations. Ground cracked conspicuously.
X. Some well-built wooden structures destroyed. Most masonry and frame structures destroyed. Ground badly cracked.
XI. Few, if any (masonry) structures remain standing. Bridges destroyed. Broad fissues in ground.
XII. Damages total. Waves seen on ground surfaces. Objects thrown upward into air.

Table 2-2 Modified Mercalli Intensity scale [Tarbuck et all]

2.2.3 Earthquake predicting theories

There is one main theory available on how earthquakes are generated; the elastic rebound theory. Though the theory seems promising, it is not complete and there is no agreement in earthquake science on the value of it. The elastic rebound model states that stress occurs between two moving plates. This stress occurs in three main steps of rock deformation (Figure 2-5), the original position (a), build-up of strain (b), and afterwards strain release (c).

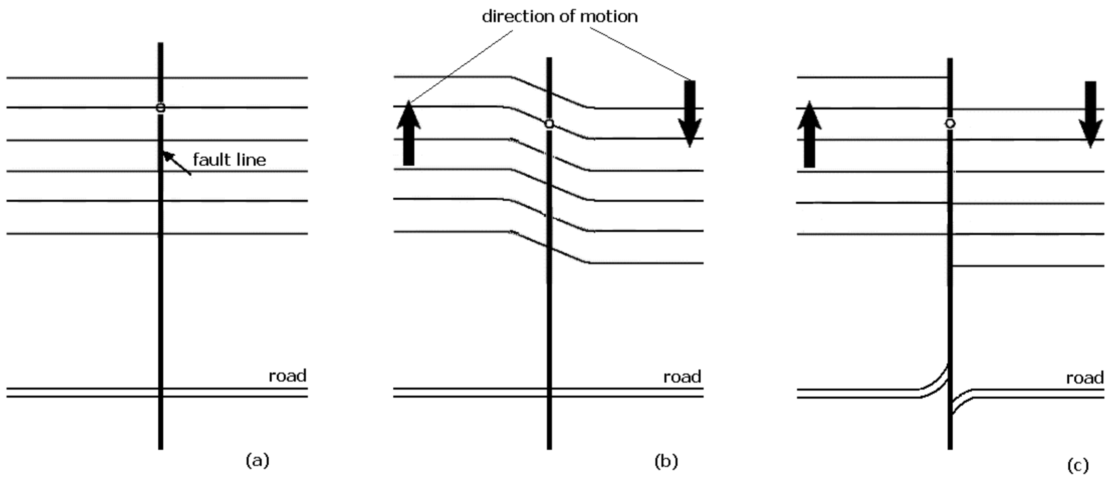

Figure 2-5, Elastic rebound model [Sandhaas, 2004]

If the fault creeps, it will produce frequent micro-earthquakes; if it binds together and then slips, it will produce large earthquakes. Stress will then quickly be released; sides of the fault will become offset; rocks will rebound to their initial state of stress. The problem with this theory is that earthquakes do not produce the large drop in stress required for this model. The elastic rebound theory can be supplemented with the seismic gap theory. The seismic gap theory states that strong earthquakes are unlikely in regions where weak earthquakes are common and the longer the period without earthquakes, the stronger the earthquake will be when it finally occurs. The problem is that the boundaries between crust plates are often fractured into a immeasurable network of minor faults that intersect the major fault lines. When an earthquake releases the stress in these faults, it may load additional stress on another fault in the network. This contradicts the seismic gap theory because a series of small earthquakes in an area can then increase the probability that a large quake will follow. Although the seismic gap theory can suggest areas that are likely for earthquakes, it does not enable scientists to predict when that earthquake will occur.

2.2.4 Earthquakes in Europe

Though the most hazardous earthquake zone is not much represented in Europe (Romania and Greece only), other earthquake classes are widespread. The most destructive zones are in the Mediterranean countries, particularly Greece, Italy and Turkey (Figure 2-6). These countries are in the collision zone between the Eurasian and African tectonic plates (see Figure 2-2) .

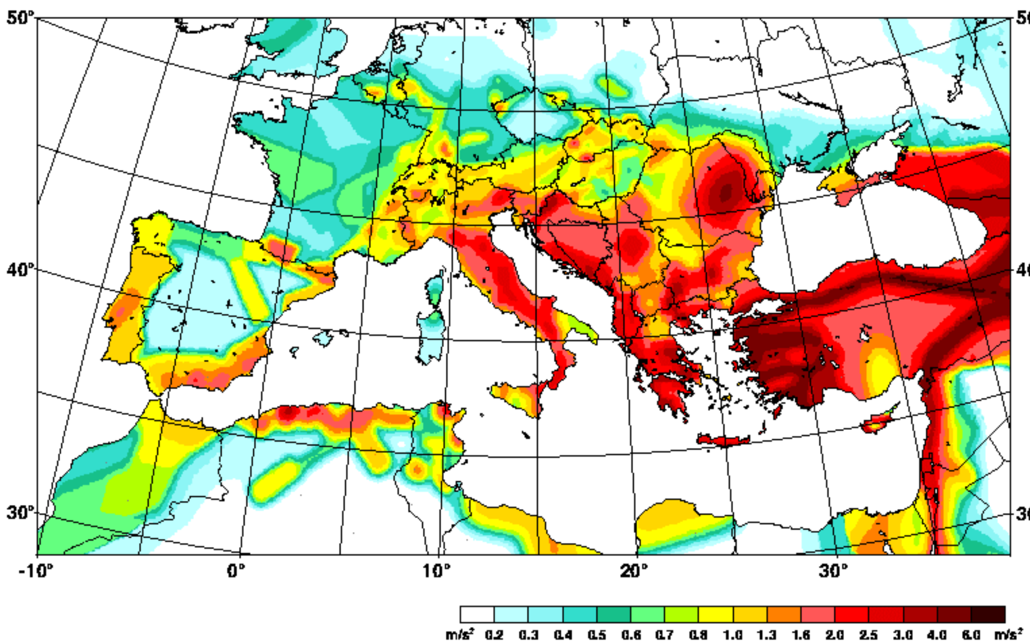

Figure 2-6, earthquake risk in Europe [www.neic.usgs.gov]

Figure 2-6 reproduces the earthquake acceleration over the different areas in Europe. Though this is not a Richter or MMI scale classification, it gives good awareness of the countries where larger earthquakes occurred in the past and will take place in the future.

Some examples of destructive earthquakes that have occurred since 1976 in Europe with impact included are given in Table 2-3.

YEAR	COUNTRY/ REGION	IMPACTS
1976	Greece, Thessaloniki	45 dead, 220 injured, major damage
1976	Italy, Frioul (twice)	997 dead, 2400injured, 189000 homeless
1979	Italy, Umbria	5 dead, numerous injured, 2000 homeless
1980	Italy, Campania	2739 dead, 8 816 injured, 334000 homeless
1980	Portugal, Azores	50 dead, 86 injured, 21296 homeless
1981	Greece, south regions	19 dead, 500 injured, 12220 buildings damaged/destroyed
1983	Belgium	1 dead, 26 injured
1984	Italy, central regions	7500 homeless
1986	Greece, Kalamata	20 dead, 300 injured, 2000 buildings damaged/destroyed
1990	Romania, Bucharest-Braila - Brasov area	9 dead, 700 injured, severe damage
1990	Italy, SW Sicily	19 dead, 99 injured, 14596 homeless
1992	Netherlands, Limburg	Extensive damage
1992	Turkey, north-west area	498 dead, 2000 injured, 2200 building damaged
1995	Cyprus, Paphos	2 dead, 5 injured, several damages
1995	Greece, Egion	26 dead, 60 injured, extensive damage
1995	Greece, Grevena-Kozani	25 injured, 5000 homes destroyed, 7000 homes damaged
1997	Italy, central region	11 dead, more than 100 injured, 80000 destroyed/damaged
1999	Turkey, Bolu-Duzce	894 dead, 4948 injured, extensive damage
1999	Greece, Athens	143 dead, 1600 injured, 50000 homeless
1999	Turkey, Istanbul area	17118 dead, 50000 injured, 500000 homeless
1999	Spain, Mula area	20 injured, buildings damaged
2002	UK, Mansfield	minor damage
2002	Italy, south regions	29 dead, 135 injured, 70% of the houses damaged

Table 2-3, most destructive earthquakes in Europe [www.neic.usgs.gov]

2.2.5 Italy

Seven of the major earthquakes since 1976 occurred in Italy. According to the official numbers almost 4000 people died in this country. Due to its cultural heritage Italian cities are especially vulnerable to earthquakes that would not be as dangerous in other countries. Damage to the frescoed vault of the San Francesco basilica in Assisi during the 1997 Umbria-Marche earthquake (Mw 6.0) shows Italy's special vulnerability. Saving lives and protecting Italy's cultural heritage are important reasons for earthquake research.

Because the wish to save the cultural heritage and the large amount of deaths in history a large budget is available for earthquake research. Therefore, the seismological research projects are large compared to some other earthquake sensitive countries. For example, the Italian earthquake record can be exploited at time scales from 10,000 years to seconds. This record allows several aspects of the earthquake process to be investigated simultaneously. Next to several earthquake prediction investigations, Italy is one of the leading European countries for earthquake resistant design. This is where the SOFIE project fits that will be introduced in section 2.3 and will be discussed in detail in chapter 3.

2.3 Earthquake design

Figure 2-7, the full scale seven storey SOFIE building [www.progettosofie.it]

At the moment of writing, the last experiment in the SOFIE project was a full scale earthquake experiment on an X-lam seven-storey building (Figure 2-7). The building that is used for the full scale test is described here in general. It is chosen to describe the building in this chapter shortly. In this way it is possible to use the SOFIE building as an example when presenting the European standard for earthquake design, Eurocode 8 (EC8). The current section describes the basic structural principles in the European standard and to what extent the SOFIE structure satisfies these principles. Detailed information on the complete project is found in section 3.5 where all the structural properties of the building are found.

The seven-storey SOFIE building is designed with a ground plan of 13.44x7.68. The design is a slice of a large and already completed project that was designed by Renzo Piano. This project was build out of steel and concrete.

For the SOFIE building the same layout is used, but the building material is changed into timber. The building is completely built with cross laminated panels. A total of 250 m3 of spruce timber is used for the wall and floor panels.

2.4 The lay-out of the building

The arrangement of panels is given in Figure 2-8. A coordinate system with axes x and y is given. The axes x and y are used in the text several times for discussing the properties of the building.

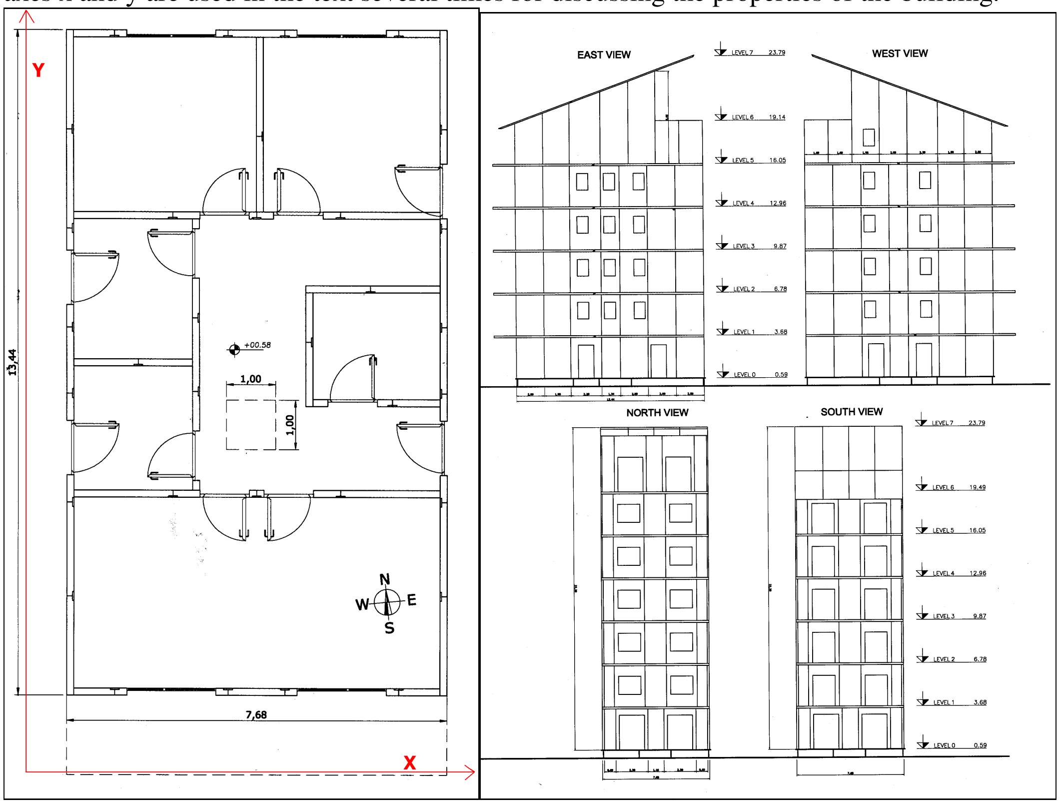

Figure 2-8, layout of the ground floor[SOFIE project, 2007]

On the right side in Figure 2-8 views on the four sides of the total SOFIE structure are given. The wind rose in the figure is used to indicate the different views on the right.

2.4.1 X-lam timber panels

The main structural element in the SOFIE structure is the cross-laminated panel, abbreviated as X-lam panel. Different producers of X-lam exist. From one of the producers (KLH in Austria) a good description of the production process is available which is cited here.

"Cross-laminated timber (X-lam) is produced from spruce timber strips. The strips are stacked crosswise on top of each other and glued with a high pressure vacuum system. This arrangement of the longitudinal and crosswise lamellas reduces the swelling and shrinkage in the board plane to an insignificant minimum. Also the static strength and shape retention increase considerably. The spruce timber used consists only of technically dried wood with wood moisture of 12% (+/- 2%). This process rules out any damaging pest, fungus and insect attacks. All boards used are subject to a visual and mechanical quality sorting procedure. The gluing takes place using solvent-free and formaldehyde-free PUR adhesive from Purbond (HB 110, HB 530). This adhesive is tested according to German standard, DIN 68141. The glue is applied automatically over the whole surface - the percentage of adhesive is 0.2 kg/m² and glue seam. A very high-quality level of adhesion is achieved as a result of the pressing power of approx. 6 kg/cm2.The factory cutting and beaming of X-lam solid cross-laminated timber boards takes place using state-of-the-art CNC technology. Depending on the purpose and static requirement, the plates are available in 3, 5, 7 or more board layers."[www.klh.at]

The X-lam panel is presented in Figure 2-9. The X-lam panel on the picture consists of five layers where the outer layers are parallel to each other. This parallelism is characteristic for the product.

Figure 2-9, X-lam panels just after production[www.progettosofie.it]

2.5 Earthquakes, structures and the European standard

Earthquakes generate very complex loading and movement patterns. No earthquake is similar to another in direction, power and duration. To make design and engineering possible, this variety in earthquakes is standardised. In Europe this is done in EC8. The earthquake motion (direction, power, duration etcetera) is represented by an elastic ground acceleration response spectrum. The structural design considerations are also standardised in EC8. EC8 is taken as the guideline to this section. The text is not reproduced one to one but it is changed for legibility. For the same reason figures are added, together with texts based on other literature.

2.5.1 Basic principles of earthquake design

Introduction

Earthquake forces and accelerations can be resisted with a good design of elements and joints. In earthquake resistant design, starting points are general, independent of the type and duration of the earthquake and the type of construction material.
These principle starting points are:

- structural simplicity
- uniformity and symmetry
- torsional resistance and stiffness
- diaphragmatic behaviour at storey level
- foundation

The starting points are elaborated in the following section. After each aspect, the properties of the SOFIE structure are discussed according to the starting point.

Starting points

Structural simplicity is characterized by the existence of clear and direct paths for the transmission of forces. Structural simplicity is an important design aspect because the modelling and the analysis in this way are less uncertain. The prediction of the seismic behaviour of structures with structural simplicity is more reliable.
The layout of the SOFIE building indicates a good structural simplicity. Vertical loads are transferred directly to the foundation by the wall panels. No large spans are present. Horizontal loads are transferred in a direct way by the shear connectors (see section 3.5.3).

The general masses (floors and roofs) and the stiffening lateral force-resisting mechanisms (shear walls) are preferably located symmetrically. With this symmetrical lay-out, short and direct transmission of the inertia forces is created and torsional forces are avoided. Graphical explanation of torsion in structures is given in Figure 2-10. Another aspect to anticipate on high torsional forces is a close relationship between the distribution of masses and the distribution of force resisting elements.

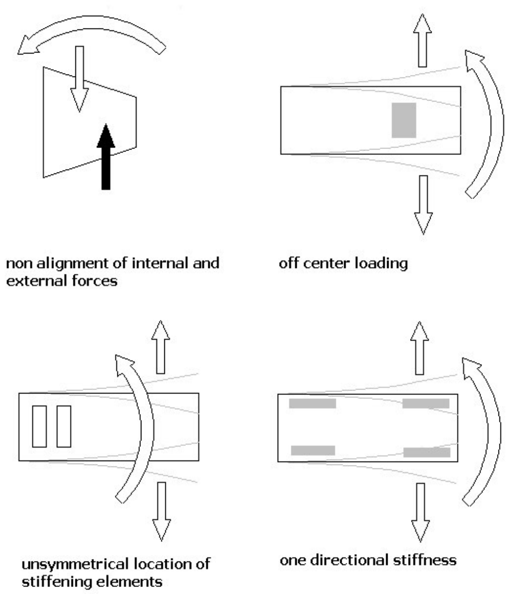

Figure 2-10, torsion in structure [Shodek,2001]

The wall panels are the only stiffening elements that are located almost symmetrically as found in Figure 2-8. Calculations (Appendix A) show that the centre of rotation is almost in the middle, which indicates the uniformity and symmetry of the masses and stiffening elements in both directions (x and y).

The torsional resistance of the structure should be adequate in order to limit torsional motions. Torsional motions stress the different structural elements in a non-uniform way. Torsional resistance is designed with the main resisting elements distributed close to the boundaries of the floor plan.
The external walls of the SOFIE structure are the longest and hence the stiffest shear wall elements. Torsional resistance is satisfied with these walls.

Elements such as floors and roofs are important for the resistance of the structure in horizontal loading, because of their diaphragmatic behaviour. They transmit the horizontal inertia forces to the vertical structural system and also ensure that the structural system is acting together in resisting the forces. A proper joint design is needed next to sufficient properties of the horizontal slabs.
The properties of the X-lam timber applied for the floors/roofs provide enough diaphragmatic behaviour to fulfil this requirement. On the capacities of the connection between the floor panels, more research is needed to get exact properties. But with engineering experience and the positive results from the experiment it is stated that these connections were designed with adequate capacity to allow for diaphragmatic behaviour.

The main purpose in the design of the foundations and the connection of the building to the foundation is that they must ensure that the building is subjected to a uniform seismic excitation. To cover these aspects, the foundation must be able to take the high seismic forces and the connections must have a high load bearing capacity. Since the foundation in the experiment consists of a steel base (see section 3.6), no problems are expected here.

Earthquake-resistant timber buildings are designed either as dissipative or low-dissipative structures. In Figure 2-11 the dissipated energy is indicated by the diagonal hatched surface.

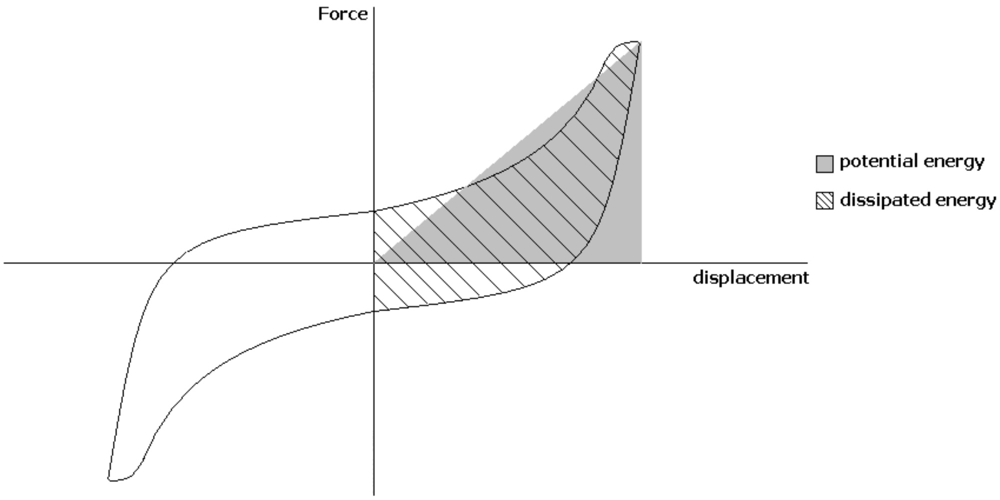

Figure 2-11, amount of dissipated energy [Sandhaas,2004]

Energy dissipation in timber structures is present in the breaking the timber and plastic deformation of the steel connectors. In dissipative structures the plastic capability of the connections is taken into account. For this type of building the behaviour factor (q explained in section 2.5.2) is larger than for low-dissipative structures. The value of q depends on the ductility class, which is explained later in section 2.5.2.
The location of the dissipative zones should be in joints and connections to have proper building behaviour. Properties of hystersis are determined in accordance with the European standard EN 12512. In low-dissipative structures, non-linear material behaviour is not taken into account (behaviour factor is equal to 1). The capacity of the members is calculated according to the European standard EN 1995-1:2004.

2.5.2 Behaviour factors

In the European standard for earthquake engineering (EC8) the capacity of structural systems to resist seismic actions is established. An elastic analysis is carried out where de elastic forces are reduced by the behaviour factor. The elastic analysis is based on the response spectrum (section 4.5). The capacity is reflected in the behaviour factor q. With q, an approximation is done of the seismic forces that the structure is subjected to (See also the lateral force method 4.6) The values for q are depending on the construction material and the structural system.
EC8 classifies timber buildings in three ductility classes; low, medium and high. Buildings are classified depending on their ductile behaviour and energy dissipation capacity. Description of the properties and their corresponding behaviour factors are given in Table 2-4.

Design concept and ductility class	q	Examples of structures
Low capacity to dissipate energy - DCL	1,5	Cantilevers; Beams; Arches with two or three pinned joints; Trusses joined with connectors.
Medium capacity to dissipate energy - DCM	2	Glued wall panels with glued diaphragms, connected with nails and bolts; Trusses with doweled and bolted joints; Mixed structures consisting of timber framing (resisting the horizontal forces) and non-load bearing infill.
	2,5	Hyperstatic portal frames with doweled and bolted joints (see **8.1.3(3)**P).
High capacity to dissipate energy - DCH	3	Nailed wall panels with glued diaphragms, connected with nails and bolts; Trusses with nailed joints.
	4	Hyperstatic portal frames with doweled and bolted joints (see **8.1.3(3)**P).
	5	Nailed wall panels with nailed diaphragms, connected with nails and bolts.

Table 2-4, seismic behaviour factors according to the European standard [Eurocode 8]

If the building is non-regular in vertical development the q-values listed in Table 2-4 should be reduced by 20% with a minimum of 1.5. Structures could have different and independent properties in the two horizontal directions. When this is the case, the behaviour factors in each main direction should correspond to the properties of the structural system in that direction.

The SOFIE building consists of glued wall panels with glued diaphragms. The connections consist of nails. Therefore, the SOFIE building can be classified as a medium dissipative building with a behaviour factor q equal to 2.

2.6 Structural dynamics

2.6.1 Introduction

In this section, the basic principles in structural dynamics are described. The general equation of motion is presented in section 2.6.2 together with the explanation of damping in the equation.

2.6.2 Equation of motion

Structures loaded by earthquakes respond with respect to its vibration properties. The general mathematical representation is a differential equation in the form of:

$F = m\ddot{u} + c\dot{u} + ku$

where:

F = force

m = mass

c = damping

k = stiffness

u = displacement

The factors influencing the structural behaviour of a system are though mass, damping and stiffness. For a good design of the building and to model the structure these are the main properties to determine.

Mass and stiffness can be directly read from the building properties but the damping term c needs some explanations using the equation of motion. The damping, c, can have different values that do have influence on the behaviour of the system. To show this the equation of motion will be solved: $m\ddot{u} + c\dot{u} + ku = 0$. To solve the equation parameters for the damping ratio ζ and the un-damped natural frequency ω_0 are defined:

$\omega_0 = \sqrt{\frac{k}{m}}$ and $\zeta = \frac{c}{2\sqrt{km}}$

The equation of motion

$\ddot{u} + 2\zeta\omega_0\dot{u} + \omega_0{}^2 u = 0$

By assuming a solution $x = e^{\gamma t}$ that is substituted in the equation of motion the following expression is obtained.

$\gamma^2 + 2\zeta\omega_0\gamma + \omega_0{}^2 = 0$

With solutions: $\gamma = \omega_0(-\zeta \pm \sqrt{\zeta^2 - 1})$

As can be concluded from the solutions to the equation of motion obtained above, the system is dependent on the value of the damping ratio ζ and the natural frequency ω_0. The qualitative behavior of the system depends directly on whether the solution for γ has one real solution (critical damping), two real solutions (over-damping), or two complex conjugate solutions (under-damping). The three cases are explained below.

\When $\zeta = 1$, there is a double root which is real, the system is said to be critically damped. A critically damped system converges to zero faster than any other without oscillating.

When $\zeta > 1$, there are two different real roots; now the system is over-damped. An over-damped system will take longer to converge to zero than a critically damped system.

When $0 \leq \zeta < 1$ the system is under-damped; in this situation, the system will oscillate at the natural damped frequency ω_d , which is a function of the natural frequency and the damping ratio. The expression for the damped frequency is given as $\omega_d = \omega_0\sqrt{1 - \zeta^2}$.

All three damping systems can be graphically visualized which is done in Figure 2-12.

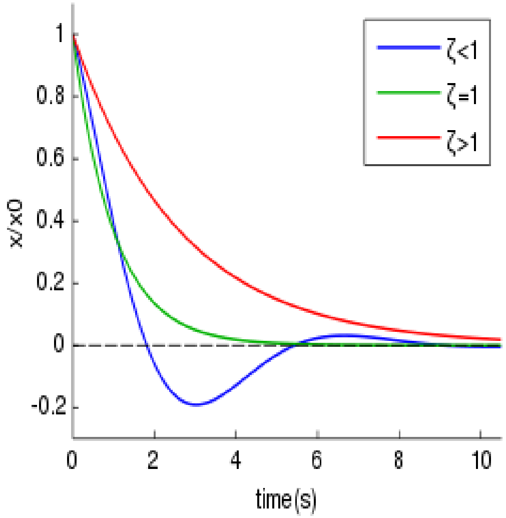

Figure 2-12, the three different types of critical damping [dynamics of structures, 2006]

2.6.3 Damping

In the section above damping in the equation of motion is explained. In this section, the damping as physical aspect is treated. Damping is the dissipation of mechanical vibration energy from the system. Energy dissipation in timber structures is present in hysteretic behaviour (factor q, see section). Hysteresis in timber structures takes place in the connections and in the material around the fastener, in term embedding. A system with hysteretic behaviour exhibits path-dependence, or "rate-independent memory". Hysteretic damping is the phenomenon that the link between stress and strain not only depends on the size of the stress, but also the stress direction.[Shodek, 2001]

2.6.4 Mathematical representation of damping mechanisms

Damping in timber structures (at the joints and surrounding materials) is a complex phenomenon. Generally a large number of factors (dissipation mechanisms e.g. friction) are involved. Therefore the damping is approximated in the design. Different methods for approximation of the dissipation in structures are available. Most approximations make use of the critical damping. Therefore critical damping is explained first after which the different models are discussed briefly in this paragraph.

The mathematical modelling of damping can be done with the following methods:[1]

- Constant viscous damping
- Frequency dependent viscous damping
- Quadratic damping
- Friction/Coulomb damping
- Elastic plastic damping

Hysteretic damping, as found in timber structures, is a combination of the constant and frequency dependent viscous damping. Therefore, these types of damping are explained in more detail. These two types of damping are modelled as a percentage of the critical damping in a viscous damped system. For a detailed explanation of the quadratic, Coulomb and elastic-plastic damping please refer to the literature.

2.6.5 Constant viscous damping

Constant viscous damping implies that the damping force is proportional to the velocity of the damped element. The system vibrates around the equilibrium position with decreasing amplitude. The damping force enforces this behaviour. Per oscillation the friction force follows the ellipse displayed in Figure 2-13. The hatched area of this ellipse is equal to the energy dissipation per period (cycle) of the vibrating system.

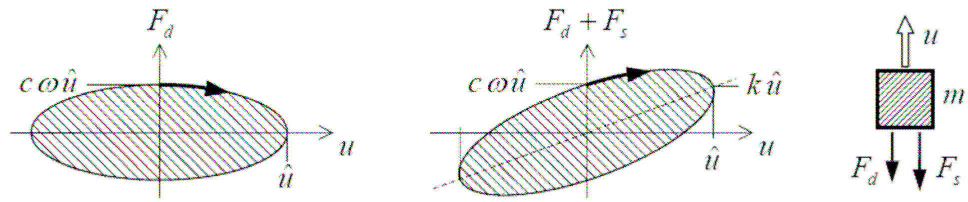

Figure 2-13, development of the forces in spring and damper [dynamics of structures,2006]

2.6.6 Frequency dependent viscous damping

For a number of materials the energy dissipation grows with the square of the amplitude, independent from the excitation frequency. The hysteresis loop that remains is similar as shown in Figure 2-14.

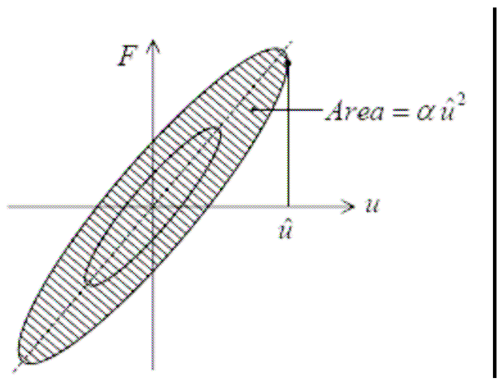

Figure 2-14, similar hysteresis loop [dynamics of structures,2006]

The area of the ellipse grows quadratic with the amplitude of motion

2.6.7 Damping in DRAIN 3D

The software used for the modelling of the SOFIE structure (DRAIN 3D, see chapter 0) uses a coefficient (β) for the proportional viscous damping. The factor β is obtained from the fundamental period of motion (see chapter 0). The viscous element stiffness is multiplied by the factor β for determining the damping C. The relation of the stiffness (K) and the damping (C) is $C = \beta K$ and $\beta = \dfrac{T g\xi}{\pi}$. ξ is the damping rate, being the variable to determine in order to get a good fitting. The lumped damping percentage of the critical damping for X-lam structures is approximately 10%. [Cecotti et all]

2.6.8 Resonance and earthquakes

Oscillations of a system decrease in time because of damping. If a part of the system is translated, the mass of the system would initially tend to resist translation because of inertia.

If the system is moved back and forth continuously as is the case for earthquakes, the structure continues to vibrate as long as the ground motion is present. In cases where the frequency of the ground motion is approximately the same as that of the construction, resonance would occur. In the event of resonance, the oscillations cause the building to vibrate and when these oscillations continue, the amplitude of the vibration increases and thus the forces on the structure.

3 SOFIE PROJECT

3.1 Introduction

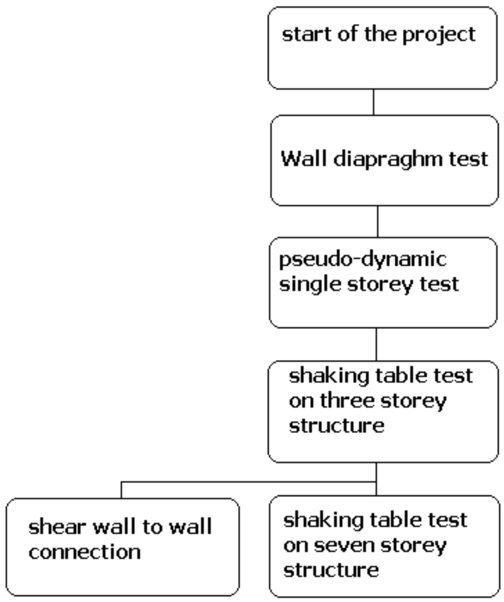

Figure 3-1, project path for the SOFIE project

Several experiments and research studies are completed within the SOFIE project. First some small scale tests are done on the material after which the scale of the experiments was increased. The first experiment to mention was a 2D wall diaphragm test whereupon the project path in Figure 3-1 is followed. Outcomes of these tests will be discussed shortly in the current chapter.

As presented in the project path diagram, the final project at the moment of writing is a shaking table test on a seven-storey timber structure. The seven-storey test and its results are discussed in detail because it forms the base of the thesis.

In sections 3.2 to 0, the three preliminary tests are discussed shortly. For these preliminary tests only the goal of the experiment, the test set-up and the conclusions are described. For more information about the experiments please refer to the published papers within the SOIFE project.
The test on the seven storey structure is described in detail in section 3.5 because it forms the base of this report. The shear wall to wall experiment is documented in chapter 5. Though the shear wall to wall experiment is not a part of the current chapter, it is mentioned here to gain an overview of the report.

3.2 In-plane cyclic tests on X-lam wall panels

The first experiments to mention are the in plane cyclic tests on a single panel. The tests are done to determine the lateral resistance of the panel and its connections. Different configurations of X-lam panels are used in ramp and cyclic tests according to European standards EN26891 and EN12512. The differences in layout can be found in the anchoring system, the layout of the opening and the interstorey connection.

The in plane cyclic and ramp tests are done on four different configurations. Panels have dimensions 2.95mx2.95m as given in Figure 3-3. All panels have a thickness of 85 mm and consist of five layers of 17mm. Vertical loads are applied for representing loading on the panel as would be the case in a complete building. The vertical loading is calculated from a three storey building. The three storey building at the time was defined as the final goal of the project. The test setup can be found in Figure 3-2 and the configuration of the panels in Figure 3-3.

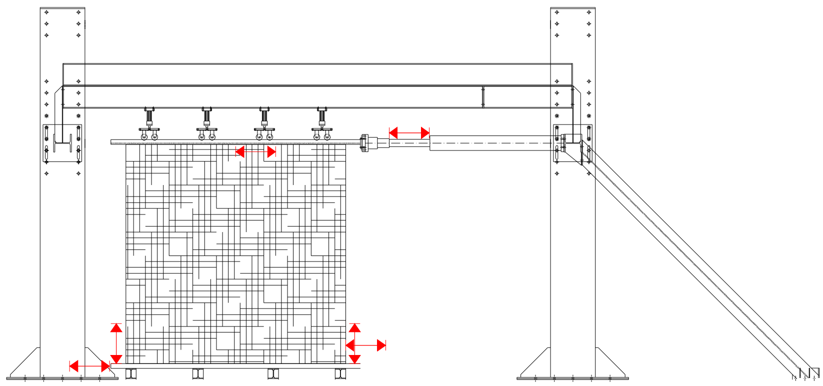

Figure 3-2, test setup for the single panel test [quasi-static and pseudo-dynamic tests on XLAM walls and buildings]

- Configuration A: a normal panel connected to the base with two holddowns and three shear connectors (ground level in three storey building). A vertical load of 18.5 kN/m2 is applied to represent vertical load from the upper two storeys.
- Configuration B: a normal panel connected to a floor panel with two shear connectors and two holddowns (second storey panel in three storey building). The extra vertical load is 10.2 kN/m2.
- Configuration C: a normal panel with a floor slab on top (ground level panel) . The panel is connected with the base with two holddowns and with the resting floor with two holddowns. The applied vertical load is 18.5 kN/m2
- Configuration D: a panel with an opening connected to the base with two holddowns and two shear connectors (ground level panel) with 18.5 kN/m2 of vertical load.

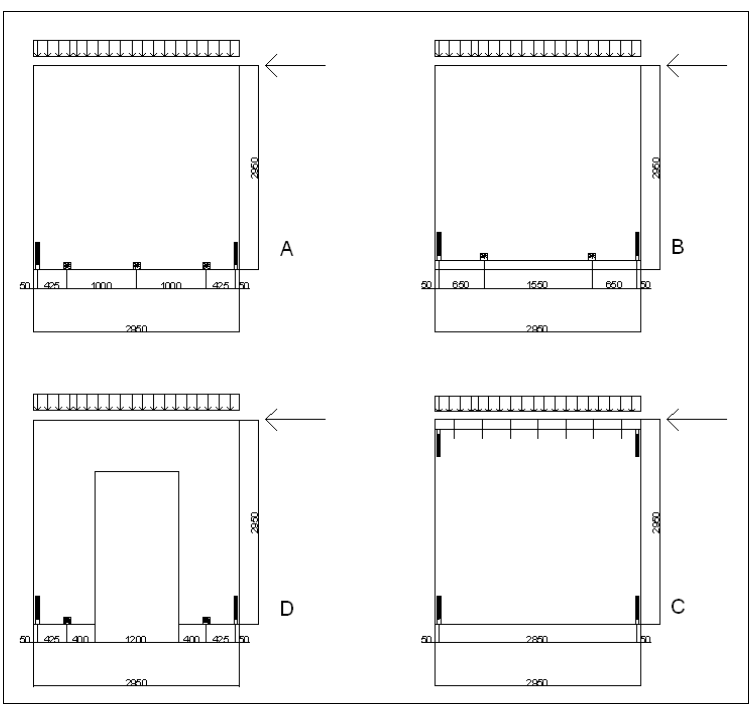

Figure 3-3, configuration for single panel tests [quasi-static and pseudo-dynamic tests on XLAM walls and buildings]

The behaviour of the panels under cyclic loading is strongly influenced by the design and layout of the joints. The X-lam timber panels behave almost completely rigid under cyclic loading in the different configurations. All energy is dissipated at the connections and viscous damping can be determined as 14%. This is a value comparable with timber frame systems, hence it promises to be suitable for seismic purposes.

3.3 Pseudo-dynamic tests on a one storey specimen with three different layouts

After the positive results of the experiments on the single panels (see section 3.2), the next step was to do an experiment on a single storey structure. This was done at the Trento University, Italy. The layout of the tested single storey was a floor plan of Length x Width x Height = 8850x8850x2950mm. The force on the structure is applied on the middle panel (see Figure 3-4). Three configurations are used for the three panels parallel to the direction of the force the red coloured walls in the figure. The last panel with an opening of 4 meters wide is used in the last test at only one outer wall. In this way an unsymmetrical building layout is created.

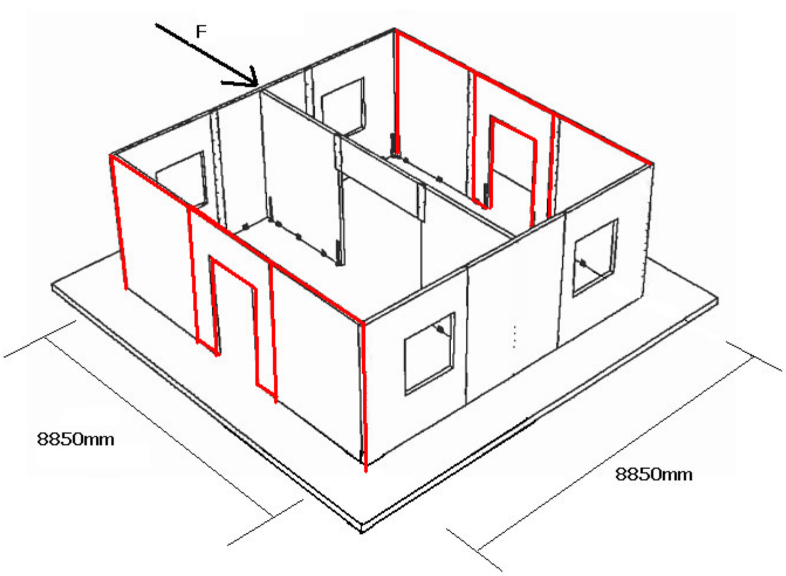

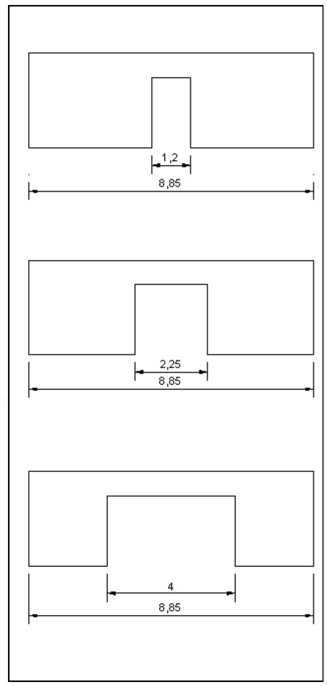

Figure 3-4, configuration for single storey test [quasi-static and pseudo-dynamic tests on XLAM walls and buildings]

Earthquake loading is approached by a pseudo-dynamic loading. The forces applied with a horizontal jack are calculated considering weight of the structure and acceleration values of real earthquakes. No vertical load was applied. From the ramp test and the cyclic test it is concluded that the size of the opening is not of a large influence on the behaviour of the structure. The behaviour of the single storey building is dependent on the joint design. . Again, the wooden panels proved to be very rigid, giving the whole structure a very high stiffness. At the same time, the connections were able to dissipate energy.

3.4 Shaking table test on a three-storey building

The experiment on a three storey timber X-lam structure is done on a building with the same floor plan as for the single storey test (section 3.3). The height of the building is approximately 10 meter. The experiment consists of earthquake loading in the direction indicated by the arrow in Figure 3-5.

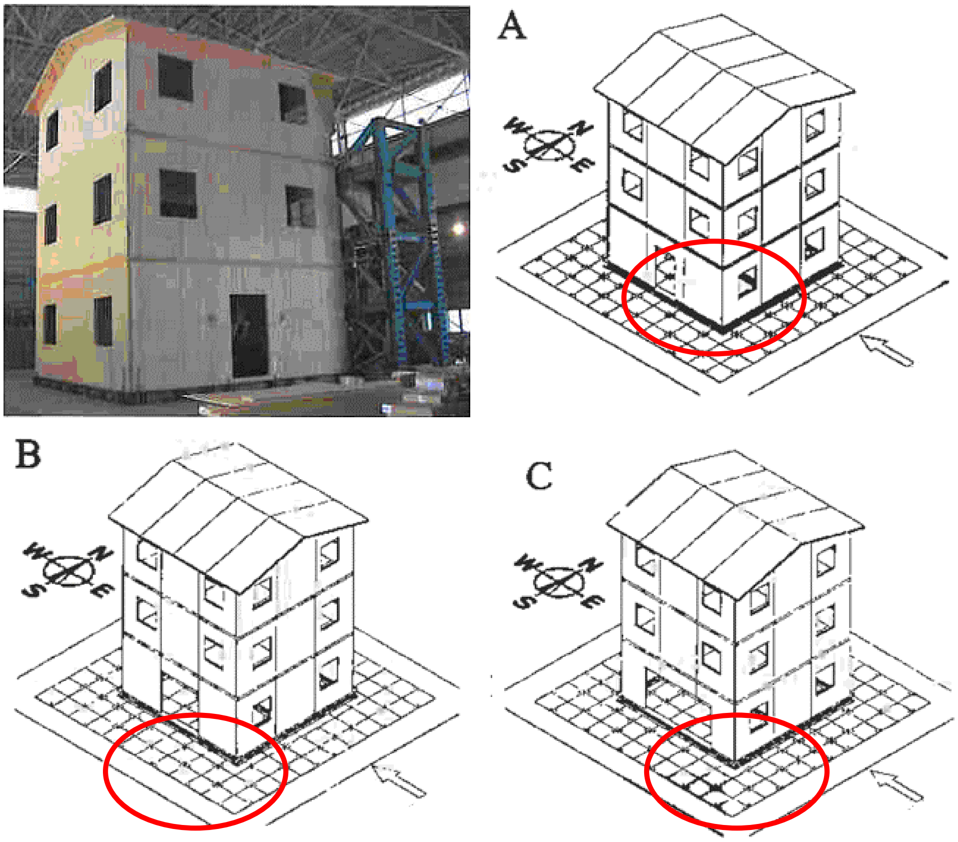

Figure 3-5, the three different setups for the three storey test [Seismic behaviour of multi-storey Xlam buildings]

A total of three configurations are tested. Again (as for the single storey test) the variance in the specimens is found in the layout of the panels parallel to the direction of the earthquake (indicated by the circles in Figure 3-5). In configuration C, the larger opening is applied only on one side to create asymmetry.

Conclusions from test results

Asymmetric locations of the horizontal force resisting elements do not lead to a large torsional force. Large openings do not have significant influence on the behaviour of the building, because the wooden panels proved to be very rigid, giving the whole structure a very high stiffness The shaking table tests confirmed the impression obtained from the cyclic tests that the construction technique with X-lam panels is promising for seismic purposes.. At the same time, the connections were able to dissipate energy.The importance of a good joint design is obvious. Energy dissipation takes place only in the joints. Joints must be designed strong enough to take the high forces maintaining ductility.
At the same time, the connections have to be designed for different levels of strength. The vertical corner joints must be very rigid in order to ensure “box behaviour” of the whole structure. Other connections must have sufficient level of strength to accommodate the high forces and contemporarily remain ductile without brittle failures. X-lam construction system taken as a whole is suitable for seismic regions. Special attention is paid to the good design of joints and to the load transfer points.

3.5 Seven storey structure

3.5.1 Introduction

This section is about the seven storey structure. The section describes the properties of the applied materials as well as the connections in the building. The full scale test details can be found in this section also. First the panels that are used in the building are described in section 3.5.2. The connections present in the building are mentioned in section 3.5.3. The experiment consists of a full scale test on a shaking table. The properties of the shaking table are given in section 3.6. In section 3.7.1 the measuring instruments are described followed by the results in section 3.8. With the properties of the building, some preliminary calculations are possible. These calculations are computed according to the European standard, EC8, in the next chapter, chapter 0.

3.5.2 Applied X-lam panels

The construction system of the SOFIE building consists of timber X-lam panels for walls and the floors. General properties are given here.

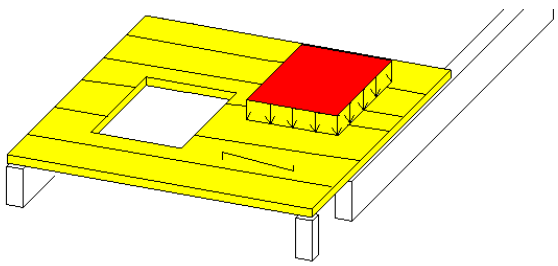

Figure 3-6 Load applied perpendicular to the panel[www.klh.at]

Mechanical strength	Strength
Modulus of elasticity Parallel to the direction of the panel grain (E0,mean) Normal to the direction of the panel grain (E90,mean)	 12000 N/mm2 370 N/mm2
Shear modulus Parallel to the direction of the panel grain (E0,mean) Normal to the direction of the panel grain (E90,mean)	 690 N/mm2 50 N/mm2
Bending strength Parallel to the direction of the panel grain	 24 N/mm2

Table 3-1, properties of X-lam parallel to facing grain [www.klh.at]

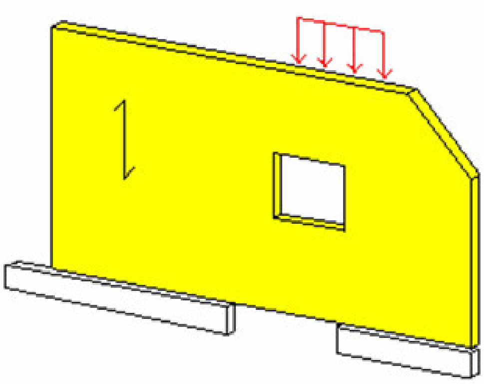

Figure 3-7, Load applied in plane of facing grain [www.klh.at]

Mechanical strength	Strength
Modulus of elasticity Parallel to the direction of the panel grain (E0,mean)	12000 N/mm2
Shear modulus Parallel to the direction of the panel grain (E0,mean)	250 N/mm2
Bending strength Parallel to the direction of the panel grain	23 N/mm2

Table 3-2, X-lam properties in plane of facing grain [www.klh.at]

The specific panels used in the SOFIE project are described here. The thickness of the applied walls is varying over the height of the construction. This is because the lateral forces due to horizontal loading are varying also. Shear forces at the base are higher then shear forces at the top (see section 4.6). The thickness of the X-lam panels is 142 mm at the 1st and 2nd storey. On storey 3 and 4, a thickness of 125 mm is used. At the top levels 5, 6 and 7, the thickness of the wall panels is 85 mm. All floor panels have a thickness of 142 mm. The properties of the used panels given by the producer are listed in Table 3-3.

The characteristic properties of panels cannot be determined directly from the general properties. An important parameter for determining strength is the direction of the layers in the panel. This is explained here in detail as it is a specific property of the X-lam panels.
Under a load perpendicular to the panel the layers perpendicular to the force direction are used for load restraining as is indicated for a five layered panel in Figure 3-8.

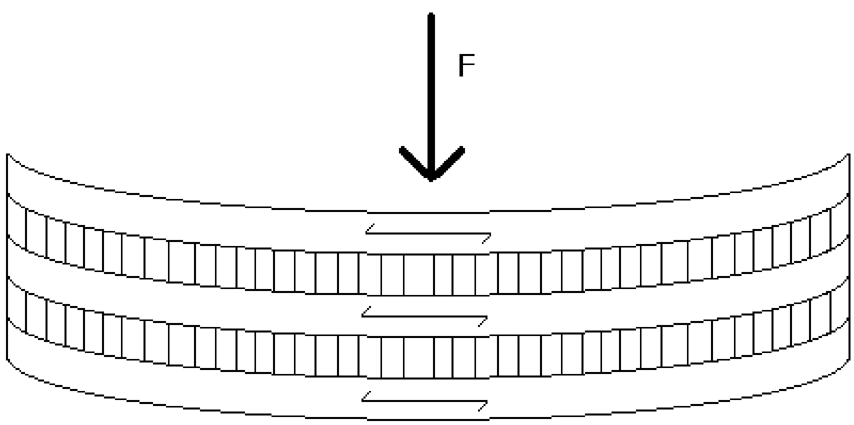

Figure 3-8, five layered panel under out-of-plane loading in bending

Panel type	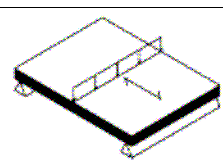	Parallel to the grain of the outer layer		
Lenotec	Emean	Rigidity= $E_{mean} \cdot J$	Fm,k	Fv,k
	N/mm^2	$10^{12}\,Nmm^2$	N/mm^2	N/mm^2
81	10590	0.469	23.11	0.92
125	9010	1.466	19.66	0.85
142	8990	2.145	19.61	0.93

Table 3-3, properties of X-lam in SOFIE project [www.klh.at]

Panel type	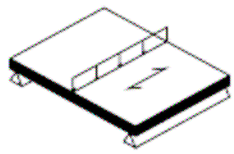	Perpendicular to the grain of the outer layer		
Lenotec	Emean	Rigidity= $E_{mean} \cdot I$	Fm,k	Fv,k
	N/mm^2	$10^{12}\,Nmm^2$	N/mm^2	N/mm^2
81	410	0.018	2.68	0.67
125	1990	0.324	7.64	0.42
142	2010	0.480	7.08	0.54

Table 3-4, properties of X-lam in SOFIE project [www.klh.at]

The shear modulus of X-lam panels is determined as G = 60 N/mm2.

3.5.3 Connections

The connections in the building are explained first for the ground floor. The layout of the panels on the ground floor is presented in 3D in Figure 3-9.

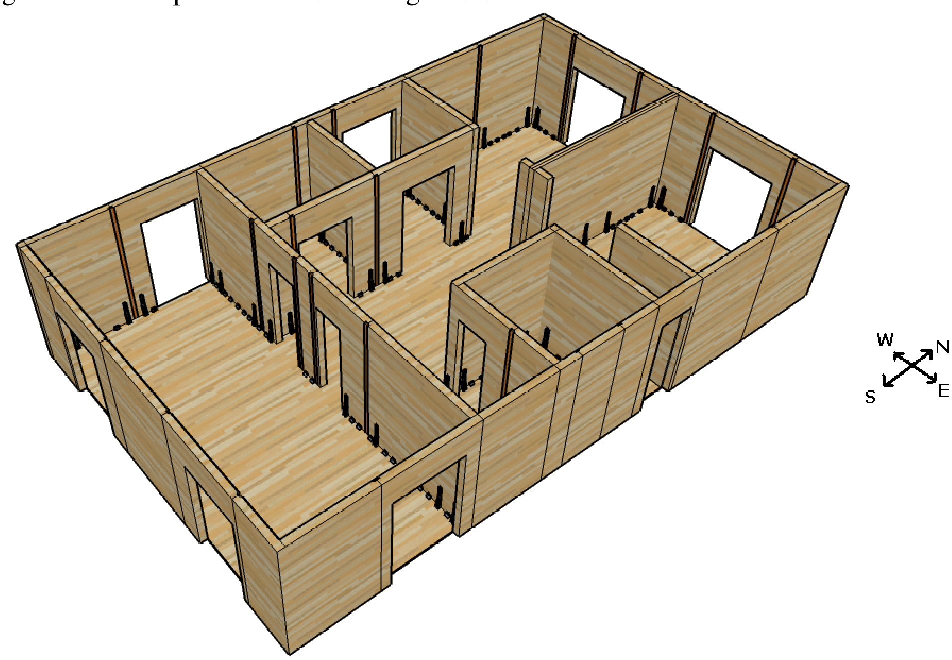

Figure 3-9, 3D drawing of the ground level

The different connections are named in the closer view in Figure 3-11. A total of six different connections are used in the SOFIE structure. These connections are: holddown; shear connector, kerto-Q LVL, wall to wall in corner, the floor panel to floor panel connection and the floor to wall connection (not presented in the figure). The different types of connections are described in detail in the next section.

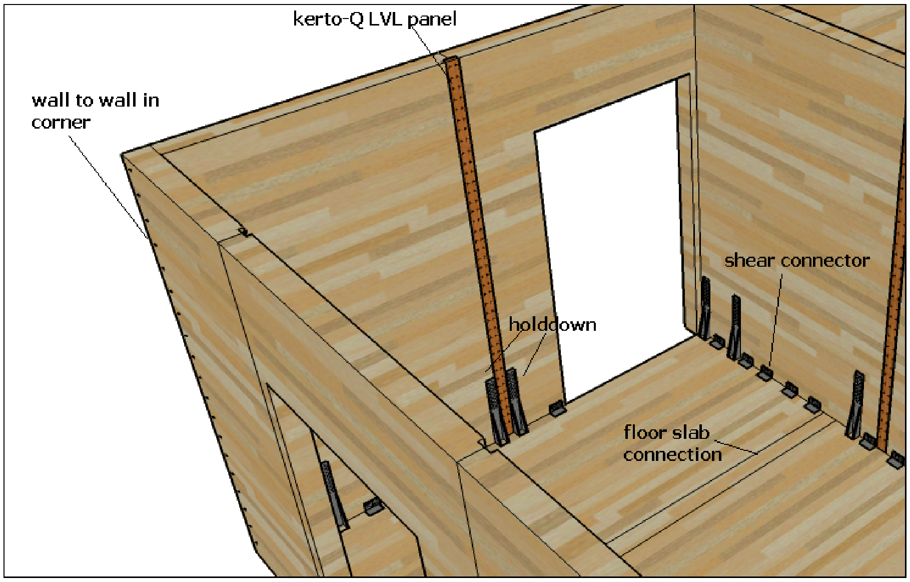

Figure 3-10, detailed overview of the applied connections

The steel connector types that are used in the connections viewable in Figure 3-10 are presented in the technical drawings of Figure 3-11.

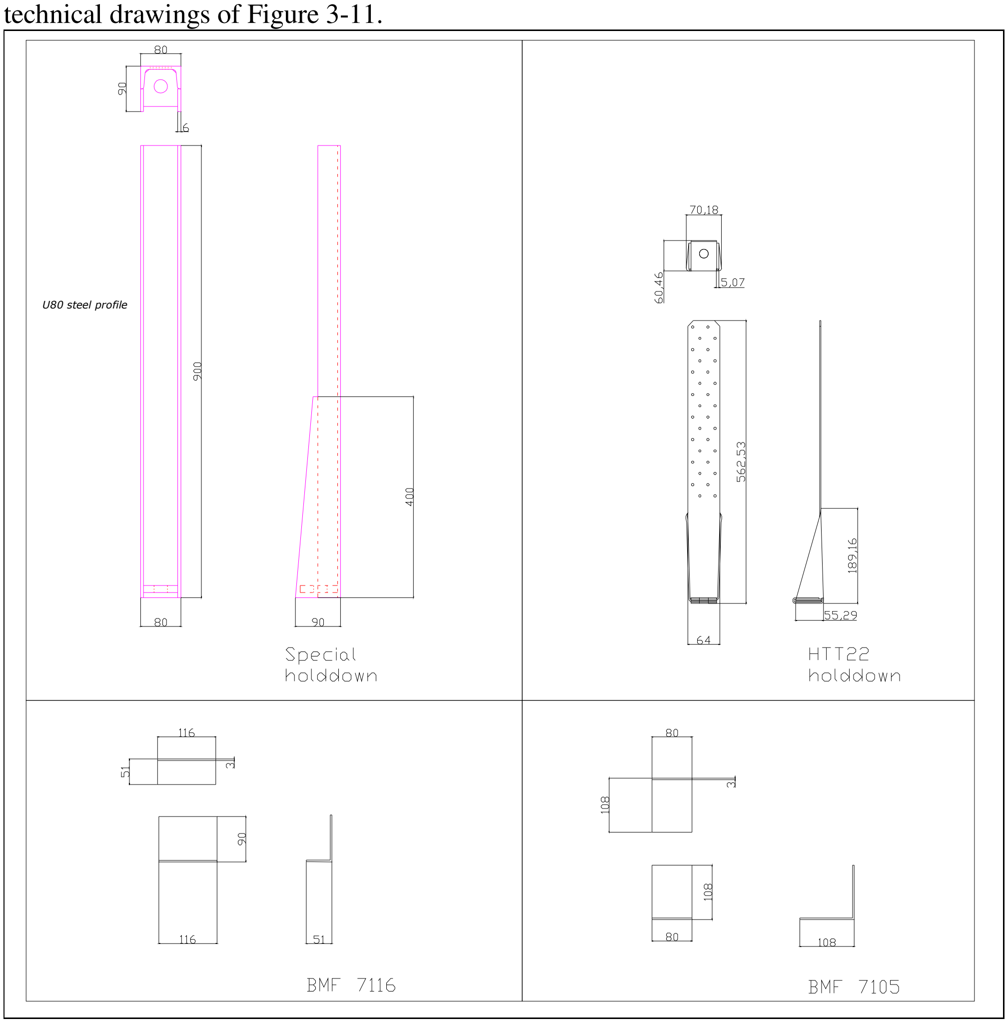

Figure 3-11, steel connector types in SOFIE project [SOFIE project,2007]

3.5.4 Layout of the connections

The set up of the different connections is described in detail in this section. Except for the top view of the floor slab connection all connections are shown in the direction indicated by the red arrow in Figure 3-12.

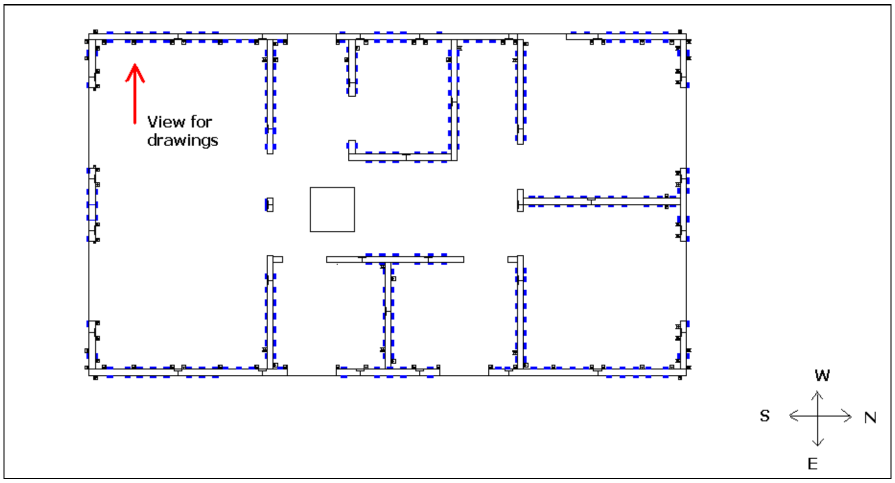

Figure 3-12, location of holddowns, shear connectors and presentation of the view direction[SOFIE project,2007]

Interstorey wall panel to wall panel connection

Floor to wall connections consist of all four types of steel connectors drawn in Figure 3-13. The number and type of fasteners are given in Table 4-12. The BMF 7116 connection is used for the shear connection between building and steel shaking table. BMF 7105 connections are used for the shear forces between the wall panels and the floor panels. The holddowns are used for vertical forces. The wall to wall connection is explained in the next section.

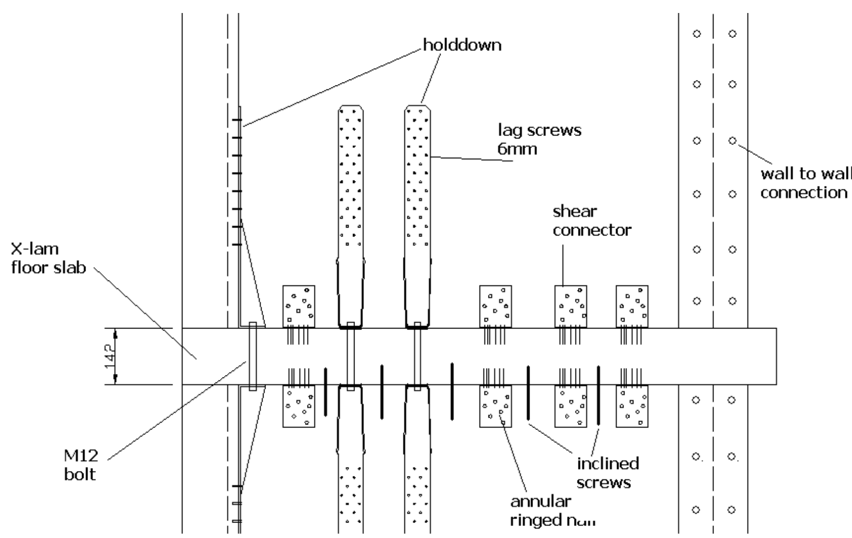

Figure 3-13, interstorey wall panel to wall panel connection

Wall panel to wall panel in plane connection (but joint)

The wall to wall connection is constructed with a Kerto-Q LVL panel screwed with self drilling 8mm screws to the X-lam panels (Figure 3-14). Kerto-Q laminated veneer timber is produced from 3 mm thick, rotary-peeled softwood veneers that are glued together to form a continuous billet. The billet is cut to length and sawn into beam, plank or panel sizes according to the customer's order. Kerto-Q is cross-bonded Kerto. One-fifth of the veneers are glued crosswise. With this structure the lateral bending strength and stiffness are improved.

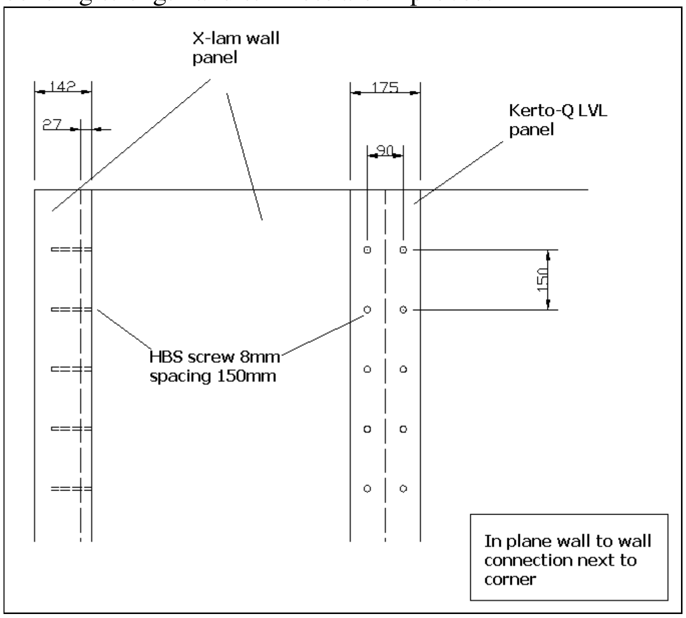

Figure 3-14, wall panel to wall panel in plane connection

Floor slab connection (but joint)

The technique that is used for the floor slab connection is given in cross section in Figure 3-15. The connecting fasteners are 8mm screws applied every 100mm.

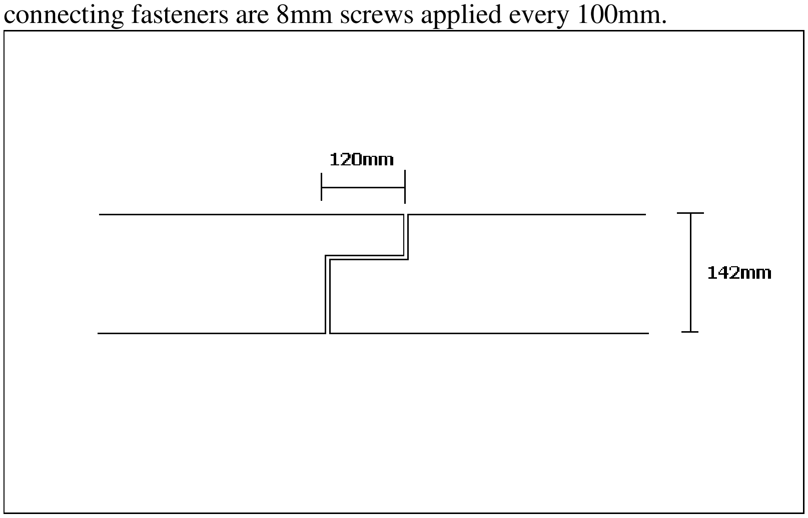

Figure 3-15, floor slab connection

Wall panel to wall panel in corner connection

In the corners the connection consists of self drilling screws 8x180mm. In the corners multiple holddowns are present to secure rigid behaviour of the corners. These screws are inclined also.

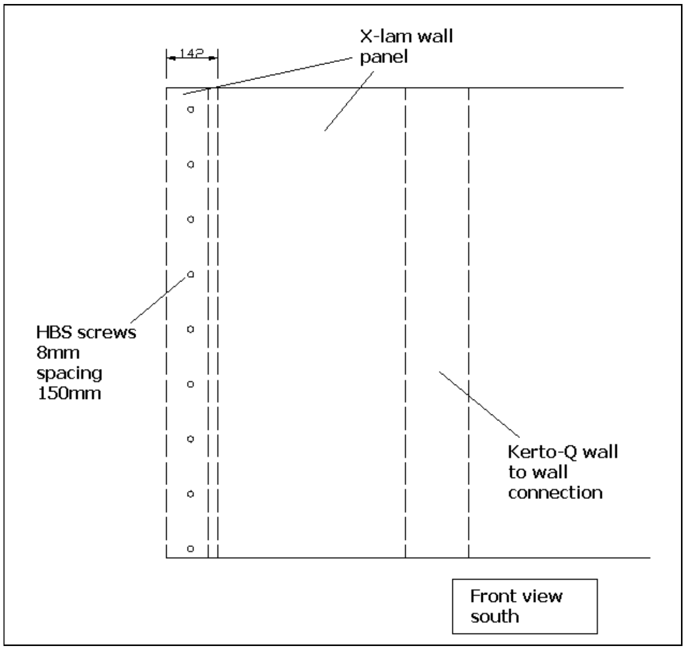

Figure 3-16, wall panel to wall panel in corner connection

Interstorey connection

The wall to floor to wall interstorey connection consists of inclined HBS 8 mm screws as indicated in Figure 3-17. For a clear figure, other connectors are left out.

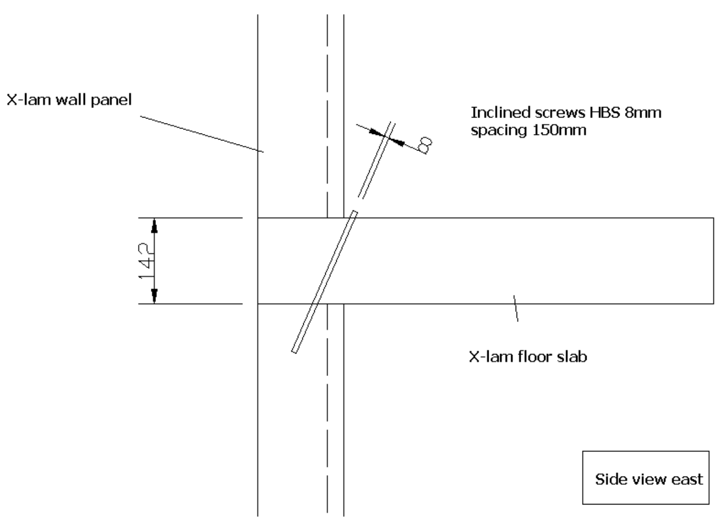

Figure 3-17, interstorey connection

3.6 Test facility

Figure 3-18 Miki shaking table from outside [www.bosai.go.jp]

The test on the seven storey building was done on the earthquake table of in Miki, Japan. The National Research Institute for Earth Science and Disaster Prevention (NIED) constructed a 3D Full-Scale Earthquake Testing Facility, nicknamed "E-Defense" in the city of Miki. Construction of this facility began in 1999 and was completed in 2005. The initiative for the table arises after the The Hyogoken Nanbu (Kobe) Earthquake occurred on January 17, 1995. Almost 6,500 citizens of Kobe and the surrounding region lost their lives, and tens of thousands more lost their houses. The economic consequences exceeded US$100 billions, making it one of the most expensive natural disasters on record. Many earthquake-resistant structures were destroyed by recent earthquakes, such as the Kobe Earthquake(1995) in Japan, the Kocaeli Earthquake(1999) in Turkey, Niigataken-Chuetu Earthquake(2004) in Japan. The reliability of structures during earthquakes must be checked again using rational design methods. For this purpose, existing design methods must be confirmed by full-scale experiments. The opportunities and challenges provided through this facility are great. It has a focus on full-scale testing of structures with high-intensity earthquakes. Important properties of the Miki shaking table are found in Table 3-5.

Table size	20x15 (m)	
Payload	12 (MN)	
Driving type	Accumulator Charged/Elcotro Hydraulic Servo Control	
Shaking direction	X,Y-horizontal	Z-vertical
Max acceleration	9m/s2	1,5m/s2
Max velocity	2m/s	0,7m/s
Max displacement	1m	0,7m
Max moment	150MNm	40MNm

Table 3-5, properties of the Miki shaking table [www.bosai.go.jp]

In Figure 3-19 the installation of the horizontal and vertical actuators and their number can be found. On the right an overview of the building site is given.

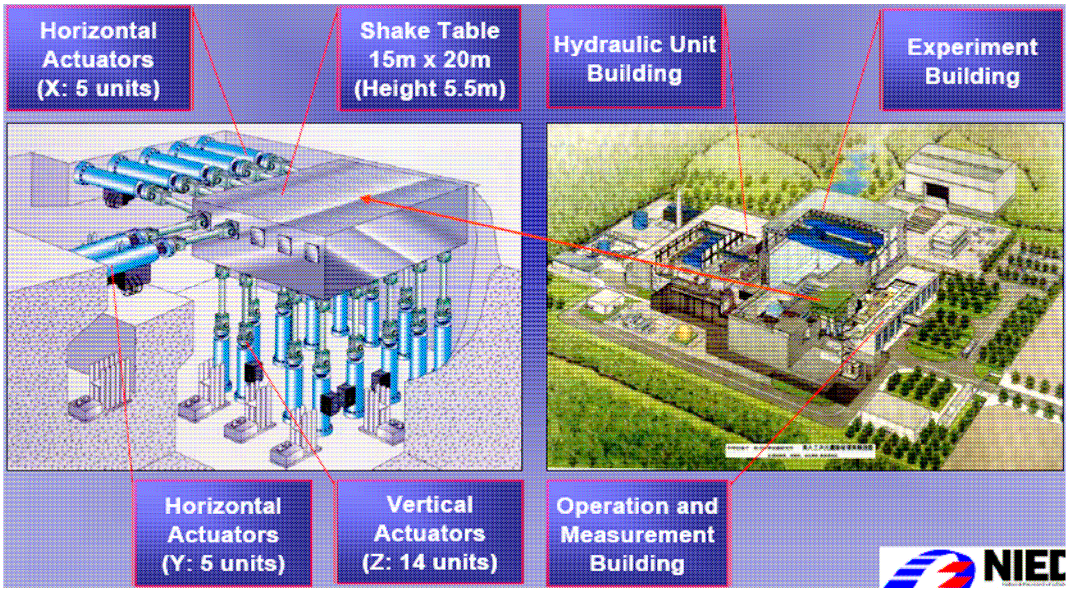

Figure 3-19, installation of Miki shaking table [www.bosai.go.jp]

3.7 Applied earthquakes

Input of the earthquake shaking table in Miki is in the form of accelerograms. The earthquakes applied on the SOFIE structure are the Nocera Umbra (1997), the JMA Kobe(1995) and the El Centro (1940) earthquake. The first tests with the structure are done with a modified PGA (peak ground acceleration) of 0.3 g ascending to 0.82 g (the maximum PGA value for the Kobe earthquake). The accelerograms of the three earthquakes are given below in order of testing. It should be mentioned that the duration of the earthquakes is not similar. The time scale of the accelerograms below is different to get clear diagrams.

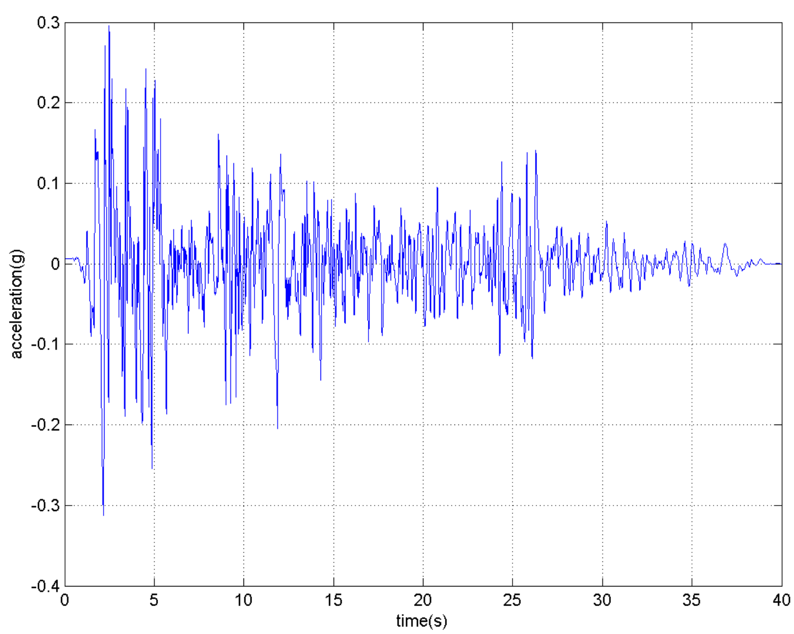

Figure 3-20, accelerogram El Centro (north-south) [SOFIE project, 2007]

Delft University of Technology

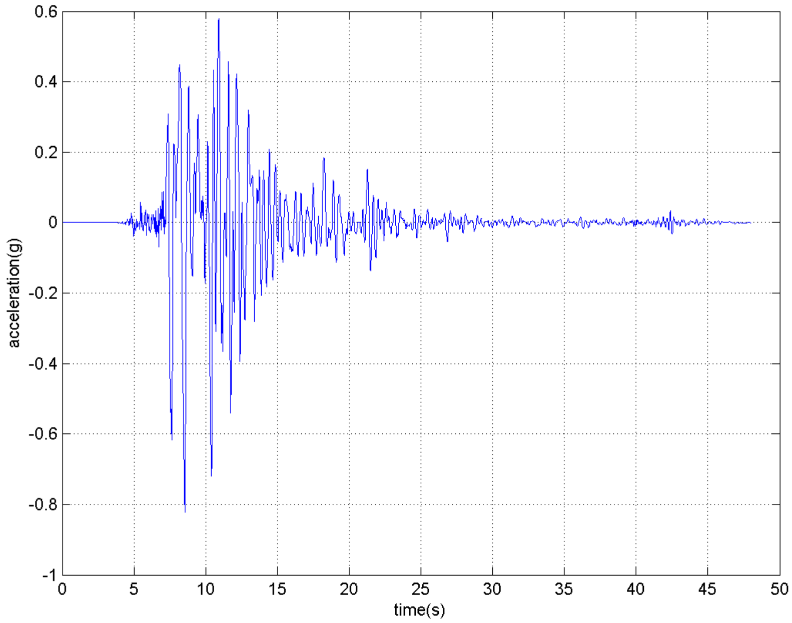

Figure 3-21, accelerogram Kobe 1995 (north-south) [SOFIE project, 2007]

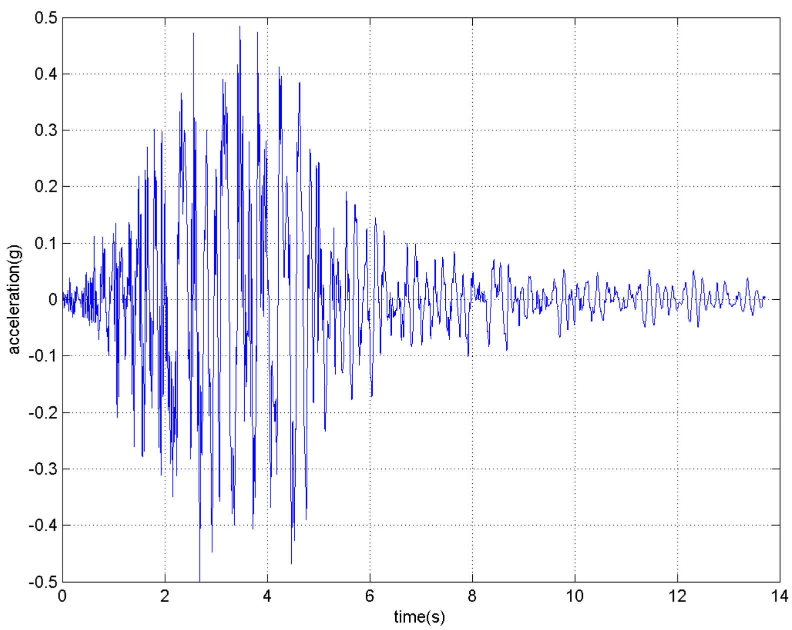

Figure 3-22, accelerogram Nocera Umbra (east-west) [SOFIE project, 2007]

3.7.1 Measuring equipment

The building movement was measured with a total of 265 instruments. The instruments are measuring:

- Acceleration per storey, the acceleration is measured with a 3D accelerometer on each floor level as indicated in Figure 3-24. On each storey eight 1D accelerometers are measuring the three coordinate directions separately. The accelerometers are installed to measure the buildings natural frequency.
- The interstorey drift is measured by displacement transducers as presented in Figure 3-23. For the horizontal drift between storeys six transducers are installed on levels 1 to 3 and 4 are installed on levels 4 to 7.
- Uplift is measured with 6 transducers at lower part of the floor and 4 transducers at the ceiling part of the floor. A picture of these transducers is found in Figure 3-25.
- vertical slip between vertical joints is measured with 4 transducers per storey
- horizontal slip between floor slab and walls is measured with 4 transducers per storey

Figure 3-23, transducers for interstorey drift [SOFIE project, 2007]

Figure 3-24, 3D accelerometer [SOFIE project, 2007]

Figure 3-25, transducer for measuring uplift [SOFIE project, 2007]

3.8 Results

3.8.1 Frequency

A total of 10 earthquake tests are carried out on the same building. Before the first earthquake loading, a step loading is applied to determine the first natural frequency. Before each next earthquake loading, the natural frequency was determined in this way. This was done because the change in frequency indicates the amount of damage occurred during the tests.

The frequency of the structure is obtained from step loading. The step loading is applied in two directions. After each earthquake test the step loading was 0.3g. The measured natural frequency from step loading before all tests is 2.3 Hz in x-direction (the short wall) and 3.5 Hz in y-direction (the long wall). The frequency is decreasing after each earthquake test, which indicates damage of the building (i.e. from 2.3 to 1.9 in x-direction). It is that concluded the building had performed very well. A diagram of the decrease in frequency is given in Figure 3-26. In the line for the x-direction some increases can be found. This increase is due to small repairs during the experiment.

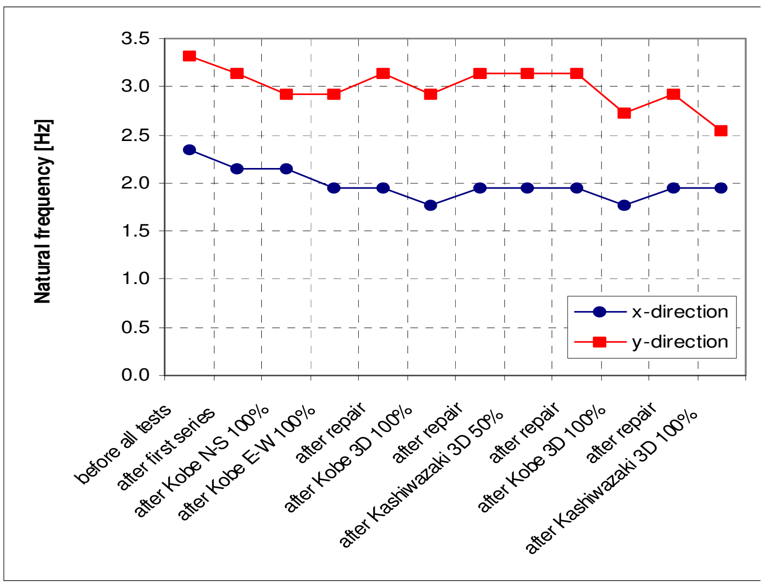

Figure 3-26, Diagram of frequency decrease

3.8.2 Interstorey drift

The critical displacements of the building the results for the interstorey drift are given here for the JMA Kobe earthquake.

Level	South wall	North wall	East wall	West wall
1	18.97	29.01	38.52	21.55
2	28.70	44.44	46.95	26.83
3	25.54	42.32	53.31	27.58
4	26.53	31.45	42.58	26.72
5	22.42	24.81	27.65	28.12
6	8.31	7.19	13.33	26.21
7	11.83	6.11	21.62	-
SUM	142.30	185.33	243.97	157.01

Table 3-6, JMA Kobe 3D 100%, interstorey drift maximum values[SOFIE project, 2007]

Level	South wall	North wall	East wall	West wall
1	-17.66	-25.19	-38.33	-21.92
2	-21.24	-32.43	-50.61	-39.10
3	-26.20	-28.26	-68.61	-53.67
4	-13.76	-20.41	-43.18	-44.90
5	-11.25	-17.68	-36.89	-45.21
6	-7.97	-8.72	-12.04	-16.88
7	-8.28	-5.06	-21.58	0
SUM	-106.35	-137.75	-271.24	-221.68

Table 3-7, JMA Kobe 3D 100%, interstorey drift minimum values [SOFIE project, 2007]

A diagram of the cumulative interstorey drift presents the shape of the building in x-direction (Figure 3-27) and y-direction (Figure 3-28)

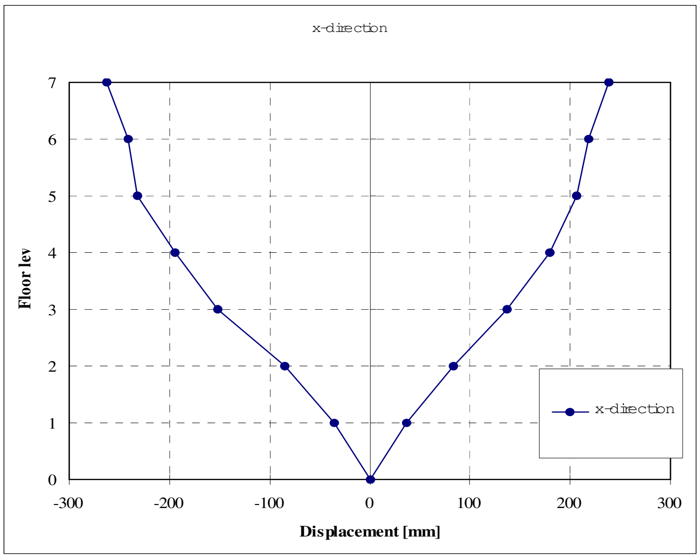

Figure 3-27, diagram of the maximum deformation of the building in x-direction

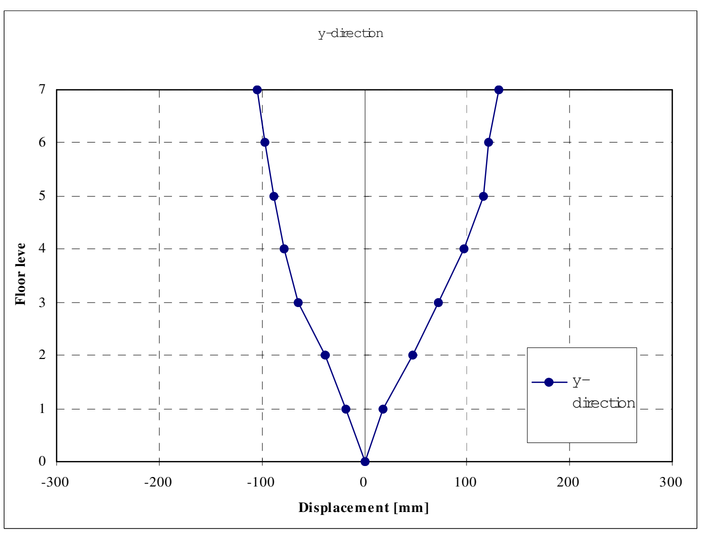

Figure 3-28, diagram of the maximum deformation of the building in y-direction

3.8.3 Uplift

Another important measurement is the uplift. The uplift resulting from the JMA Kobe earthquake is given in Table 3-8 and graphical cumulative in Figure 3-26.

Level		S-E corner	N-E corner	S-W corner	N-W corner
1	Bottom	5.87	13.19	4.88	4.96
	Top	3.21	3.32	4.16	4.54
2	Bottom	4.67	16.43	5.41	8.12
	Top	5.52	5.64	2.70	4.57
3	Bottom	4.17	10.25	4.22	9.32
	Top	4.58	2.23	2.65	4.25
4	Bottom	3.12	2.46	4.16	6.55
	Top	3.75	1.61	1.54	3.73
5	Bottom	2.37	1.49	2.15	5.10
	Top	1.89	0.90	1.27	1.37
6	Bottom	0.60	0.46	1.04	1.63

Table 3-8, JMA Kobe uplift in millimeters [SOFIE project, 2007]

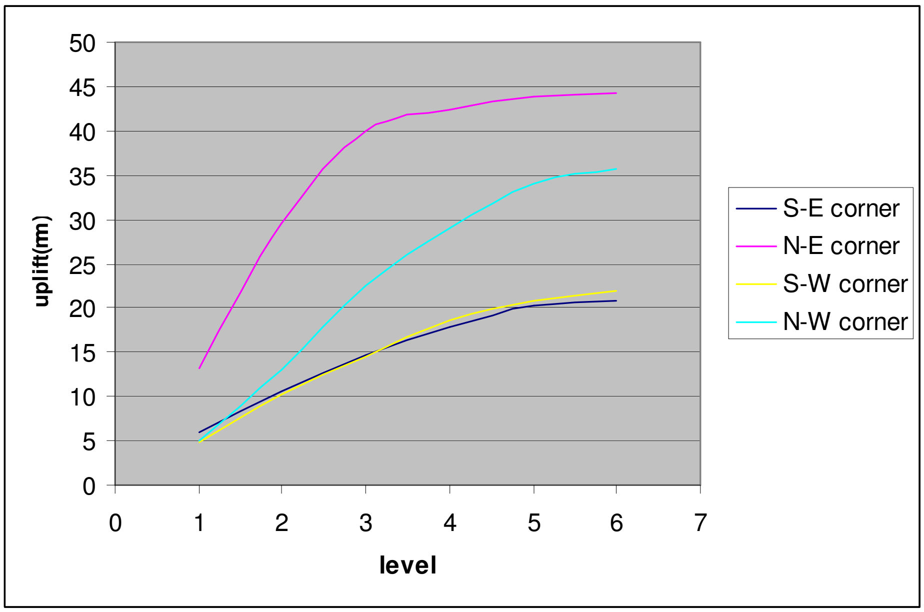

Figure 3-29, uplift in millimeters

The test outcomes confirmed the X-lam structures being earthquake resistant because no permanent deformations had taken place after the tests.

4 Estimating the building behaviour with calculations

4.1 Introduction

The experiment results showed good behaviour of the building under the applied earthquakes as is described in chapter 3. In this chapter the tested SOFIE building is checked with the. The forces from the earthquake can be calculated with the methods in EC8. The load bearing capacity of the structure is determined from EC5. In timber calculations according to EC5 material factors and modification are needed. Both factors are equal to 1 in special load combinations, which is the case for earthquakes. Next to check whether the building could resist the earthquake according to the European standard it is also a useful step in the process of designing a computer model. These calculations require good knowledge of the building that can be used in the computer model.

It is chosen to check the shear force capacity of the applied connections in the SOFIE project. The horizontal shear forces are transferred by the connections that consist of BMF steel angles. The holddowns are designed for vertical uplifting forces and it is assumed that these holddowns do not have significant contribution to the horizontal shear force capacity.
In EC8 methods for preliminary calculations are presented. In this thesis, the lateral force method is used to check the horizontal shear capacity of the connections in the structure.
The equation for the horizontal shear forces is: $F_b = S_d(T_1)m\lambda$.
Where:
Sd(T1) = the ordinate of the design spectrum

T1 = the fundamental period of vibration

m = the total mass of the building

λ = the correction factor

First some building and ground parameters are needed that are calculated in section 4.2 to 4.5. The lateral force method is applied in section 4.6.2. In sections 4.7.2 to 4.8, the capacity of the connections is calculated and checked with the results for the horizontal shear force obtained from the lateral force method. In 4.3 and 4.4 the natural frequency T1 is determined. In section 4.5 Sd(T1) is computed and λ, the correction factor is determined.

4.2 Masses

An important property of the building is the mass. Mass of the seven storey building exists out of mass of the wall panels and floor panel mass. Additional vertical load is applied to represent live load and finishing load. A calculation of the mass is found in Appendix A. In Table 4-1 an overview of the total vertical load per level is found.

Level	Mass wall panels (kN)	Mass floor panels(kN)	add mass(kN)	Total mass(kN)
0	212			287
1	215	75	294	584
2	197	75	294	566
3	197	75	294	566
4	163	75	294	532
5	128	75	294	497
6	61	75		136
total	1175	450	1470	3095

Table 4-1, masses of the structure [SOFIE project, 2007]

4.3 Calculation of the natural frequency with rules of thumb

In EC8 multiple ways of determining T1 are found. Two of them that are used in this section are rules on thumb.

The first rule on thumb is:

$T_1 = C_t H^{\frac{3}{4}}$ =0.05*23$^{3/4}$ =0.52s

Where

C_t is a factor dependent on the material of the structural system (C_t=0.05 for timber structures).

H is the height of the building.

The other rule on thumb is:

$$T_1 = 2\sqrt{d} = 2\sqrt{0.243} = 0.98s$$

With d= the lateral elastic displacement of the top of the building, due to gravity loads applied in horizontal direction.

The lateral *elastic* displacement is read from the output from the full scale earthquake test (see section 3.8.2). It is hard to determine whether the displacements in the test are still elastic or already plastic. The maximum displacement from the test is used here. Therefore, the estimation by the rule will be too high.

4.4 Calculation of the natural frequency with structural dynamics

As written before, it is allowable within EC8 to determine natural frequencies from dynamics. The methods used in this thesis are respectively:

- Standard mechanical formulas
- Lumped mass model
- Improved Rayleigh method

The standard mechanical formulas and the lumped mass model are applied on two extreme situations: the bending beam and the shear beam. The real SOFIE situation is somewhere in between these two. The third method, the improved Rayleigh method normally is used to calculate the first natural frequencies without testing. Because of the data of the SOFIE project that are available, it is possible to use the real data in the method and in this way a natural frequency is calculated.

For the calculation extreme situations are defined. A tree of the calculated models is given in Figure 4-1. A total of seven results are obtained for the natural frequency. The calculations of all methods are described in detail in Appendix B. Only results are given here.

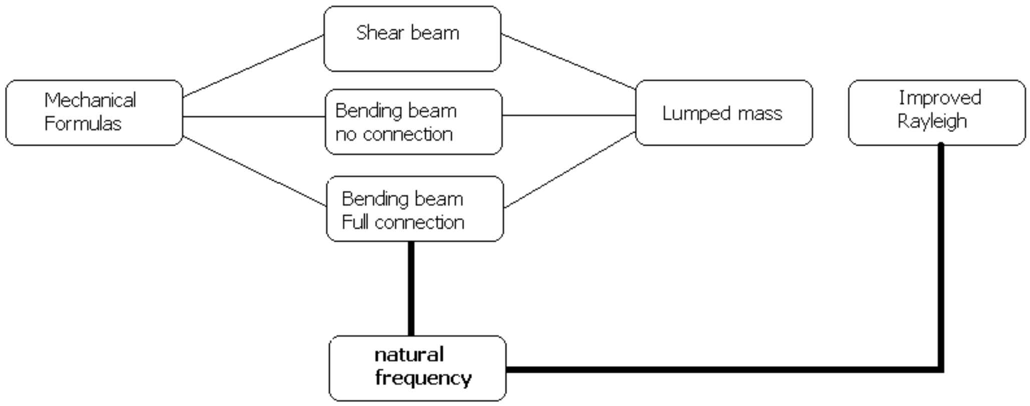

Figure 4-1, tree of calculated models

4.4.1 Standard mechanical formulas

Figure 4-2, bending and shear beam

For the calculation with the basic mechanical formulas, a distinction in two extreme response cases is needed. These extreme situations consist of a shear beam response (Figure 4-2 on the right) or a bending beam response (Figure 4-2 on the left).

The parameter E (modulus of elasticity) is needed. The modulus of elasticity perpendicular to the grain of the upper timber layer is 12000 N/mm^2. The shear modulus G is 60N/mm^2.[www.finnforest.com]

The complete calculations can be found in Appendix B. Results of each method are presented in this section. Results are presented in two different directions x and y. These directions can be found in Figure 2-8.

Shear beam

Shear stiffness in x-direction $k = \sum GA = \frac{2.42 \cdot 10^8}{6} = 0.4 \cdot 10^8 \, N / rad$

Shear stiffness in y-direction $k = \sum GA = \frac{6.12 \cdot 10^8}{6} = 1.02 \cdot 10^8 \, N / rad$

$$\left.\begin{array}{l} \omega_0 = \sqrt{\frac{k}{m}} \\ m = 3170 kN \\ k_y = 1.02 \cdot 10^8 \\ k_x = 0.4 \cdot 10^8 \end{array}\right\} \begin{array}{l} \omega_y = 5.67 \, rad / s \\ \omega_x = 3.57 \, rad / s \end{array}$$

Bending beam

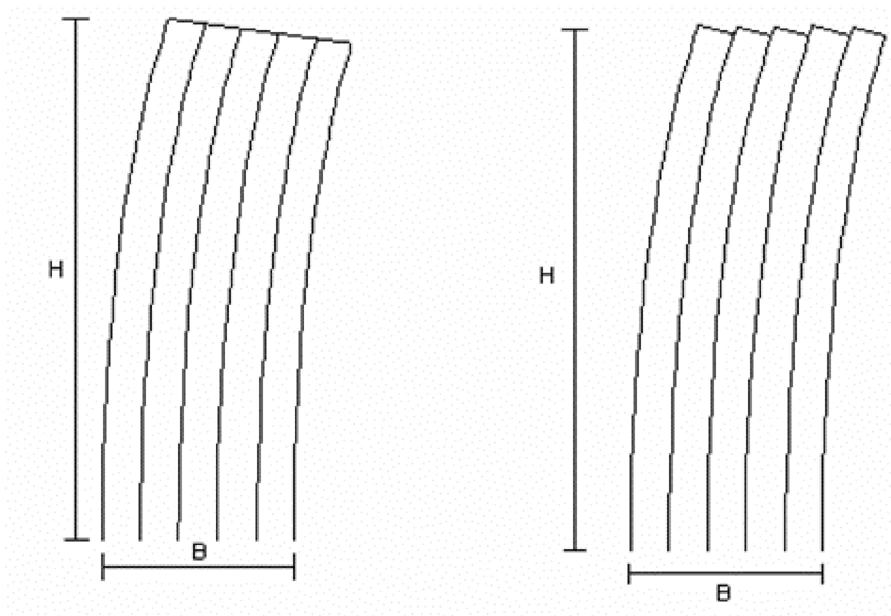

Figure 4-3, two situations for bending beam, left: full bending beam behaviour, right: mechanically jointed beam behaviour with joint slip

Full resistant vertical connections (Figure 4-3 left)

Applying the standard mechanical formula for a cantilevered bending beam:

$$k_y = \frac{6\sum EI}{H^2} = \frac{6*10000*1,03*10^{14}}{7*23500^2} = 1,59*10^9 \, N / rad$$

$$k_x = \frac{6\sum EI}{H^2} = \frac{6*10000*1,93*10^{13}}{7*23500^2} = 0,299*10^9 \, N / rad$$

$$\left.\begin{aligned} &\omega = \sqrt{\frac{k}{m}} \\ &\text{m=3170 kN} \\ &\text{k}_y = 1{,}59 * 10^9 \\ &\text{k}_x = 0{,}299 * 10^9 \end{aligned}\right\} \begin{aligned} &\omega_y = 22.4 rad/s \\ &\omega_x = 9.71 rad/s \end{aligned}$$

<u>Negligible vertical connections (Figure 4-3 right)</u>

$$k = \frac{6EI}{H^2} = \frac{6*10000*2{,}19*10^{12}}{7*23500^2} = 33{,}99*10^6\, N/rad$$

$$k = \frac{6EI}{H^2} = \frac{6*10000*1{,}13*10^{12}}{7*23500^2} = 20{,}46*10^6\, N/rad$$

$$\left.\begin{aligned} &\omega = \sqrt{\frac{k}{m}} \\ &\text{m=3170 kN} \\ &\text{k}_y = 33.99 * 10^6 \\ &\text{k}_x = 20.46 * 10^6 \end{aligned}\right\} \begin{aligned} &\omega_y = 3.27 rad/s \\ &\omega_x = 2.54 rad/s \end{aligned}$$

4.4.2 Calculation of the natural frequency with the lumped mass model

For the purpose of dynamic analysis, it is possible and preferable to treat inertial forces of a rigid body as if the mass and mass moment of inertia were concentrated at the centre of the mass. The lumped mass model that is created in this way is preferable, because the problem of the structure with an infinite number of degrees of freedom is transformed into a system with many degrees of freedom. For the lumped mass model some assumptions are needed [Structural Dynamics, theory and application, Paz and Leigh]:

- The total mass of the structure is concentrated at the floors
- The slabs or girders are infinitely rigid as compared to the columns
- The deformation of the structure is independent of the axial forces present in the columns

A lumped mass model can be created for which it is possible to set up equations in the form of: $F = m\ddot{u} + c\dot{u} + ku$.

The timber X-lam building consists of seven storeys; hence a 7 degree of freedom system can be set up. Equations of motion for an undamped multi-degree-of-freedom (MDOF) system can be obtained by omitting the damping matrix. $m\ddot{u} + ku = 0$. Assume the free vibration motion is expressed as $u(t) = u\sin(\omega t + \varphi)$. By filling in the free vibration mode into the equations of motion the following expression for the construction can be obtained:
$k - \omega^2 m = 0$.

With the theory of multiple degree of freedom systems, a matrix calculation can be found as in the Table 4-2.

$$
\begin{vmatrix}
m1 & 0 & 0 & 0 & 0 & 0 & 0 \\
0 & m2 & 0 & 0 & 0 & 0 & 0 \\
0 & 0 & m3 & 0 & 0 & 0 & 0 \\
0 & 0 & 0 & m4 & 0 & 0 & 0 \\
0 & 0 & 0 & 0 & m5 & 0 & 0 \\
0 & 0 & 0 & 0 & 0 & m6 & 0 \\
0 & 0 & 0 & 0 & 0 & 0 & m7
\end{vmatrix}
\begin{vmatrix}
\ddot{u}1 \\ \ddot{u}2 \\ \ddot{u}3 \\ \ddot{u}4 \\ \ddot{u}5 \\ \ddot{u}6 \\ \ddot{u}7
\end{vmatrix}
\qquad
\begin{vmatrix}
k1+k2 & (-k2) & 0 & 0 & 0 & 0 & 0 \\
(-k1) & k2+k3 & (-k3) & 0 & 0 & 0 & 0 \\
0 & (-k3) & k3+k4 & (-k4) & 0 & 0 & 0 \\
0 & 0 & (-k4) & k4+k5 & (-k5) & 0 & 0 \\
0 & 0 & 0 & (-k5) & k5+k6 & (-k6) & 0 \\
0 & 0 & 0 & 0 & (-k6) & k6+7 & (-k7) \\
0 & 0 & 0 & 0 & 0 & (-k7) & k7
\end{vmatrix}
\begin{vmatrix}
u1 \\ u2 \\ u3 \\ u4 \\ u5 \\ u6 \\ u7
\end{vmatrix}
$$

Table 4-2, mass matrix and stiffness matrix

Again the same distinction for the shear beam and bending beam are used as in the section on standard mechanical formulas.

Shear beam

By using Maple, eigenvalues can be found (Table 4-3). The first eigenvalue is corresponding to the eigen frequency.

	Y direction	Frequency(Hz)	X direction	Frequency (Hz)
Ω1	3.33	0.52	2.14	0.34

Table 4-3, outcome for the lumped mass shear beam

Bending beam

Negligible vertical connections

With the properties of the panels, the stiffness of the wall panels is calculated. From these stiffness values of the walls, the stiffness per direction per floor level can be calculated (Table 4-4). These values are used to construct the stiffness matrix. The complete construction of the stiffness matrix can be found in Appendix B.

	x-direction	y-direction
level0	2.61E+09	4.03E+09
level1	2.74E+09	4.30E+09
level2	1.80E+09	2.83E+09
level3	1.80E+09	2.83E+09
level4	1.03E+09	2.04E+09
level5	1.03E+09	1.12E+09
level6	1.04E+08	2.74E+08

Table 4-4, stiffness per level per direction

By using Maple eigenvalues can be found. The first eigenvalue is corresponding to the eigen frequency.

	Y direction	Frequency(Hz)	X direction	Frequency (Hz)
Ω1	17.74	2.82	14.02	2.23

Table 4-5, outcome for the lumped mass bending beam with negligible connections

Full resisting vertical connections

Because of the high stiffness of the outer walls, modelled as full bending beam, the inner walls are not taken into account.

	x-direction	y-direction
level0	3.70E+10	1.98E+11
level1	3.70E+10	1.98E+11
level2	3.25E+10	1.74E+11
level3	3.25E+10	1.74E+11
level4	2.21E+10	1.19E+11
level5	2.21E+10	1.19E+11
level6	2.21E+10	1.19E+11

Table 4-6, stiffness per level per direction

With the theory of MDOF systems a stiffness and mass matrix can be established and with Maple the eigenvalues and vectors are determined.

	Y direction	Frequency(hZ)	X direction	Frequency (hZ)
Ω1	57.97	9.22	55.08	8.76

Table 4-7, outcome for the lumped mass bending beam with full connections

4.4.3 Vibration analysis by Rayleigh's method

[Dynamics of structures, Clough and Penzien, 1993]

The theory, an example and application of the method to the SOFIE building are found in Appendix B.

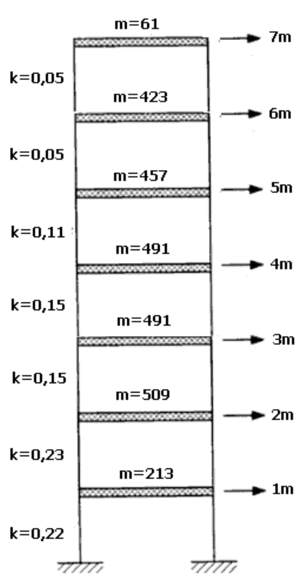

Figure 4-4, the Rayleigh starting point for the SOFIE structure

Assumed shape(mm)	Mass(kN)	Cumulative mass(kN)	Stiffness*1e9(N/mm)	mass* assumed shape	Total deflection (mm)
1	287	3168	0.22	14666.67	14666.67
2	584	2881	0.23	24836.21	39502.87
3	566	2297	0.15	45039.22	84542.09
4	566	1731	0.15	45254.90	129796.99
5	532	1165	0.11	53440.37	183237.36
6	497	633	0.05	75207.92	258445.28
7	136	136	0.05	18851.49	277296.76

Table 4-8, output of the Rayleigh method

In the last column Ψ can be found with its transpose being:

$$\psi^T = [14666, 39502, 84542, 129796, 183237, 258445, 277296]$$

$$\omega^2 = \frac{\psi_0^T M \psi_0}{\psi_1^T M \psi_0}$$

→ The natural frequency is calculated as 0,0053√(k/m)=5.3 rad/s.

4.4.4 Summary calculated frequencies

The different methods used for calculating the natural frequencies of the seven storey building can be checked with the frequency measured after the step loading in the test (see section). These values are found in the last two columns in Table 4-9.

Method		Natural frequency f (y)	Natural frequency f (x)	Natural period (y)	Natural period (x)	Period in test (y)	Period in test (x)
Mechanical formulas	Shear beam (1)	0.90	0.56	1.11	1.79	0.29	0.43
	Bending beam (2)	0.52	0.40	1.92	2.50		
	Bending beam (3)	3.56	1.54	0.28	0.65		
Lumped mass	Shear beam (4)	0.52	0.34	1.92	2.94		
	Bending beam (5)	2.82	2.23	0.35	0.45		
	Bending beam (6)	9.22	8.76	0.11	0.11		
Improved Rayleigh (7)		5.9		0.17			
Method 1 EC8 (8)				0.52	0.52		
Method 2 EC8 (9)				0.98	0.98		

Table 4-9, feedback table

Standard mechanical formulas can be used for estimating the beam behaviour. With the lumped mass model for a bending beam with negligible connections between the walls in plane the natural frequency obtained from the experiment is closely approximated. Although the improved Rayleigh method seems a promising method, it is a laborious method with a not very accurate outcome.

4.5 Calculation of the design spectrum

The seismic response of the ground, Sd(T), is defined in EC8 by the following diagrams a, b, c, d and e. The line that has to be chosen is dependent on the type of ground.

Ground type	S	T_B (s)	T_C (s)	T_D (s)
A	1,0	0,05	0,25	1,2
B	1,35	0,05	0,25	1,2
C	1,5	0,10	0,25	1,2
D	1,8	0,10	0,30	1,2
E	1,6	0,05	0,25	1,2

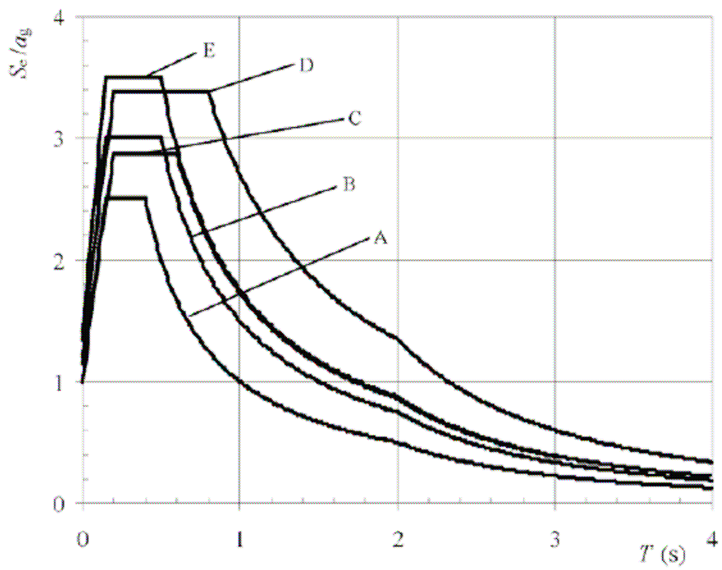

Figure 4-5, design spectrum [Eurocode 8]

The diagram is a graphical representation of the equations in Figure 4-6. With the natural periods are obtained in section 4.3 and 4.4 the variable $S_d(T)$ can be obtained. This variable is needed for calculating the shear forces in the building.

a) $0 \le T \le T_B : S_d(T) = a_g S \left[\frac{2}{3} + \frac{T}{T_B} \left(\frac{2,5}{q} - \frac{2}{3} \right) \right]$

b) $T_B \le T \le T_C : S_d(T) = a_g S \frac{2,5}{q}$

c) $T_C \le T \le T_D : S_d(T) \begin{cases} a_g S \frac{2,5}{q} \left[\frac{T_C}{T} \right] \\ \ge \beta a_g \end{cases}$

d) $T_D \le T : S_d(T) \begin{cases} a_g S \frac{2,5}{q} \left[\frac{T_C T_D}{T^2} \right] \\ \ge \beta a_g \end{cases}$

Figure 4-6

Almost every time the criteria for equation c are satisfied $T_c \le T \le T_d$; equation b is valid for the calculations 6 and 7. Equation c is valid for calculations 1,3,5,8 and 9. Equation d fits to cases 2 and 4

T is the vibration period of a linear single-degree-of-freedom system;
a_g is the design ground acceleration on type A ground ($a_g = \gamma_1 a_{gR}$);
T_C is the upper limit of the period of the constant spectral acceleration branch;
of the spectrum;
S is the soil factor;
S_d (T) is the design spectrum;
q is the behaviour factor ;
β is the lower bound factor for the horizontal design spectrum.

Most of the parameters in the equation are dependent on the soil type. The soil type in the SOFIE project can be taken equal to 1 (rock or rock-like material in EC8). This is because of the fact that the building is tested on a steel base, hence a very stiff and good base. The other parameters:
Ag=design ground acceleration. The analysis of the SOFIE building is done for the Kobe earthquake with a ground acceleration of 0.82g, which is the design ground acceleration.
T; in sections 4.3 and 4.4 natural frequencies are determined.
Tb=0.1
Tc=0.25
Td=1.2
Q (behaviour factor) = 2 for glued timber wall panels
Following the code, the recommended value for the factor β is 0.2.

The equations in the Eurocode 8 for the design spectrum are varying for different natural frequencies. The lowest frequency fitting the conditions is used for calculating the different equations as this gives the largest shear forces.

Equation b

$$T_B \le T \le T_C : S_d(T) = a_g S \frac{2,5}{q} = 1.02$$

Equation c

$$T_C \leq T \leq T_D : S_d(T) \begin{cases} a_g S \dfrac{2,5}{q}\left[\dfrac{T_C}{T}\right] \\ \geq \beta a_g \end{cases} = \begin{cases} 0.82 \cdot 1 \cdot \dfrac{2,5}{2}\left[\dfrac{0.25}{0.28}\right] = 0.91 \\ \geq 0.2 \cdot 0.82 = 0.164 \end{cases}$$

Equation d

$$T_D \leq T : S_d(T) \begin{cases} a_g S \dfrac{2,5}{q}\left[\dfrac{T_C T_D}{T^2}\right] \\ \geq \beta a_g \end{cases} = \begin{cases} 0.82 \cdot 1 \cdot \dfrac{2,5}{2}\left[\dfrac{0.25 \cdot 1.2}{1.92^2}\right] = 0.08 \\ \geq 0.2 \cdot 0.82 = 0.164 \end{cases}$$

Correction factor

The value for the correction factor λ is equal to: λ = 0,85 if T1 < 2 TC and the building has more than two storeys. The SOFIE structure satisfies these conditions.

4.6 Calculation of shear forces and connection check

4.6.1 Introduction

In the European standard (EC8) different methods are available to determine the structural forces in buildings to make earthquake resistance possible. These methods are:

Linear:
- The lateral force method
- The modal response analysis

Non linear:
- Non-linear static pushover
- Non linear time history analysis

In the calculation on the building the lateral force method will be used in this report. First the method and the parameters in the seismic shear force calculation are commented. The lateral force calculations can be found section 4.6.2. In section 4.7.1, the capacity of the shear force connectors is determined and the connections are checked with the lateral forces computed.

4.6.2 Lateral force method

The seismic base shear force F, for each horizontal direction in which the building is analysed, is determined in the European standard:

$$F_b = S_d(T_1) m \lambda$$

Where:
- Sd (T1) is the ordinate of the design spectrum at period T1..
- T1 is the fundamental period of vibration of the building for lateral motion in the direction considered. In Eurocode 8 methods are given to determine T1.
- m is the total mass of the building.
- λ is the correction factor, the value of which is equal to: λ = 0,85 if T1 < 2 TC and the building has more than two storeys, or λ = 1,0 otherwise.

In other words the design shear force value is specified as a function of the design weight, the fundamental period, the seismic site parameters and the type of lateral load resistance.

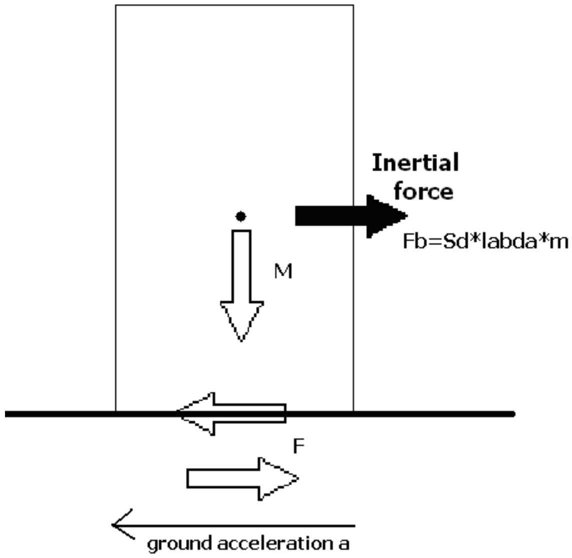

Figure 4-7, shear force presentation [Shodek, 2001]

The general equation for horizontal shear forces, $F_b = S_d(T_1)m\lambda$, can be used to calculate the base shear force as well as for the shear forces on each level (Figure 4-7). The largest seismic response factor calculated in section is used to determine shear forces. According to the equation the shear force on each level is linearly dependent to the supported mass. The shear force on each floor can be found with the method in EC8:

$$F_i = F_b g \frac{s_i g m_i}{\sum s_i g m_i}$$

where

F_i = horizontal force acting on storey i

F_b = the seismic base shear

s_i,s_j = the displacements of the masses m_i,m_j in the fundamental mode shape

m_i,m_j = storey masses

Shear forces are presented in Table 4-10. The calculation is done with an excel sheet which can be found in Appendix B.

Level	Mass(kN)	Cumulative mass (kN)	Shear force m(kN)
0	287	3170	2748
1	584	2883	2499
2	566	2299	1993
3	566	1733	1502
4	532	1167	1011
5	497	635	550
6	136	136	117
total	3170		

Table 4-10, shear forces

4.7 Shear force capacity of the connections

4.7.1 Checking the steel of the connector

With the dimensions of the steel according to figure the capacity of the connections is calculated.

Special holddown (Vertical forces)	Simpson HTT22 (Vertical forces)	BMF 7116 (horizontal forces)	BMF 7105 (horizontal forces)
w=80mm t=6mm $f_{y,k}$=360N/mm^2 F_{max}=80g6g360kN	w=70mm t=5.07mm $f_{y,k}$=360N/mm^2 F_{max}=70g5.07g360=126kN	w=116mm t=3mm $f_{y,k}$=360N/mm^2 F_{max}=116g3g360=125kN	w=80mm t=3mm $f_{y,k}$=360N/mm^2 F_{max}=80g3g360=86kN

Table 4-11, dimensions of the steel connectors [SOFIE project, 2007]

4.7.2 Checking fasteners in the connection

The number and type of nails used for the different type of connectors is summarized in Table 4-12. In the calculations it is assumed the failure of the connection will be in horizontal fasteners.

Connection	Fasteners for horizontal connection	Fasteners for vertical connection
Shear connection BMF 7116	11 angular ringed shank nails (4x 60)	M12 bolt
Shear connection BMF 7105	8 angular ringed shank nails (4x 60)	8 angular ringed shank nails (4x 60)
Simpson HTT22 Holddown	12 annular ringed shank nails diameter 4	Threaded rod trough floor
Custom made holddown	30 lagged screws diameter 6	Bolt trough floor

Table 4-12, overview of the used connections and applied fasteners[SOFIE project, 2007]

4.7.3 Failure for fasteners

The screws applied in the custom made holddown have a diameter of 6mm. For screws with a diameter < 8mm, the rules for nails may be applied in the EC5. The connection is approached as a thick steel plate to timber connection. Johansen defined two possible failure modes according to Figure 4-8 .

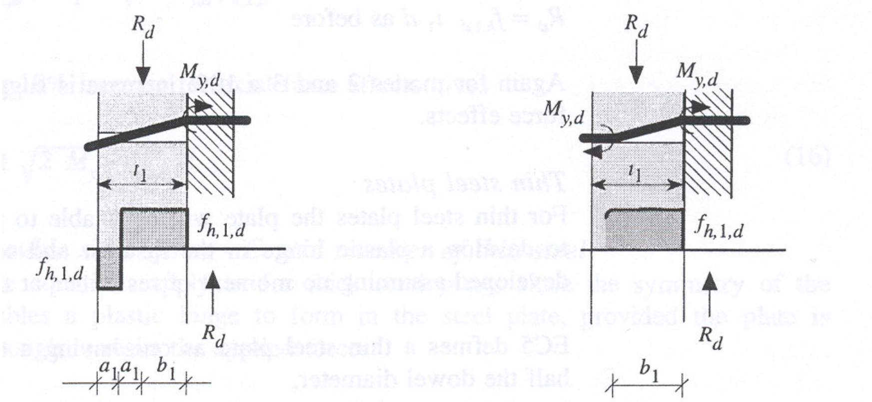

Figure 4-8, Johansen failure modes for screws. Failure mode 2 left and failure mode 3 right [Step 1, 1995]

Failure mode 2

$$R_d = f_{h,1,d} d t_1 \left[\sqrt{2 + \frac{4 M_{y,d}}{f_{h,1,d} d t_1^{\ 2}}} - 1 \right]$$

Failure mode 3

$$R_d = 1{,}4 \sqrt{2 M_{y,d} f_{h,1,d} d}$$

The embedding is calculated with the formula for non predrilled nails. In earthquake design the material factor and the modification factor are 1 since earthquakes are a special load case.

$$f_{h,k} = 0{,}082 \rho_k d^{-0{,}3} = 0{,}082 * 360 * 6^{-0{,}3} = 17.25 N/mm^2$$

$$f_{h,1,d} = \frac{k_{\text{mod}} f_{h,k}}{y_m} = \frac{1 \cdot 17.25}{1} = 17.25 N/mm^2$$

$$M_{y,d} = \frac{k_{\text{mod}} 180 d^{2,6}}{\gamma_m} = 18987 Nmm$$

With this value for f, the design resistance can be calculated for both failure modes 2 and 3.

$$R_{2,d} = 17.25 * 6 * 60 \left[\sqrt{2 + \frac{4 * 18987}{17.25 * 6 * 60^2}} - 1 \right] = 3008 N$$

In this calculation the value for t is taken as 60.

$$R_{3,d} = 1{,}4 \sqrt{2 M_{y,d} f_{h,1,d} d} = 1{,}4 \sqrt{2 * 18987 * 17.25 * 4} = 2266 N$$

Failure mode 3 is governing for the failure of the nail.

The maximum vertical force capacity for the holddown is then $R_d = n \cdot R_{3,d} = 67 kN$

4.7.4 Failure for 4 mm nails

The nails applied in the BMF steel angles have a diameter of 4mm. The connections BMF7116 and BMF7105 are approached as a thick steel plate to timber connection. The same failure modes are applicable as for the screws in the section above.

The embedding strength for a nail can be calculated with the formula for non predrilled nails. Again the material factor and the modification factor are equal to 1.

$$f_{h,k} = 0{,}082\rho_k d^{-0,3} = 0{,}082 * 360 * 4^{-0,3} = 20{,}55 N/mm^2$$

$$f_{h,1,d} = \frac{k_{\text{mod}} f_{h,k}}{y_m} = \frac{1 * 20{,}55}{1} = 20{,}55 N/mm^2$$

$$M_{y,d} = \frac{k_{\text{mod}} 180 d^{2,6}}{\gamma_m} = 6616 Nmm$$

With this value for f, the design resistance can be calculated for both failure modes 2 and 3.

$$R_{2,d} = 20.55 * 4 * 60 \left[\sqrt{2 + \frac{4 * 6616}{20.55 * 4 * 60^2}} - 1 \right] = 2197 N$$

In this calculation the value for t is taken as 60, the length of the nail because the width of the panel is larger than the length of the nail.

$$R_{3,d} = 1{,}4\sqrt{2 M_{y,d} f_{h,1,d} d} = 1{,}4\sqrt{2 * 6616 * 20.55 * 4} = 1460 N$$

Failure mode 3 is governing for the failure of the nail.

The maximum horizontal shear force capacity for the BMF steel angles is then:
BMF7116=16kN
BMF7105=11kN

4.8 Checking shear force capacity

With the capacity known the connections can be checked with the horizontal forces determined in section 4.6. This comparison is done in the diagram below (Figure 4-9).

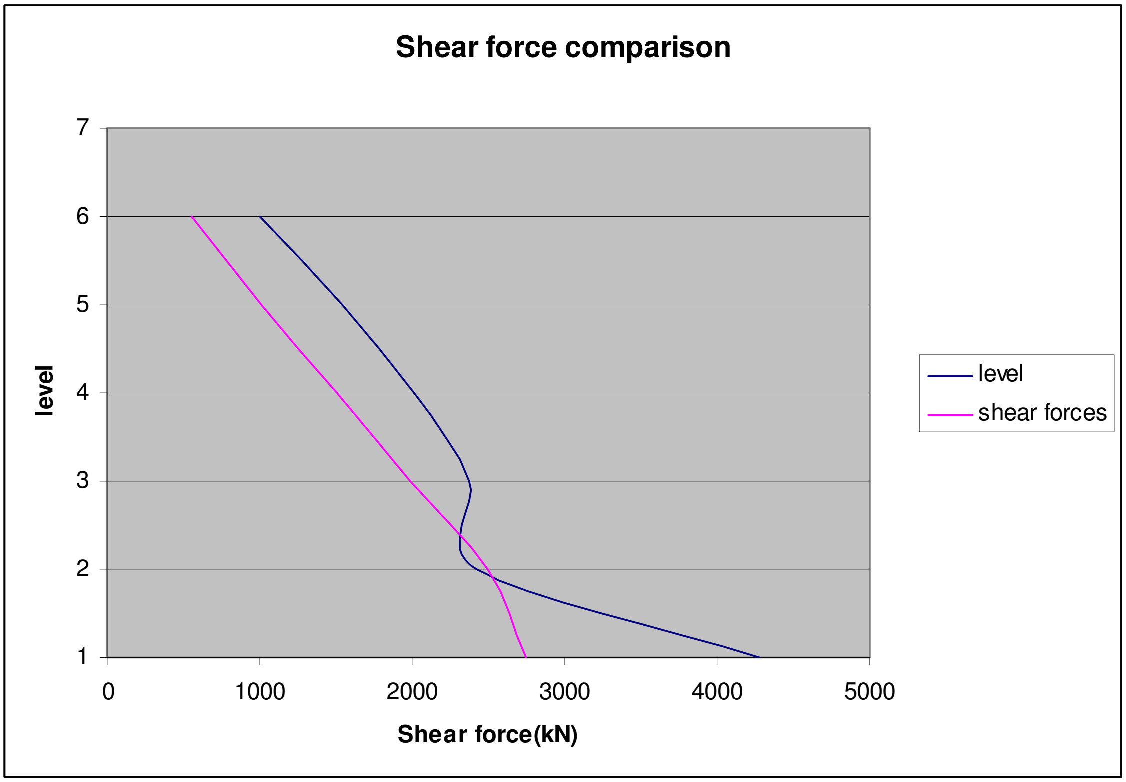

Figure 4-9, graphical check of shear force capacity

It can be concluded that the shear force capacity of the shear connectors is not sufficient for resisting the shear forces. It is concluded that the other connections and fasteners present (please refer to the publications in SOFIE) contribute to the shear force capacity of the building.

5 Panel-to-panel in-plane connection experiment

5.1 Introduction

As indicated earlier in this report, the properties of the kerto-Q laminated Veneer Lumber panel-to-panel connection are unknown. This wall connection is frequently applied in the SOFIE building. Therefore, more research on this connection is advised for a better understanding of the building behaviour and a better computer model. Within the scope of this thesis, an experiment on a downscaled specimen of the wall to wall connection is done, which is described in this chapter. The total experiment consists of ramp tests and cyclic tests according to EN12512 as will be commented in this chapter. In section 5.2 and 5.3, a description of the connection is found. Design calculations according to Johansen are computed in section 5.4. The test set-up for the ramp test is treated in section 5.5 and the results for the ramp test can be found in section 0.In the results section, some adjustments in the test setup in favour of the cyclic test are discussed also. Section 5.7 is about the cyclic test and finally, the conclusions of the total experiment are written in section 5.8

5.2 Screws

The connection between the walls has been designed using Rothoblaas screws at a spacing of 150 mm. The load carrying capacity can be theoretically derived using Johansen's equations. In section 5.3 more information about the layout of the connection is given. The Johansen failure mode for the applied screws is determined in section 5.4. The screws are 8x100 self tapping screws, steel quality $F_{u,k}$ = 1000MPa. Dimenions are according to Figure 5-1 and Table 5-1.

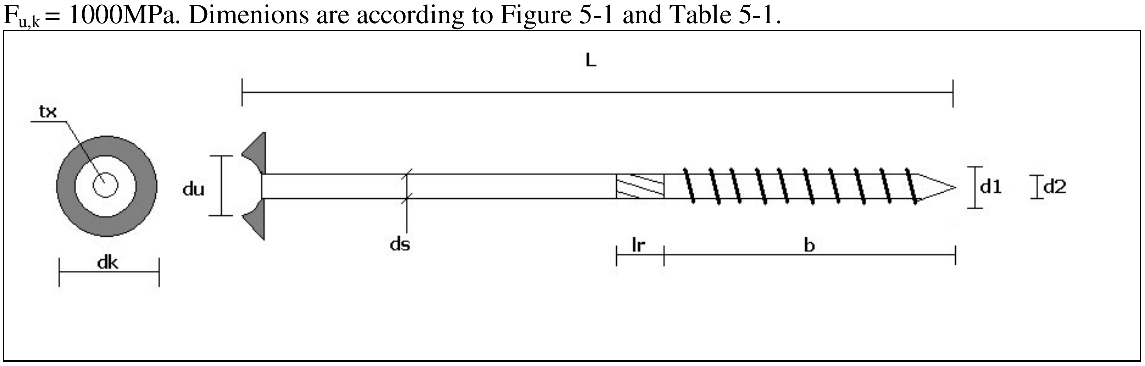

Figure 5-1, Screw applied in wall to wall connections [www.rothoblaas.com]

Rothoblaas 8x100 self tapping screw		
Var.	Name	Value(mm)
d1	Outer thread diameter	8
d2	Core diameter	5.4
b	Thread length	52
L	Total length	100
ds	Shank diameter	5.85
du	Head diameter	15
dk	Washer diameter	25
tx	Insert length	40
lr	Length, cutter	12

Table 5-1 Screw properties [www.rothoblaas.com]

5.3 The connection

In Figure 5-2, a picture and a drawing of the connection is given.

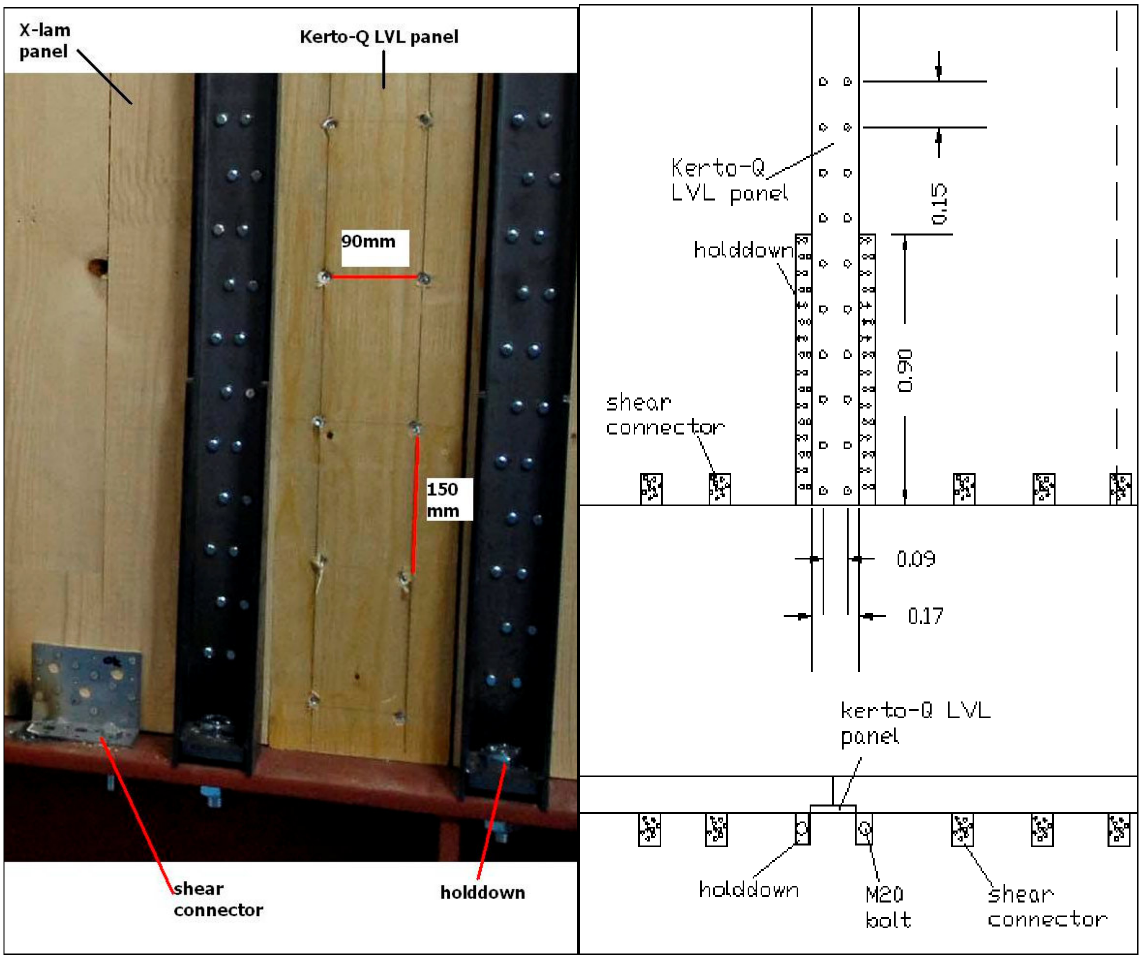

Figure 5-2, picture of holddowns and shear connectors surrounding the kerto-Q connection [SOFIE project, 2007]

The horizontal connection between X-lam panels consists of a kerto-Q LVL panel strip. Laminated Veneer Lumber (LVL), in Europe is produced within a defined production process. After heating in hot water, the panels are made by gluing rotary peeled veneers from spruce into continuous panels. The veneers (typical thickness of about 3 to 4 mm) are graded in density. The glue applied is phenol formaldehyde adhesive. After applying the glue, the veneers are pressed together mechanically or under vacuum at a temperature of about 150 degrees Celsius. In Kerto-Q LVL, every fifth veneer is laid perpendicular to the underlying mat. The structure of the Kerto-Q improves the panel's lateral bending strength and stiffness. The cross veneers improve the ductility of the product and prevent cracking when used as a beam. There is also an essential reduction in moisture-dependent variations across the width of the panel. [finnforest.com]

The Kerto-Q LVL panel is placed in a slot and is fastened with self drilling screws. The self drilling screws have a diameter of 8 mm. A picture of the connection as it is found in the building is given in Figure 5-2.

5.4 Johansen equations and checking

The failure load is determined with Johansen failure modes. 8mm screws in the wall to wall connection are loaded in single shear. Single shear timber-to-timber Johansen failure modes are graphically represented in Figure 5-3 accompanied with the equations for the ultimate load capacity $F_{v,Rk}$ in Figure 5-4.

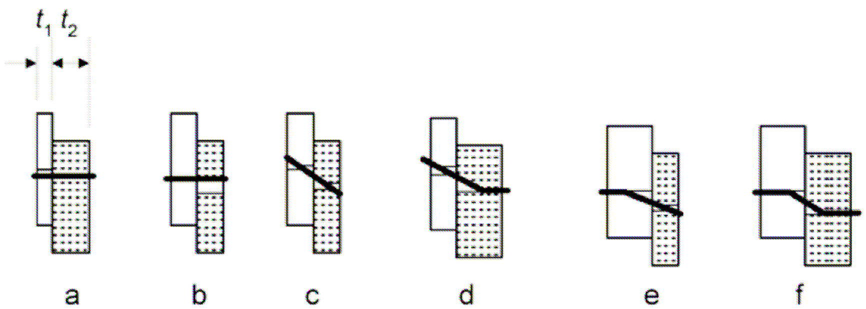

Figure 5-3, Johansen failure modes [Step 1, 2001]

$$
F_{v,Rk} = \min \begin{cases}
f_{h,1,k} t_1 d & \text{(a)} \\
f_{h,2,k} t_2 d & \text{(b)} \\
\dfrac{f_{h,1,k} t_1 d}{1+\beta}\left[\sqrt{\beta + 2\beta^2\left[1+\dfrac{t_2}{t_1}+\left(\dfrac{t_2}{t_1}\right)^2\right]+\beta^3\left(\dfrac{t_2}{t_1}\right)^2} - \beta\left(1+\dfrac{t_2}{t_1}\right)\right] + \dfrac{F_{ax,Rk}}{4} & \text{(c)} \\
1,05\,\dfrac{f_{h,1,k} t_1 d}{2+\beta}\left[\sqrt{2\beta(1+\beta)+\dfrac{4\beta(2+\beta)M_{y,Rk}}{f_{h,1,k}\, d\, t_1^2}} - \beta\right] + \dfrac{F_{ax,Rk}}{4} & \text{(d)} \\
1,05\,\dfrac{f_{h,1,k} t_2 d}{1+2\beta}\left[\sqrt{2\beta^2(1+\beta)+\dfrac{4\beta(1+2\beta)M_{y,Rk}}{f_{h,1,k}\, d\, t_2^2}} - \beta\right] + \dfrac{F_{ax,Rk}}{4} & \text{(e)} \\
1,15\sqrt{\dfrac{2\beta}{1+\beta}}\sqrt{2M_{y,Rk} f_{h,1,k} d} + \dfrac{F_{ax,Rk}}{4} & \text{(f)}
\end{cases}
$$

Figure 5-4, single shear timber-to-timber failure equations

$F_{V,Rk}$ is the characteristic load-carrying capacity

t is the timber board thickness

$f_{h,i,k}$ is the characteristic embedment strength

d is the fastener diameter

$M_{y,Rk}$ is the characteristic fastener yield moment

β is the ratio between the embedment strength of the members

$F_{ax,Rk}$ is the chracteristic axial withdrawal capacity

of the fastener. $F_{ax,Rk}$ is unknown is should be taken as zero

In the equations, two expressions need more explanation ($f_{y,k}$, $M_{y,k}$). Factor f is representing the embedment strength:

. $f_{h,1,d} = 0.082(1-0.01d_{eff})\frac{\rho_k k_{\mathrm{mod}}}{\gamma_m}$ In earthquake design the factors k_{mod} and γ_m are neglected (i.e. taken equal to 1). M_y is the yield moment of the fastener: $M_{y,d} = 0.3 f_u d_{eff}^{2.6}$.

Equations in figure are calculated for the connection and the minimum characteristic load capacity indicates the governing failure mode.

Embedding strength of the X-lam:

$$f_{h,1,k} = 0.082(1-0.054)500 = 38.78N/mm^2$$

The Kerto-Q timber embedding strength:

$$f_{h,1,k} = 0.082(1-0.054)530 = 41.11N/mm^2$$

The β-factor:

$$\beta = \frac{f_{h,2,k}}{f_{h,1,k}} = 1.06$$

$$M_{y,k} = 0.3 f_{u,k} d_{eff}^{2.6} = 0.3 g 1000 g 5.4^{2.6} = 24062Nmm$$

In the calculation, a thickness t1 and t2 are needed. T1=27mm (thickness of the Kerto-Q LVL panel) and t2=73mm(the total length of the screw is 100mm).

$$a = f_{h,1,k} t_1 d = 5654Nmm$$

$$b = f_{h,2,k} t_2 d = 16205Nmm$$

$$c = \frac{f_{h,1,k} t_1 d}{1+\beta}\left[\sqrt{\beta + 2\beta^2\left[1+\frac{t_2}{t_1}+\left(\frac{t_2}{t_1}\right)^2\right]+\beta^3\left(\frac{t_2}{t_1}\right)^2} - \beta\left(1+\frac{t_2}{t_1}\right)\right] = 5121N$$

$$d = 1.05\frac{f_{h,1,k} t_1 d}{2+\beta}\left[\sqrt{2\beta(1+\beta)+\frac{4\beta(2+\beta)M_{y,Rk}}{f_{h,1,k} d t_1^2}} - \beta\right] = 2831N$$

$$e = 1.05\frac{f_{h,1,k} t_2 d}{1+2\beta}\left[\sqrt{2\beta^2(1+\beta)+\frac{4\beta(1+2\beta)M_{y,Rk}}{f_{h,1,k} d t_2^2}} - \beta\right] = 5854N$$

$$f = 1.15\sqrt{\frac{2\beta}{1+\beta}}\sqrt{2M_{y,Rk} f_{h,1,k} d} = 3649N$$

The governing Johansen failure mode for the wall to wall connection is mode d with a load carrying capacity of 2831N per screw.

5.5 Test set-up

5.5.1 The location and loading instrument

The test set-up consists of a 250 kN pressure jack of the Delft University of Technology. A picture of the test bank and the test specimen is given in Figure 5-5. The set-up consists of a upper traverse (1), the specimen (2),the pressure jack (3) and a PC (4). In the picture, the specimen is not in the test position. In the current position, the specimen is suspended on the top traverse, which is vertically movable. This is used to get the specimen in the test position. The hydraulic of the jack is arranged by oil pressure and is controlled by a pc (left in Figure 5-5). The control software used is designed by an employee of Delft University of Technology and is installed under Windows.

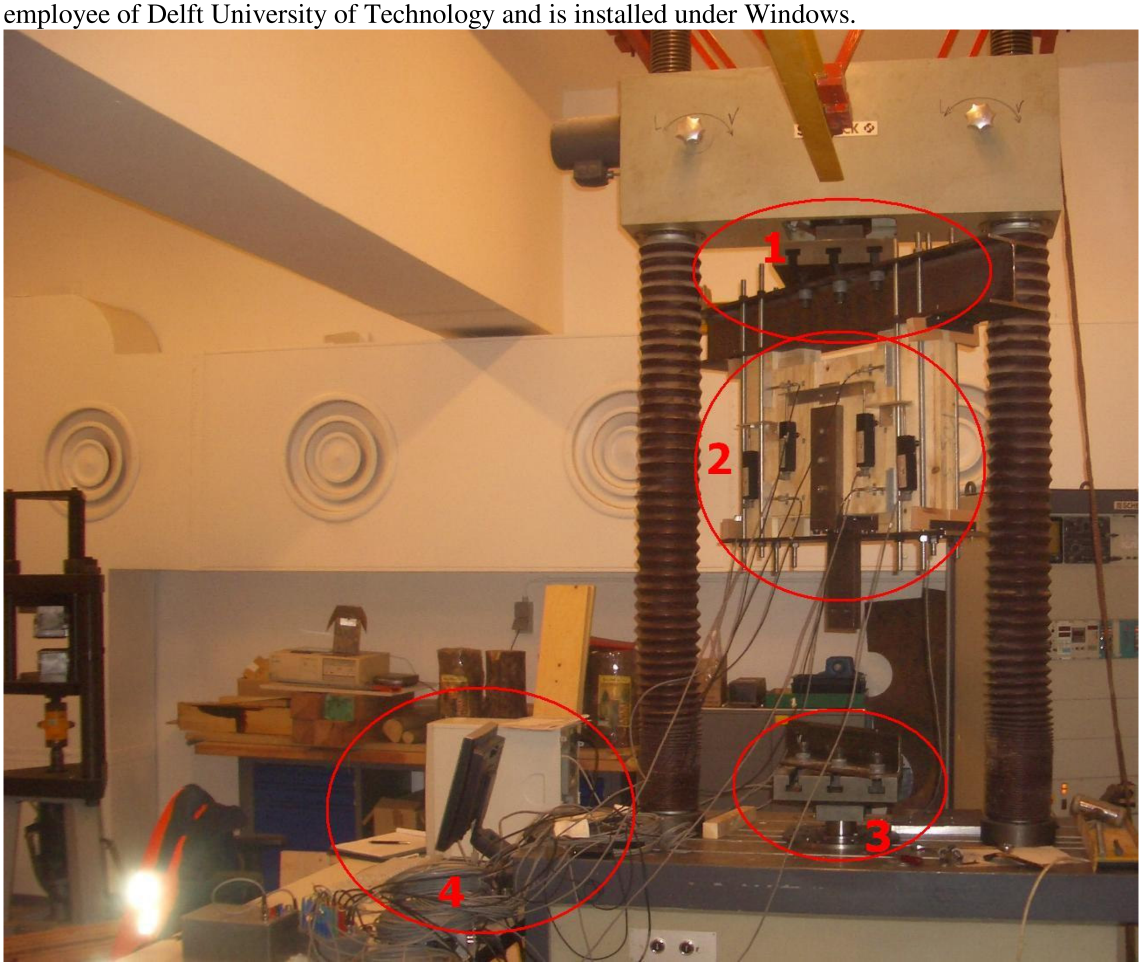

Figure 5-5, Picture of the test set-up for the experiment

5.5.2 Specimen

In the real situation, the movement is vertical, but induced by horizontal loading. The available test bank is capable of vertical loading. The loading in the test is therefore vertical, induced by vertical forces. It is assumed that no deviation will occur with the vertical setup of the test. The dimensions of the test specimen are minimized for saving timber material and to be suitable for the test bank. To anticipate on a complex test setup, the specimen is symmetrical. The X-lam panels used are three layered and five layered panels. Three screws in a row are applied on both sides of the LVL strip. Edge distances are taken in accordance with Eurocode 5. The specimen has dimensions according to Figure 5-6. The thickness of the LVL is 27mm while the thickness of the wall panel is 95 mm and 50 mm below the LVL strip

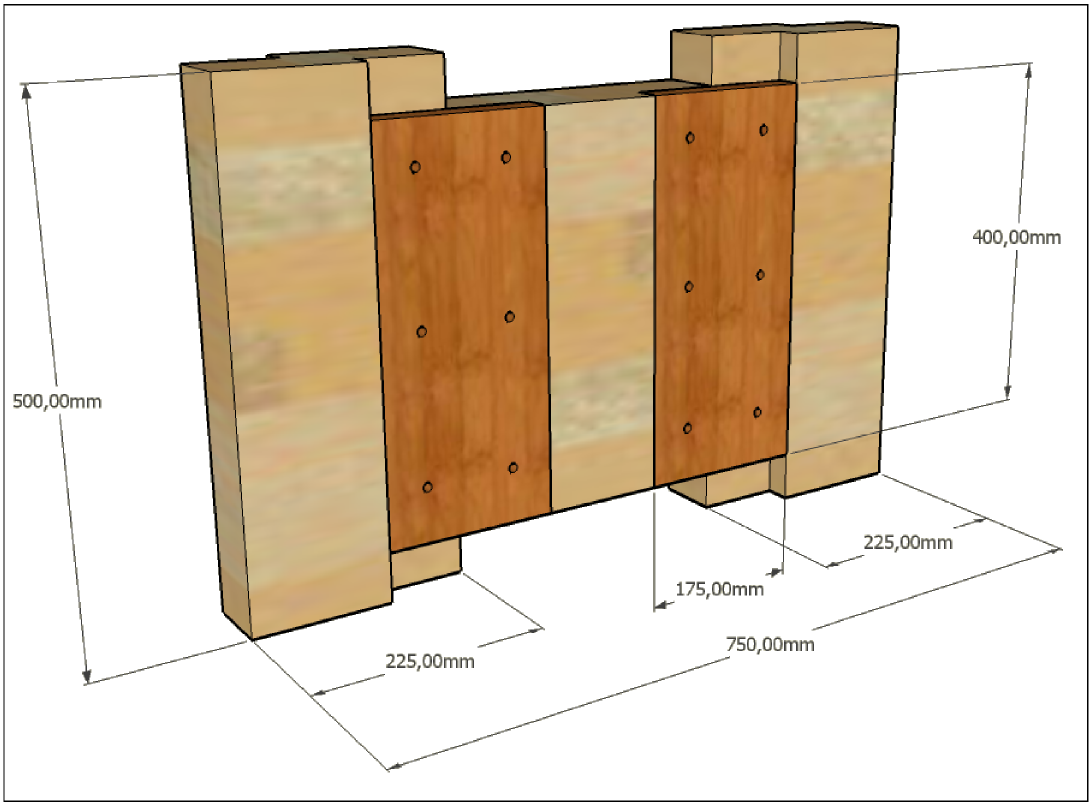

Figure 5-6, view of the specimen

The X-lam panels available at Delft University of Technology for the experiment consist of three- and five layered panels with a thickness of 95mm. It was decided to do tests on both panel types.

5.5.3 Test procedure

In the European standard EN12512, rules for determining the parameters of a timber connection in cyclic loading are given. In the European standard EN26891 the rules for ramp tests can be found. Both standards are used for testing the SOFIE connection between wall panels. The following text is obtained from the standards and adjusted for this document.

Environment parameters

Cyclic loading tests on timber connections should be carried out on specimens, which have been conditioned at the standard environment temperature of 20 ± 2 °C and a relative humidity of 65 ± 5 %. The climate room at the Delft University of Technology where the experiment is carried out complies with these requirements.

Test parameters

The test must be carried out at a constant rate of displacement between 0,02 mm/s and 0,2 mm/s. The experiment is within the scope of earthquake design. The duration of earthquakes is generally short. Therefore, it is chosen to do the experiment at a rate of displacement of 0,2 mm/s, the maximum value within the code.

Test procedure

The ramp test is carried out to determine the load slip envelope curve for the connection. The cyclic test is performed to determine the hysteresis in the connection under cyclic loading. The European standard requires a displacement driven test with the displacements as given in Figure 5-7. The test procedure is built-up from different percentages of yield displacement vy. These percentages can be found in the figure and are increasing to 4 times the yield displacement or until the displacement in the experiment is 30 mm. This 30 mm upper boundary is neglected for this experiment and the test is carried out until failure occurs. The yield displacement may be estimated or a real ramp test can be carried out to determine this parameters. The specific cyclic loading procedure for the experiment on the wall to wall connection is given in Figure 5-17.

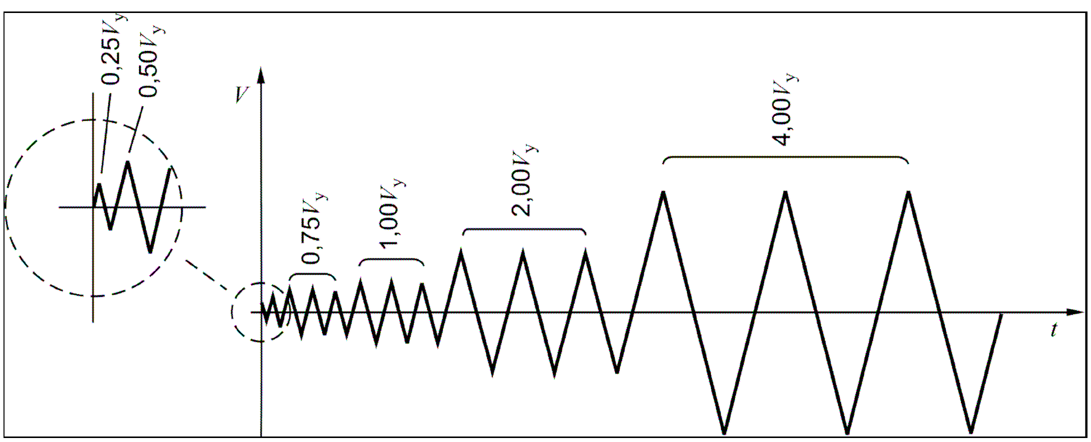

Figure 5-7, Test procedure for cyclic tests

Delft University of Technology

5.5.4 Number of experiments

In the experiment, three layered and five layered panels are tested. The total experiment consists of two ramp tests and six cyclic tests. The two ramp tests are done on a three and a five layered specimen. There are three arguments to do a ramp test:

- The test procedure (EN 12512) for cyclic loading is determined from the (estimated) yield slip and the envelope curve. A ramp test is done on the connection for determining yield slip and ultimate load. With the obtained values the parameters for the cyclic loading procedure are established.
- A ramp test on a three layered and a five layered panel is done to discover the influence of the number of layers in static loading.
- Another reason to do a ramp test is that it makes early checking of the test setup possible.

The cyclic part of the experiment consists of three cyclic tests on a five layered X-lam panel and three cyclic tests on a three layered X-lam panel.
The number of three is chosen to obtain good average properties of the connection.
Tests on the three and five layered panels are done to discover the influence of the number of layers in cyclic loading.

5.5.5 Instrumentation

All instruments used for measurement are transducers with a sensitivity classified in two types. One type is for displacements between 0 and 100mm. This type is suitable for measurement of the larger displacements. In Figure 5-8, two of the large displacement transducers are presented (number 1).

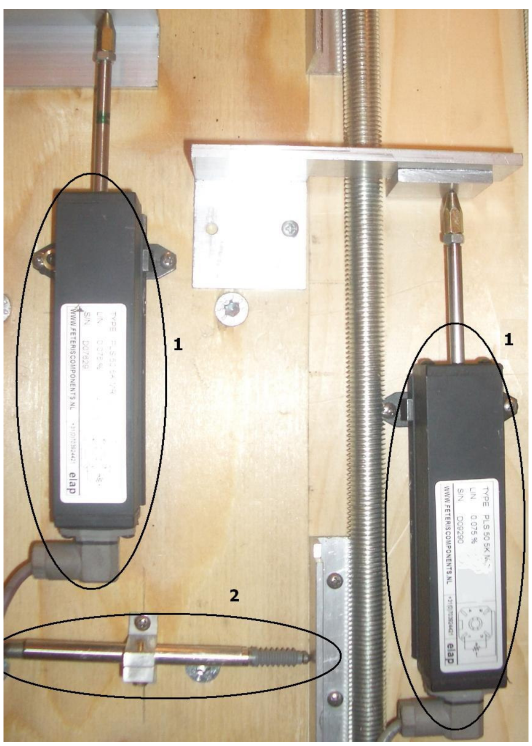

The second type used is for displacements between 0 and 10 mm, but will measure more accurately. These transducers are applicable for measurement of displacement due to rotations of the specimen (number 2 in Figure 5-8)

Figure 5-8, overview of used transducers in the ramp test

Calibration of the transducers

The output signal of the transducers is in Volts. Volts are calculated into displacement values for each transducer with a different calibration factor. Calibration factors are established with an accuracy of three digits.
The software program used for measurement has the possibility to couple calibration factors with the output signal of the transducers. In this way it is possible during the test to see the real displacement values and evaluation of results is easier.

5.5.6 Measurements

The locations of the transducers are presented in Figure 5-9.

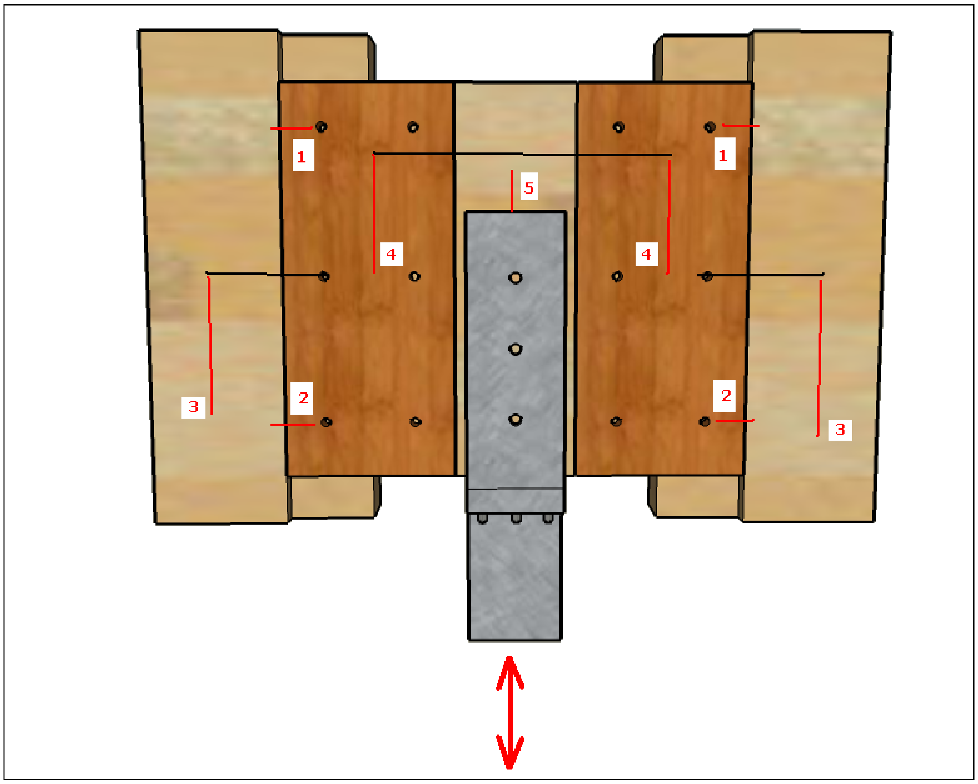

Figure 5-9, overview of measurement channels in ramp test

- Instruments 1 are measuring the horizontal displacement due to rotation between side panel and LVL panel on topside
- Instruments 2 are measuring the horizontal displacement due to rotation between side panel and LVL panel at the downside
- Instruments 3 are measuring the displacement between side panels and LVL panel
- Instruments 4 are measuring the displacement between middle panel and LVL panel
- Instrument 5 is measuring the displacement between the steel holder for applying the force and the middle panel

Locations

The channels used for measuring displacements in the specimen are given in the figures below. Figure 5-10 is representing the view, called the 'front' side of the specimen. Figure 5-11 is representing the 'back'.

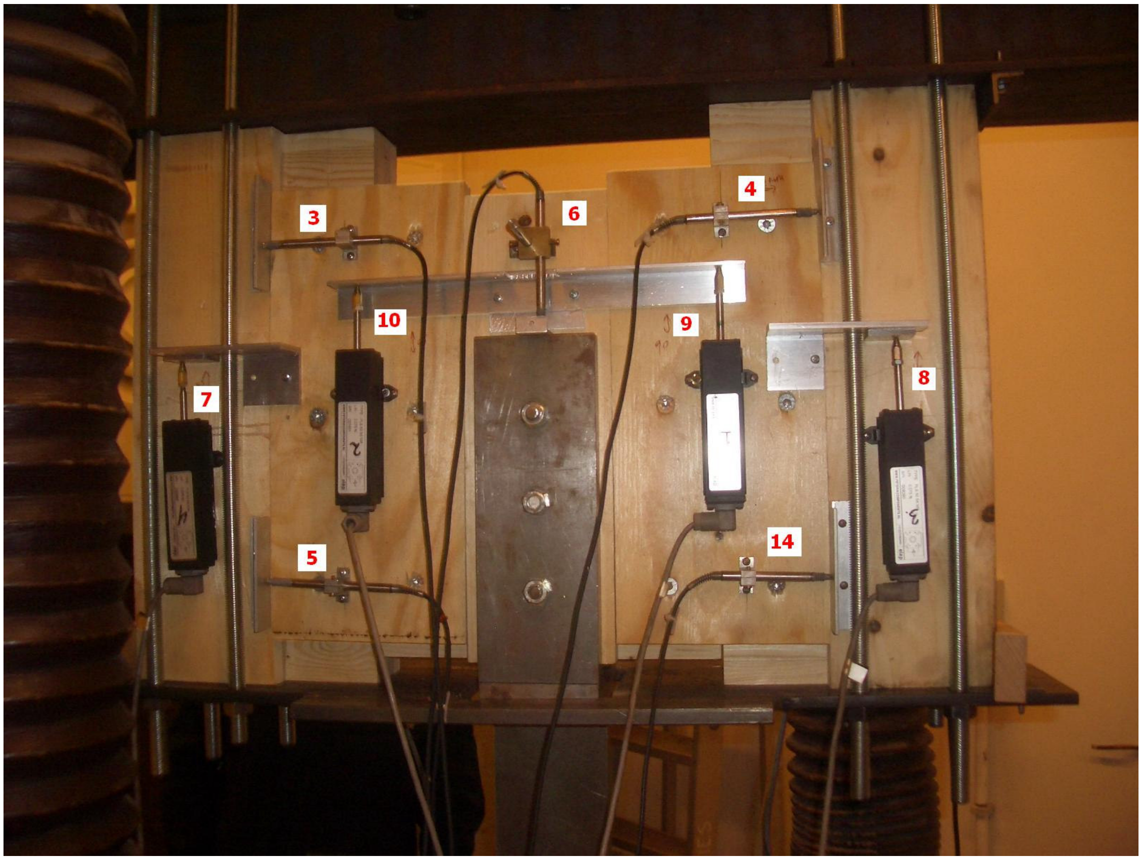

Figure 5-10, presentation of the 'front' side channels

Channels 3, 4, 5 and 14 are measuring the rotation due to loading of the specimen.
Channels 9 and 10 are measuring the difference in displacement of the middle X-Lam panel and the two connecting Kerto-Q LVL panels. Channels 7 and 8 are measuring the difference in displacement of the side X-Lam panels and the connecting Kerto-Q LVL panels. Channel 6 is measuring the difference in displacement between the steel holder and the specimen.

Figure 5-11, presentation of the 'back' side channels

Channels 11 and 12 are measuring the displacement between the side panels and the middle panel at the 'back' side.

5.6 Results

5.6.1 Screw failure

After the ramp test the specimen is scanned with an X-ray scanner. In Figure 5-12 an X-ray scan of the loaded screws can be found. The figure of the deformed screws confirms the preliminary calculated failure mode d (see chapter 0). The failure of the connection mostly can be explained by plastic deformation of the screws. The properties of the screw and the timber induce very large embedment strength, wherefore the deformation of the connection due to embedment failure can be neglected.

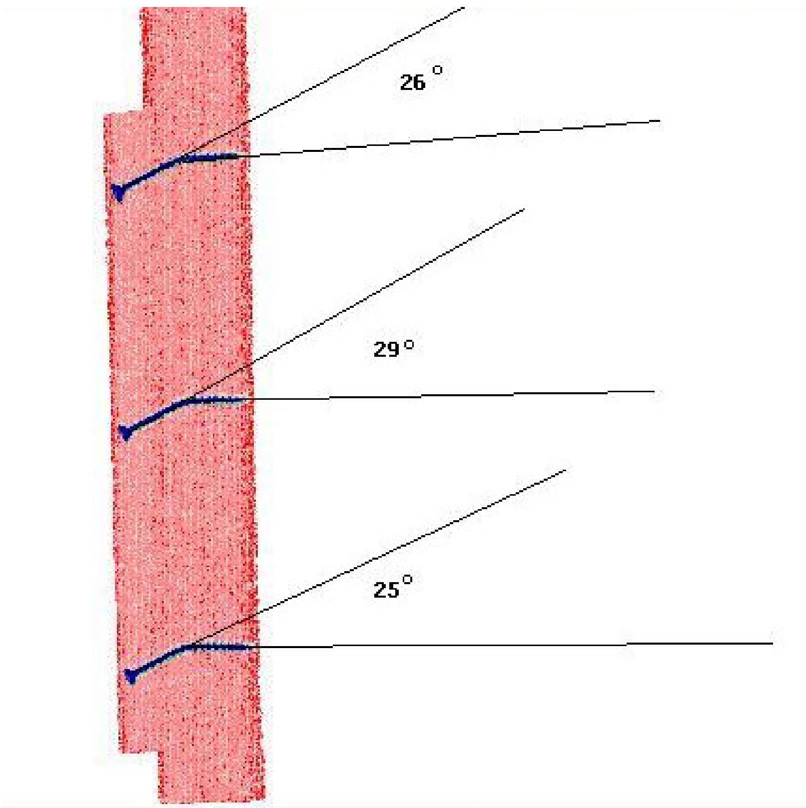

Figure 5-12, x-ray scan of the deformed screws

5.6.2 Forces and displacements

Output of the different channels is given in Appendix C. The diagram of the displacement-force diagram is given in Figure 5-13. It must be mentioned that the displacement input for the diagram is corrected with the slip between the steel holder and the specimen (measured by channel 6).

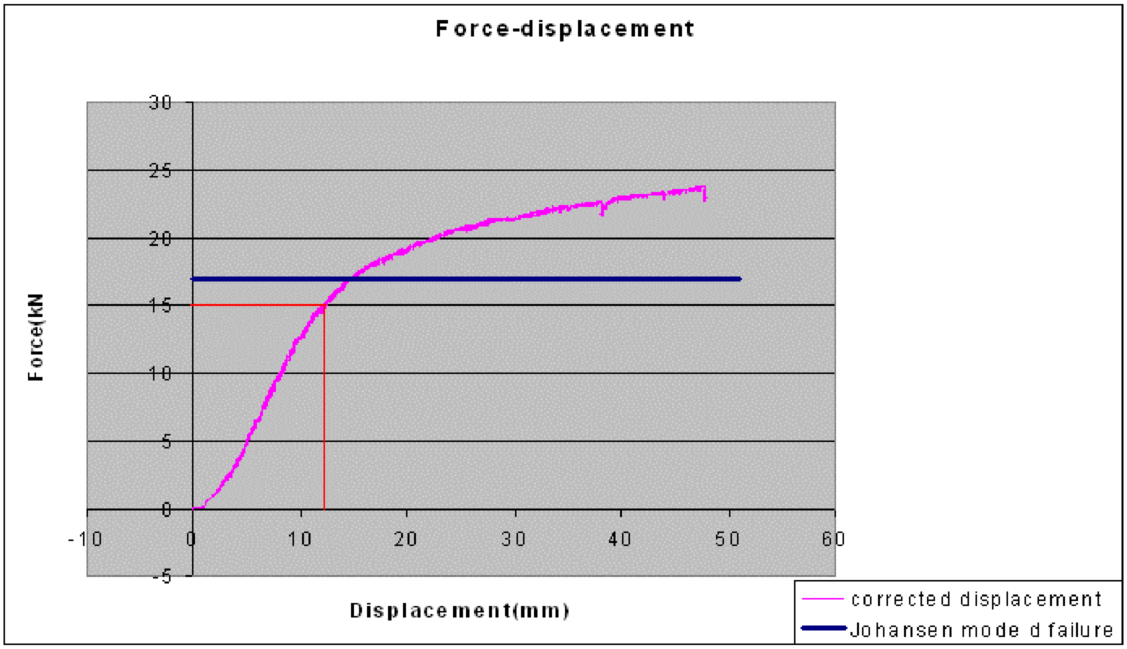

Figure 5-13, Force displacement diagram of the ramp test

At a force of approximately 15kN and a displacement of 12mm, the inclination of the line is decreasing (also 'estimated' as the yield point indicated in Figure 5-13 with the red lines). This decreasing inclination is pointing at a more plastic behaviour of the connection. Ultimate displacement in the ramp test is approximately 48mm.

5.6.3 Side restraints

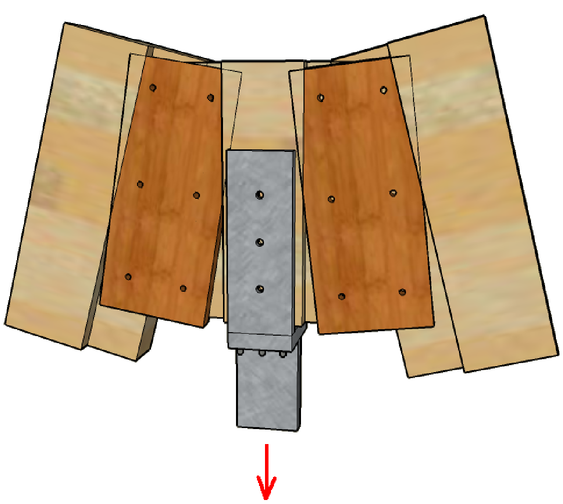

Two ramp tests are completed. In the first ramp test it there was a problem of lateral displacements (indicated exaggerated in Figure 5-14). These displacements were too high and it was concluded that a facility should be provided in order to restrain lateral displacements. Such displacements are not possible in practice, since the full wall panels are restrained both in horizontal and vertical directions

Figure 5-14, lateral displacements

This facility is realized by connecting the vertical supports. The specimen is secured with wedges on top and bottom to avoid sideways movements. Without these sideways movements, a better representation of the full wall-to-wall system is obtained. The total setup can be found in Figure 5-15.

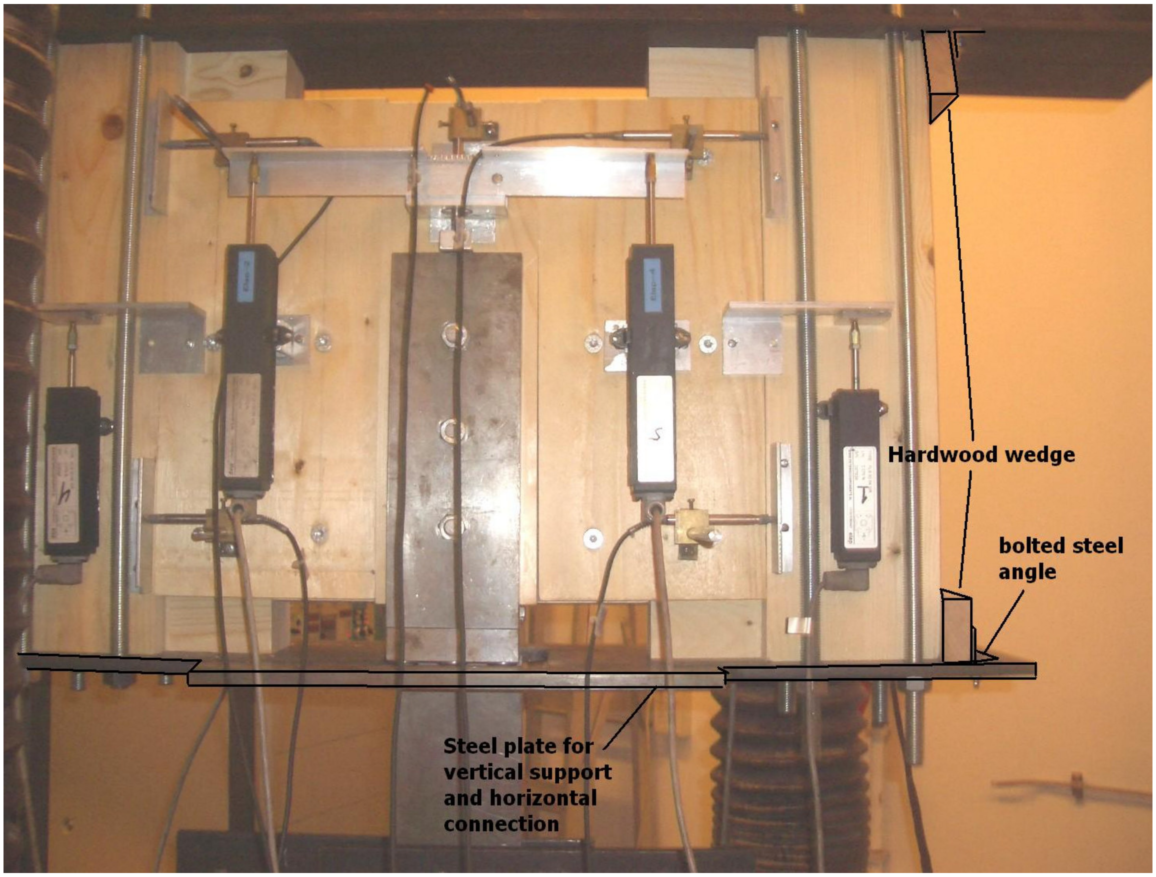

Figure 5-15, picture of the test set-up with facility to restrain lateral displacement

5.6.4 Three or five layered

In Figure 5-16, the output for both ramp tests are presented. Difference in the two ramp tests is allocated to the errors in constructing the specimen, preparing test set-up and the rate of the displacement. The rate of displacement of the jack was higher in the ramp test on the three layered specimen, but apart from a slight difference.

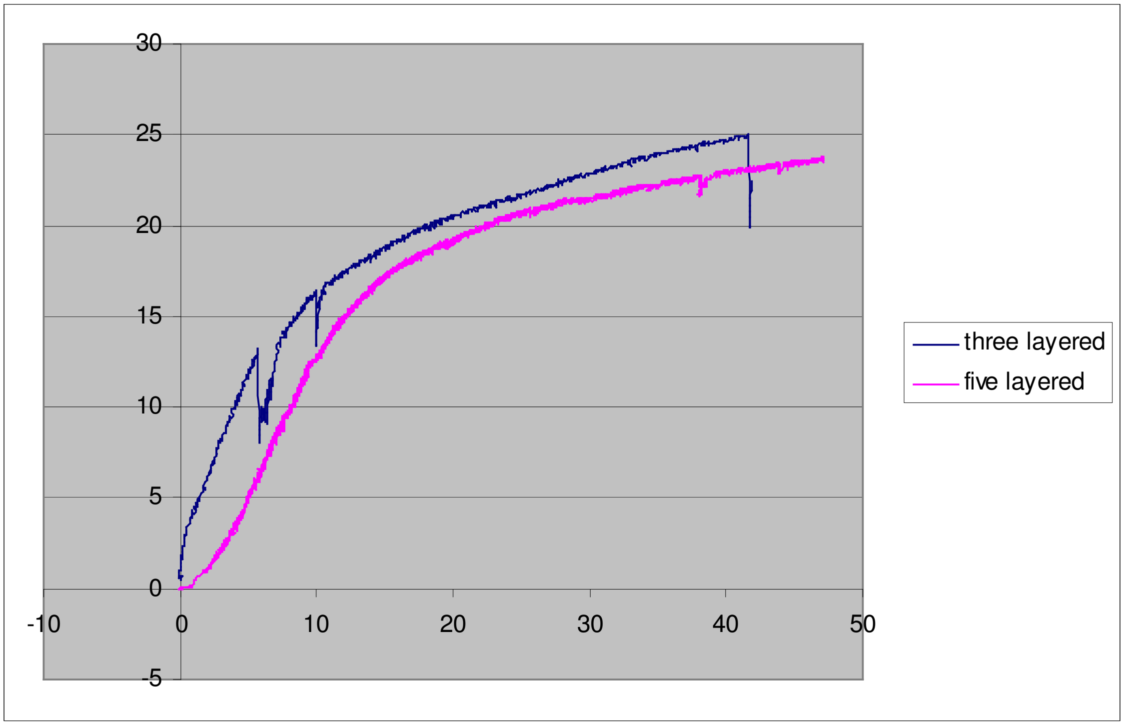

Figure 5-16, force-displacement diagrams of the three- and five layered panel experiments

There is no significant difference in the response of the three and five layered specimen in the ramp test.

5.6.5 Conclusions

Instruments

In the cyclic test the movement of the specimen will be in two directions. This means that the ultimate displacements measured in the ramp test, described above will be reached in positive and negative direction. In other words, the displacements found in the ramp test must be doubled for establishing the necessary measuring area for all instruments during the cyclic test. From this doubling it is concluded that the instruments in channel 9 and 10 must be replaced by larger transducers. Therefore, the channels as indicated in **Fout! Verwijzingsbron niet gevonden.** and **Fout! Verwijzingsbron niet gevonden.** are changed.

Yield slip

The ramp test is carried out for determining the yield slip of the SOFIE connection. In the obtained force-displacement diagram, the yield point can be estimated. The yield displacement is approximately 10mm at a force of 12kN. With the established yield displacement, the cyclic loading procedure can be established according to the European standard EN12512. The displacement diagram applied to the hydraulic jack is given in Figure 5-17. The total duration of the cyclic test is 4780 seconds.

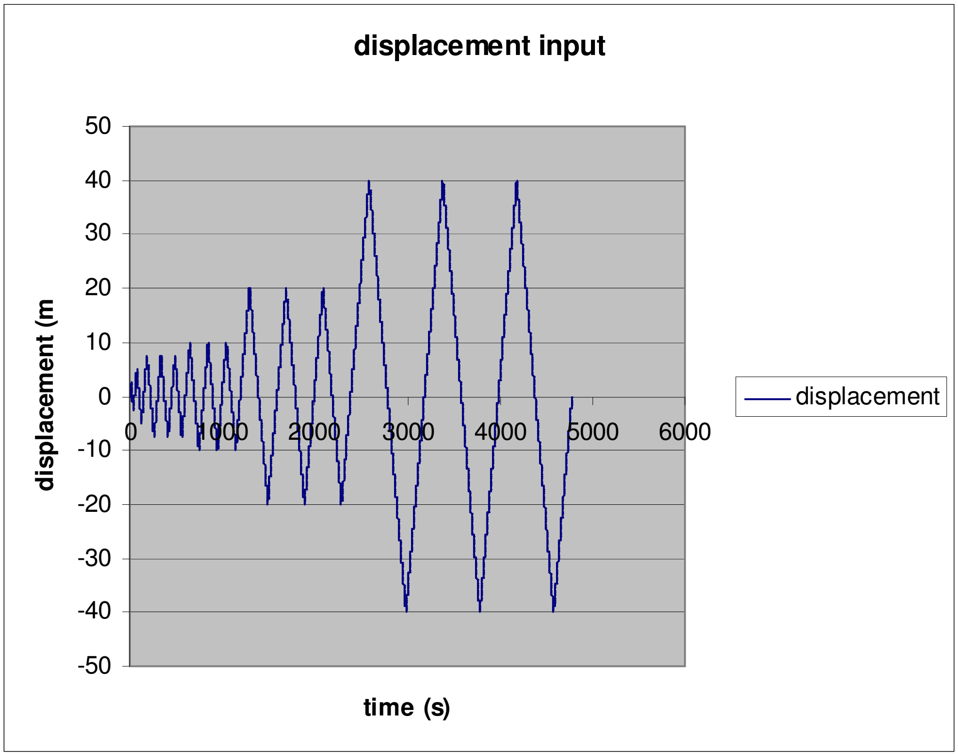

Figure 5-17, cyclic test procedure according to EN12512

Three or five layered

The five layered and three layered specimen respond in same order of magnitude to the ramp test. Therefore the displacement diagram in Figure 5-17 is used for all cyclic tests.

5.7 Cyclic test

5.7.1 Results

Some of the transducers are replaced by transducers with a larger measuring area as explained in section 5.6.5. In this way, the channels are changed also. In Appendix C all channels used can be found together with the complete results from the experiment. In this paragraph, the slip between the steel holder and the specimen and the total force-displacement diagram are presented.

Slip between steel holder and middle panel

Channel 5 is measuring the slip between the steel holder and the middle panel. The slip in time is presented in Figure 5-18. It has to be mentioned the horizontal scale is no time dependent variable. In all the results presented in this chapter as well as in Appendix C, the slip is subtracted from the results.

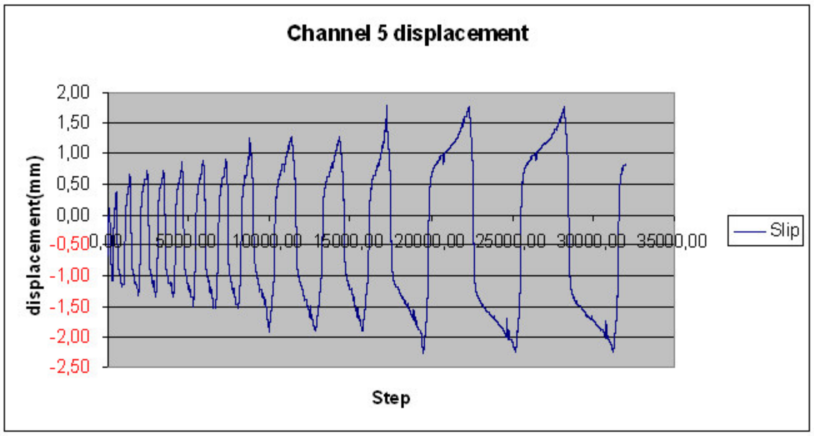

Figure 5-18, slip between steel holder and the specimen in experiment 2

Force-displacement diagram

A total of six cyclic tests are done of which force-displacement diagrams are obtained. Per test, 12 channels are used for measuring displacements. In other words, there are a lot of results available. To keep everything clear it is chosen to show only one force-displacement diagram in this report and to show the key values for the other tests in table form (Table 5-2). In Figure 5-19 the force displacement diagram of experiment number 1 on the five layered panel is shown. The force on the specimen is plotted against the displacement of the jack (the blue displacement line). In the negative quadrant the force is not changing as is indicated by the horizontal line.

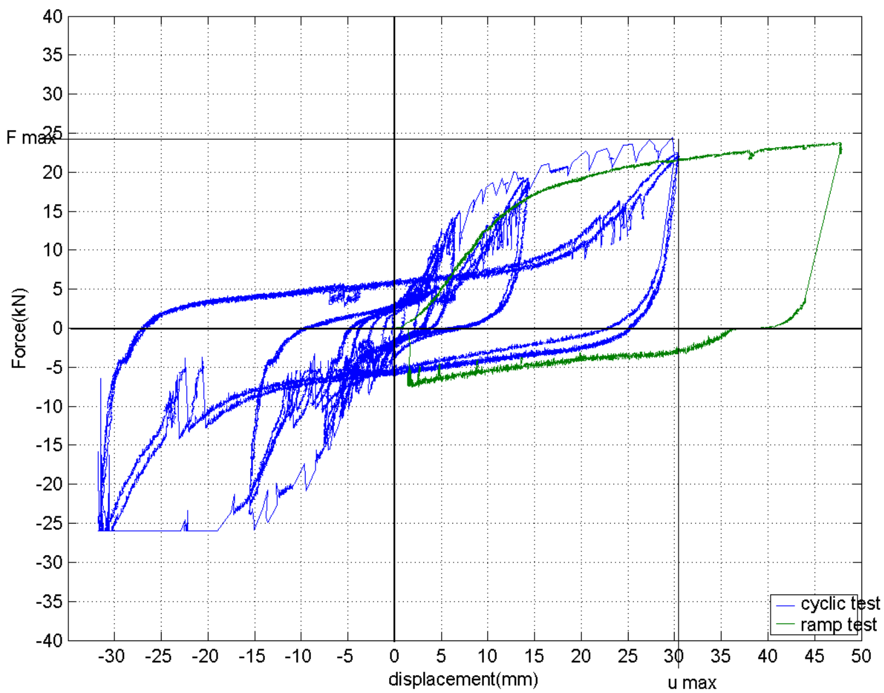

Figure 5-19, force displacement diagram of experiment 2

Experiment number		F_{max}(kN)	U_{max}(mm)
5 layered	2	**24.41**	**32.29**
	3	25.42	34.42
	4	25.82	35.58
3 layered	5	24.23	35.52
	6	25.46	35.58
	7	25.96	35.52

Table 5-2, maximum of F and d in the experiments

5.8 Conclusions from the experiment

The symmetrical setup of the test is a good way of testing the connection. Lateral restraining is necessary to avoid rotational movement. In this way a reliable representation of the full wall-to-wall connection is obtained. The number of layers in the panel is negligible for response to cyclic loading. The amount of dissipated energy in the tested connection with the test procedure in Figure 5-17 is around 3 to 4 kNm as is calculated in Appendix C.

5.9 Recommendations

The experiment is done on a relatively small and a symmetrical connection. A total of twelve screws are tested in four rows. The real SOFIE building connection has larger dimensions and more screws are applied. It is assumed that with scaling down of the connection no significant deviation occurs. In a full scale test this assumption must be checked on its correctness.
The displacement in the test is vertical induced by vertical forces. In the building the movement is vertical but induced by horizontal loading. It is assumed that this difference does not lead to severe deviations. This assumption must be checked by doing experiments on the connection with real dimensions.

6 Modelling of the structure

6.1 Introduction

The software program used for modelling is DRAIN 3D. The program was chosen because it was used in the SOFIE project and was considered good for the modelling within this project. Another advantage was that enough expertise of the DRAIN 3D was available within the graduation committee. In this chapter, basics and background of the program is explained in section 6.2 to section 6.4. In section 6.5, the geometry for the seven storey model is described. Section 6.7 treats the properties of the connections in the model.

6.2 Hysteresis

Under reversed cyclic loading of timber connections, strength and stiffness are related to load history, the hysteretic behaviour. Practically this means that the load-slip relation of each loading cycle is influenced by the magnitude and direction of the preceding cycle. It is the hysteretic behaviour that makes modelling of timber structures more complex than the formulation of a unidirectional load-displacement connection.
Due to 'memory' in the material it is not possible to apply modelling techniques for static behaviour connections under cyclic loading. The models available for describing the elastic-plastic behaviour for materials as concrete and steel are not applicable for timber connections. This is because these models do not allow for pinching, or decrease of stiffness of the surrounding material.
For the timber connections in the SOFIE structure, an analytical model is needed to describe the hysteretic response of cyclically loaded timber connections.

6.3 DRAIN 3D

DRAIN 3D was originally developed at Berkeley University of California. The first version of the DRAIN program has been programmed in Fortran 77 and is a 2D modelling program. This DRAIN 2D software was extended and modified into the 3D version. The University of Florence, one of the committed parties within the SOFIE project, developed timber fastener subroutines in the DRAIN 3D version.

The timber fastener subroutines added are based on an algorithm representing a linear simplification obtained from test data as shown in Figure 6-1. Two diagrams are available for this simplification. The first is a cycle with four different inclinations. The inclinations are K1, K2, K3 and K4. The load slip diagram is given in Figure 6-1 on the left. The six inclination diagram is presented in Figure 6-1 on the right

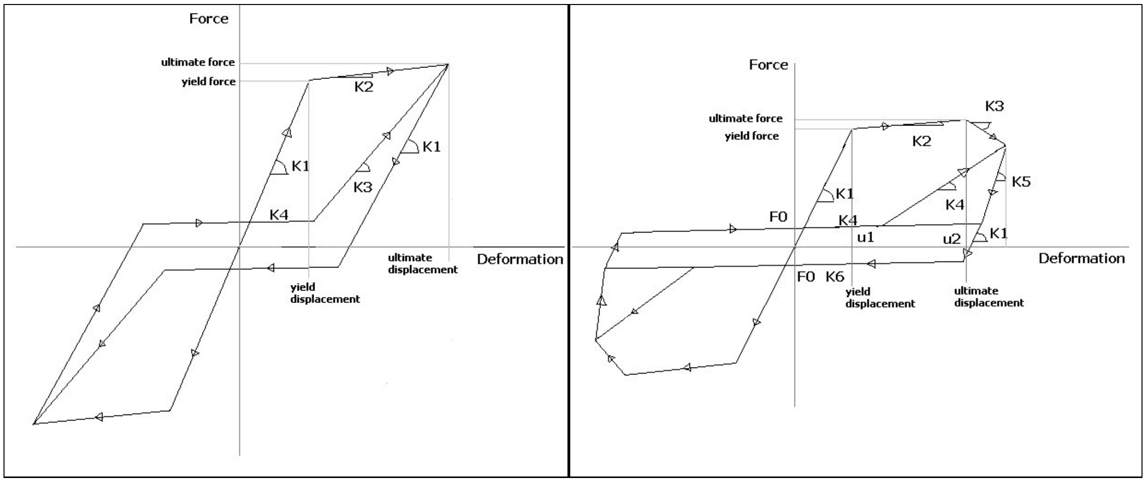

Figure 6-1, the load slip diagram with four gradients (left) and six gradients (right)

The behaviour of the timber X-lam connections is better approximated by the curve with six inclinations. Six inclinations account for six different stiffness values (K1- K6).

The subroutines developed by the University of Florence exist of three elements, which make use of the diagrams given in Figure 6-1 that can be invoked in the software. These elements are:

- Rotational semi-rigid element:
  This element is used to describe moment rotation behaviour of a semi-rigid joint.
- Translational semi-rigid element:
  This element describes the load-slip behaviour of a semi-rigid joint.
- Translational semi-rigid element with asymmetric pinching hysteretic cycle:
  This element describes the load-slip behaviour of a semi rigid joint, but the input variables can be different in the 1st and 3rd quadrant.

6.4 Development of the program within the scope of the thesis

The DRAIN 3D software version compiled at the University of Florence is available for the model within the scope of the thesis. After the first modelling steps, the software pointed out to have insufficient memory. Another problem was that it was not possible to define the number of element groups needed for the model of the seven-storey building. Therefore, the code of the program was edited to solve these two problems and compiled again. The complete code used for compiling and the new version of the DRAIN 3D software is found on the added DVD. This new version of DRAIN 3D is developed without supervision of the Universities of Florence or Berkeley.

6.5 Seven storey model

The model of the seven storey SOFIE structure is complex. To gain a better insight the presentation of the model is in steps. First a 2D model of a part of the structure is given. It is chosen to present a 2D model of multiple levels. Explanation of panel definition and the geometry of the vertical connection and horizontal connection are presented here. Secondly a model of the ground level floor is presented. The horizontal elements representing the floors are described. Furthermore on restraints, slaving, the spring elements and lumped masses are treated in this part. The layout of the wall panels is approximately the same for each level. Therefore, the geometry of the ground floor can be copied to the other levels. Only the upper storey of the SOFIE building is different. The model and its considerations for the seventh storey are described in section 6.5.

6.5.1 Two dimensional

In this paragraph, the two-dimensional structure of a part of the model is explained. In this way a clear impression is possible. The first step is to translate the panels and connections into DRAIN 3D elements. This translation is presented for a part of the structure in Figure 6-2.

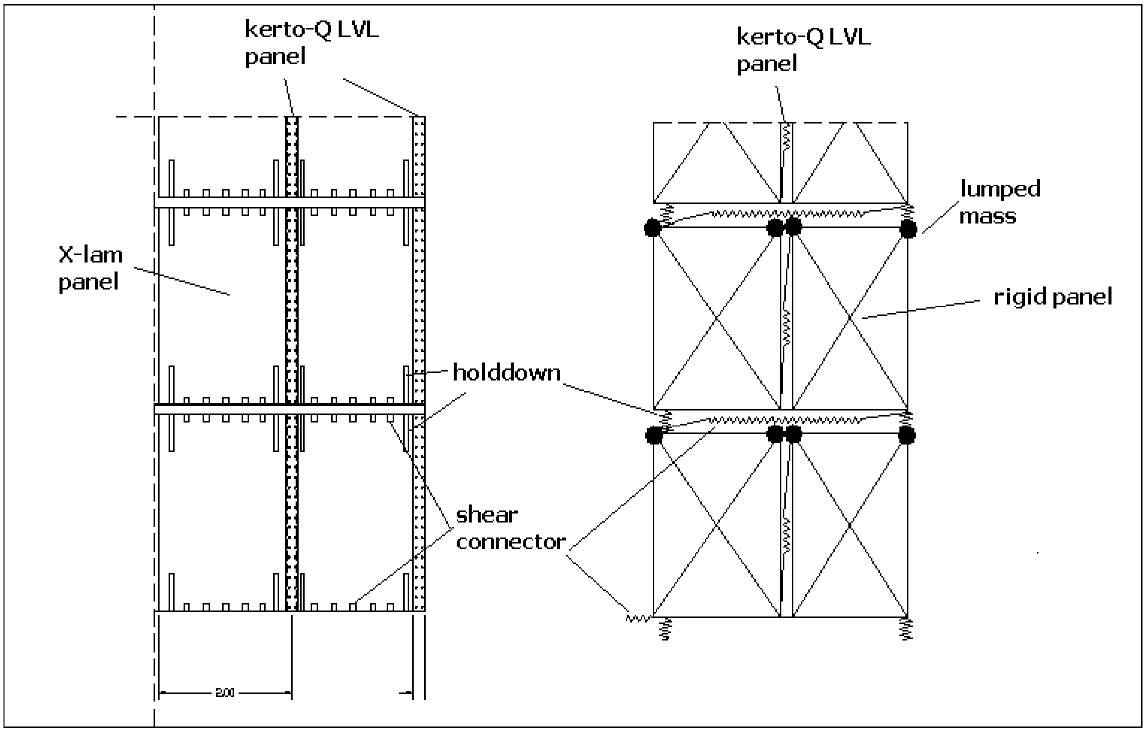

Figure 6-2, modeling of the rigid panels

The vertical spring elements are representing the holddowns in the building; horizontal springs are modelling the shear connectors. The model further consists of essentially rigid panels, modelled with rigid straight timber elements. The kerto-Q connection between the panels is represented by a spring. Masses are lumped at the top nodes of each panel. The masses are determined in chapter 0. The number of vertical and horizontal springs in the model is not corresponding to the number of holddowns and shear connectors present in the structure. A simplification is applied for modelling considerations.
In this simplification there are springs modelling 1, 2, 3, 4 or 5 holddowns. In the definition of a spring modelling 5 holddowns the properties as stiffness and strength are five times higher than the model for 1 holddown. The simplification is apparent in Figure 6-2; each floor level is connected with four holddowns, but in the model only two holddowns are defined. Panels with openings are also present in the building. Modelling of these panels is explained separately.

<u>Panels with opening</u>

Panels with openings are defined as presented in Figure 6-3. Vertical and horizontal members are present together with diagonals for rigid behaviour. The horizontal members above and under the opening consist of elements only capable of resisting tension and compression forces. In this way it is secured that both panel parts act together in structural point of view, but the weaker part of the panel is respected.

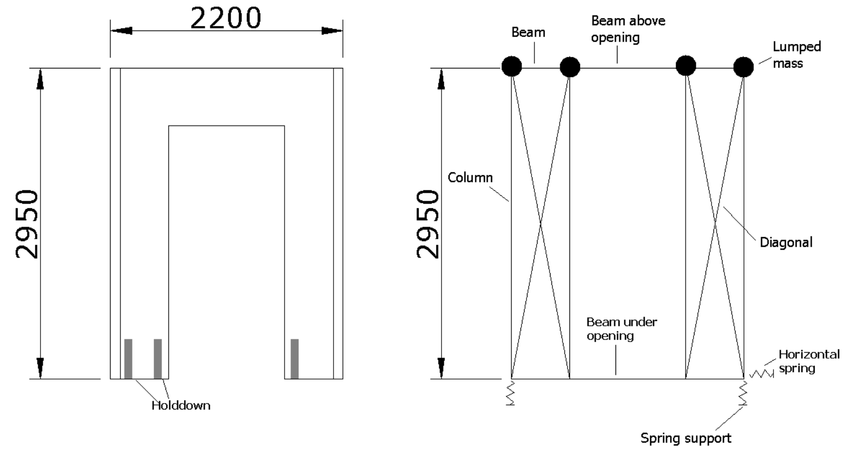

Figure 6-3, the panel with opening AutoCAD view and its wire framed model

This was the first idea to model the panels with openings. After running the complete model it was discovered that the panels must be modelled in the same way as normal panels; completely rigid. Calculations with DRAIN 3D indicated that panels with the configuration as in Figure 6-4 acted as non rigid while experiments, see section 3.2, showed rigid behaviour.

6.5.2 Three dimensional

In Figure 6-4, the 3D model of the ground level without (left) and with the floor elements (right) is presented.

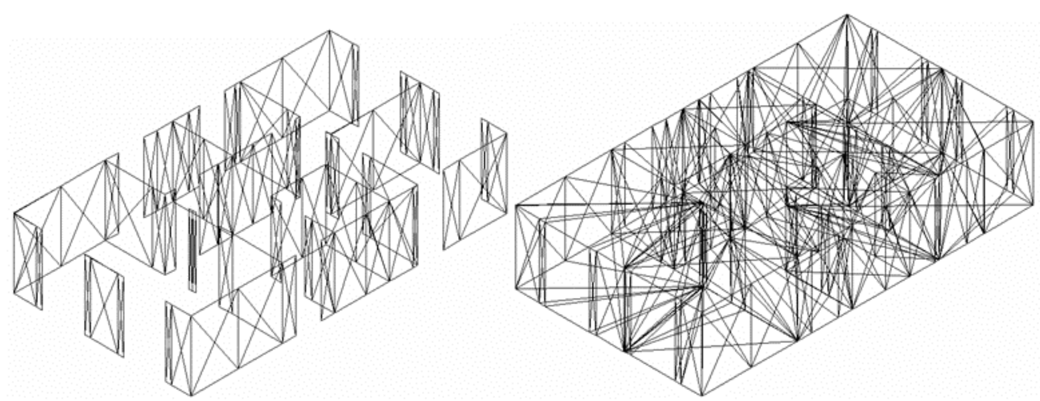

Figure 6-4, model of the ground floor

Floor generation

The floor slabs in the building are responsible for the diaphragmatic behaviour of the floor. This is a very important factor in earthquake engineering, see section 2.5.1. The definition of the floor slab elements in the DRAIN 3D model must secure diaphragmatic behaviour in the model. The generation of floors requires some more information on the method of definition. The building is divided in 9 sections according to Figure 6-5. Then each node is connected to the node in the opposite corner in the same block. For the floor elements a very stiff spring element is used. This means the stiffness of the floor in vertical direction is neglected in the model. The pattern that is generated is presented in Figure 6-6.

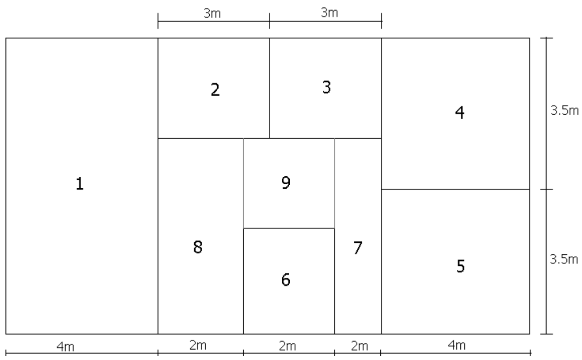

Figure 6-5, sections of the ground floor

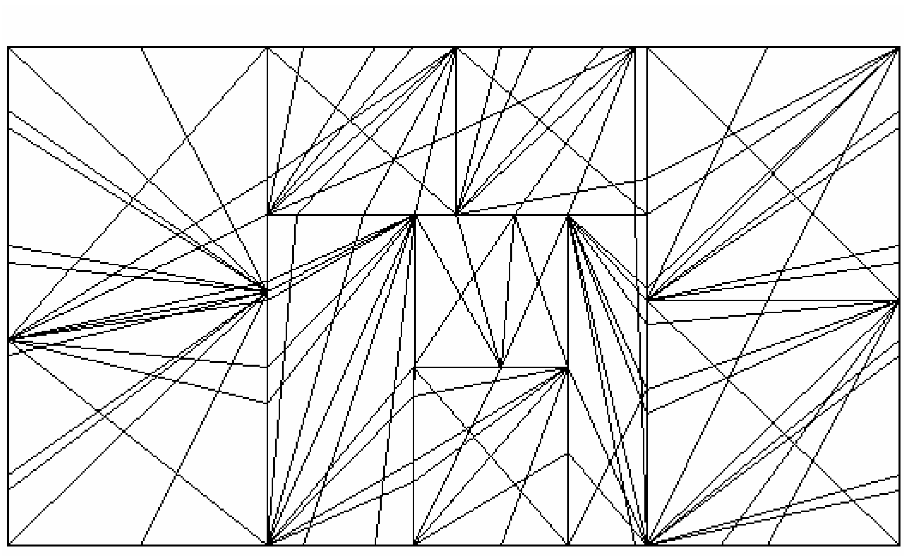

Figure 6-6, Top view on the ground floor, diagonals representing the floor slabs in the model

6.5.3 Vertical direction and restraints

On ground floor, the panels are defined by nodes on three levels: the support, the base beam and the top beam. The support nodes are resrained. The restraints in DRAIN must be given in six variables; translation in three directions and rotation in three directions. For the supports, restraints are given to the translation in three directions and rotations in three directions, for example in figure Figure 6-7 the support nodes 37, 38,43 and 44.

<u>Slaving</u>

Slaving in the program is needed to link nodes with each other and is needed for nodes next that are connected in the model by springs. In slaving the displacements and forces in the master node are copied to the slaved node.
The slaving constraints are defined for translation in three directions (x,y,z) and for rotation in three directions (x,y,z). Three main types of slaving are used in the input file for the seven storey structure; slaving in three translational degrees of freedom (x,y,z), two translational degrees of freedom (x,y)and one translation slaved (x or y). With some sketches these three different cases are elaborated.

The slaving in three directions is defined at the corners of the structure. Corners are found at every location where one panel is connected perpendicular to another panel. In the lower nodes, slaving is defined in all three directions. The upper nodes are slaved in x and y direction. In Figure 6-7 an example of the south-east corner of the building is given (location indicated red in the floor plan on the right). The nodes 40 and 45 are slaved in three directions. The nodes 42 and 47 are slaved in directions x and y.

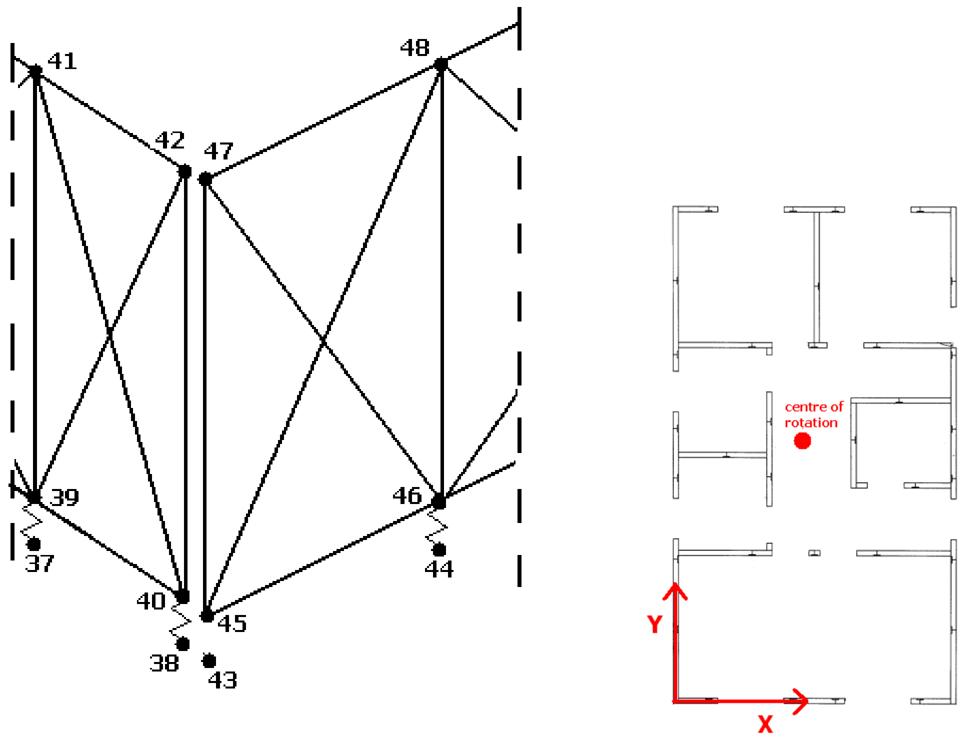

Figure 6-7, detail of the model in the south-east corner

Slaving in one direction (x or y) is defined at the panels with openings.

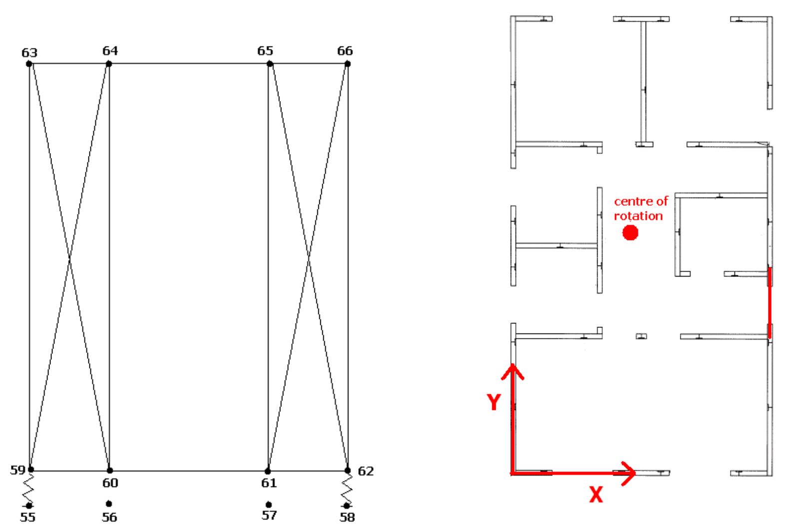

Figure 6-8, detail of panel with opening

As an example, the model of a panel with opening is given in Figure 6-8. The example is a panel in the east wall of the model (exact location is found in layout on the right). The degrees of freedom for the panel in y-direction (see layout) are restricted by the elements. However, in x-direction the nodes 64 and 65 can move out of plane. To anticipate on this movement that does not occur in the real building, slaving to node 60 and 61 is given in x-direction.

<u>Masses</u>

The masses of the panels, the floor and the live loads are lumped at the top nodes of the panel definition. The masses of the panels are determined for each panel separately and the total mass is lumped at the top nodes. The calculation can be found in the Appendix D.
Each mass is defined proportionally to the part of the building that is supported by the node. The same partition in blocks as for the floor definition is used (Figure 6-5).
The total mass of the floor and the live load in each block is divided over the total number of upper points defined. In this way for example nodes between block 1 and 2 are loaded vertically from the floor in block 1 and block 2.

6.6 Springs

In this section, the springs in the model are explained. Due to the complexity of the model, multiple renderings of the ground floor level are presented with the spring elements in it. In this way clear and well-arranged renderings are given. The properties of the spring elements are determined in section 6.7.

6.6.1 Vertical spring supports

The vertical springs in the model consist of springs representing the holddowns and springs representing the wall-to-wall connection. The location of these vertical springs is given in Figure 6-9. The lumped masses and floor are left out in this figure to get a clear figure.

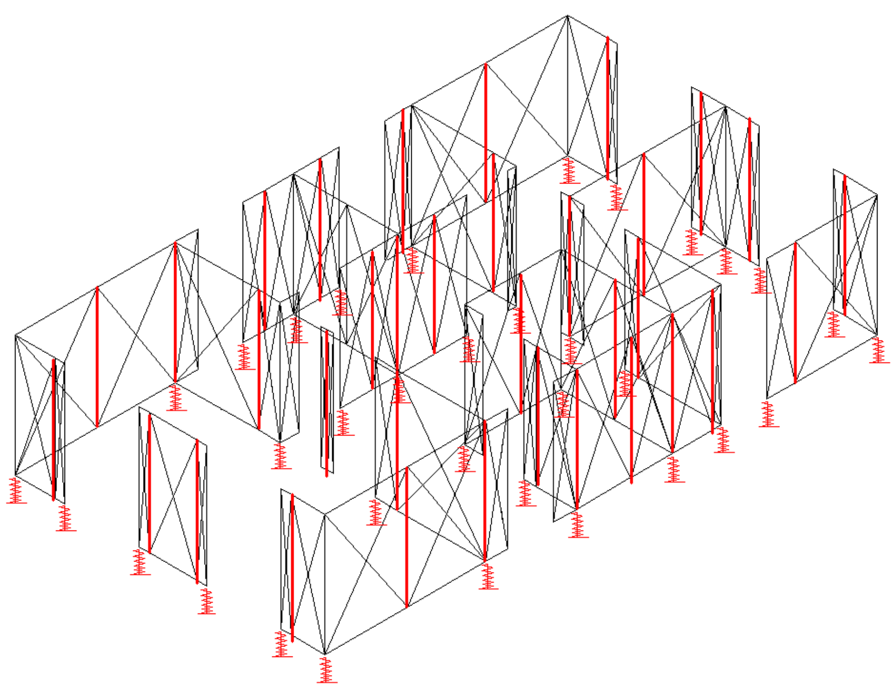

Figure 6-9, 3D presentation of vertical springs and wall to wall connection

6.6.2 Horizontal spring supports

Horizontal spring elements are representing the horizontal shear connections. The springs are defined at the location of shear walls in the building according to Figure 6-10. In the figure, the lumped masses defined are also visible.

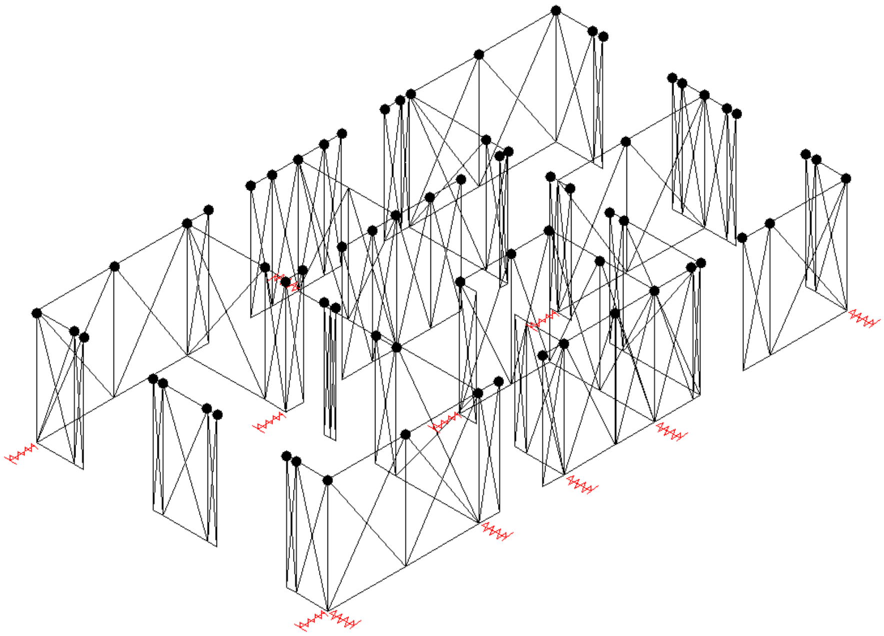

Figure 6-10, 3D presentation of the horizontal springs and lumped masses

6.6.3 Seventh storey

The geometry of the sixth and seventh storey is according to Figure 6-11. The seventh storey in the model is defined by larger panels starting at the sixth storey.

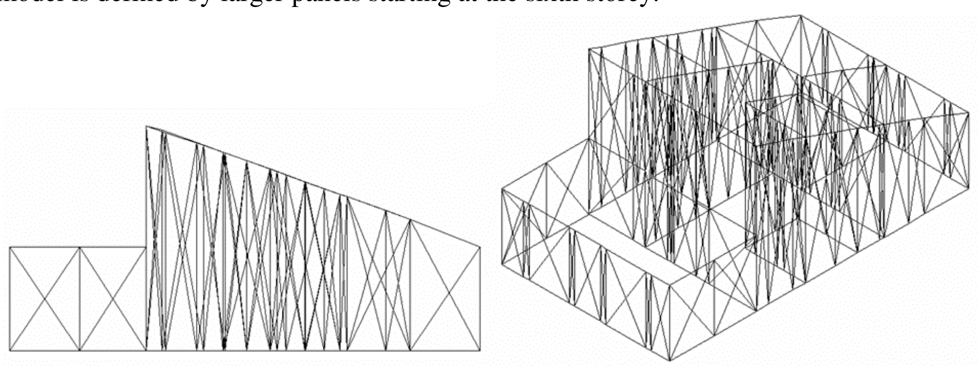

Figure 6-11, model of the seventh storey

With the geometry seventh storey known, the geometry is completed. The total model, without diagonals and floors, can be found in Figure 6-12.

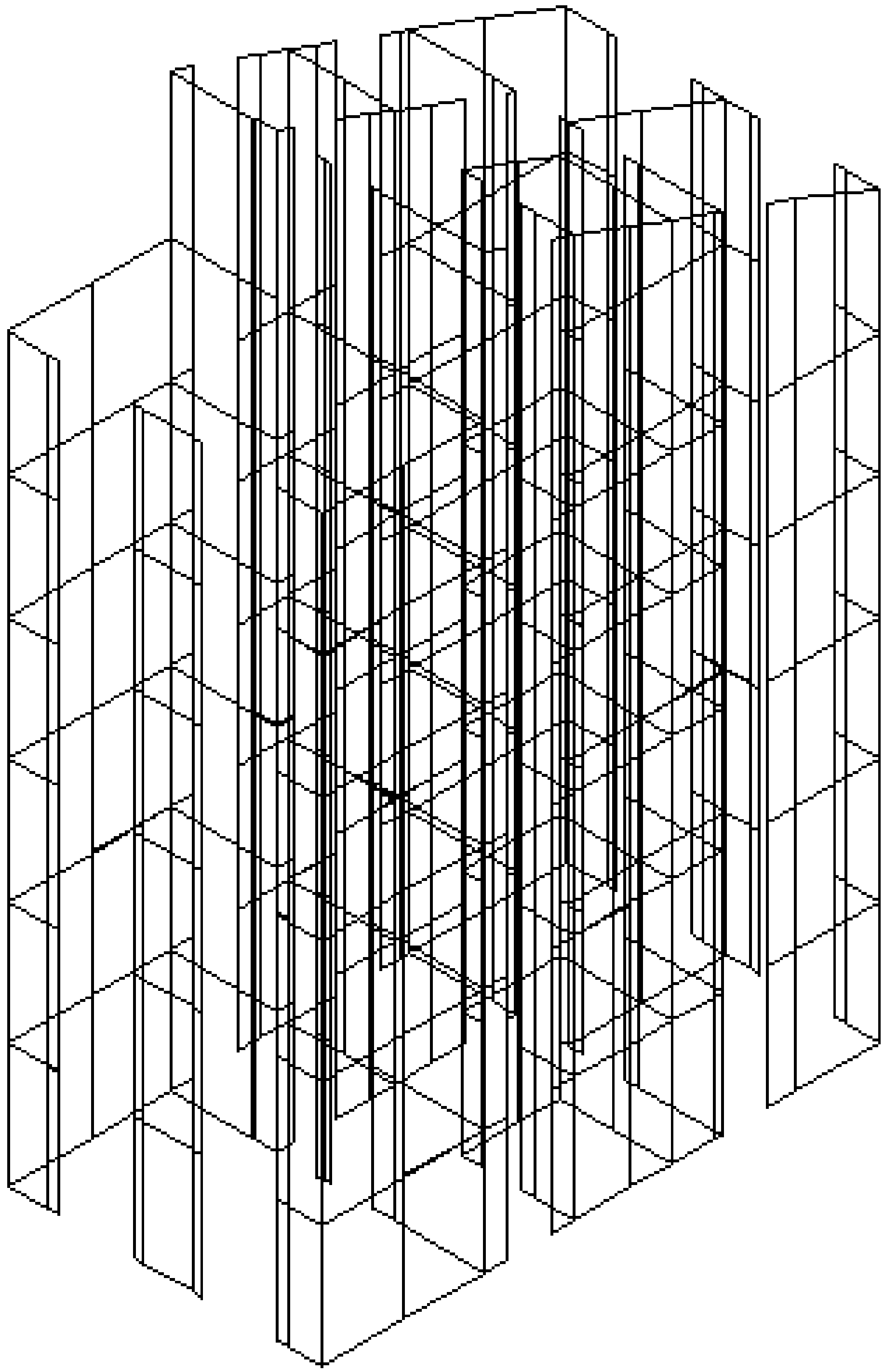

Figure 6-12, model of the complete building without diagonals and floors

6.7 Properties of the springs

The experiments described in chapter three are accompanied with modelling in DRAIN 3D. This modelling implies in most cases a DRAIN 3D model that is calibrated with trial and error to experimental results. The elements to calibrate are the spring elements. The horizontal springs are calibrated in the model for the three storey structure (refer to the SOFIE project for more information). The Simpson HTT22 spring is done before also. These calibration processes are described shortly in the next section. The special holddown and the wall to wall connection are calibrated in this chapter for the first time. Therefore, these processes are described in more detail.

6.7.1 Fitting of normal holddown + horizontal shear connectors

The model for calibration to the test results (chapter 3) is given in Figure 6-13. The XLAM panel is assumed to be rigid; the vertical, horizontal and diagonal members which are used to model the panel have an infinitely high stiffness. All ductility and energy dissipation is concentrated in the joints which are modelled as springs. The stiffness values of these springs, i.e. their hysteretic behaviour, are calibrated on the test results in terms of dissipated energy. Also the maximum force and the ultimate slip should be approximated as good as possible.

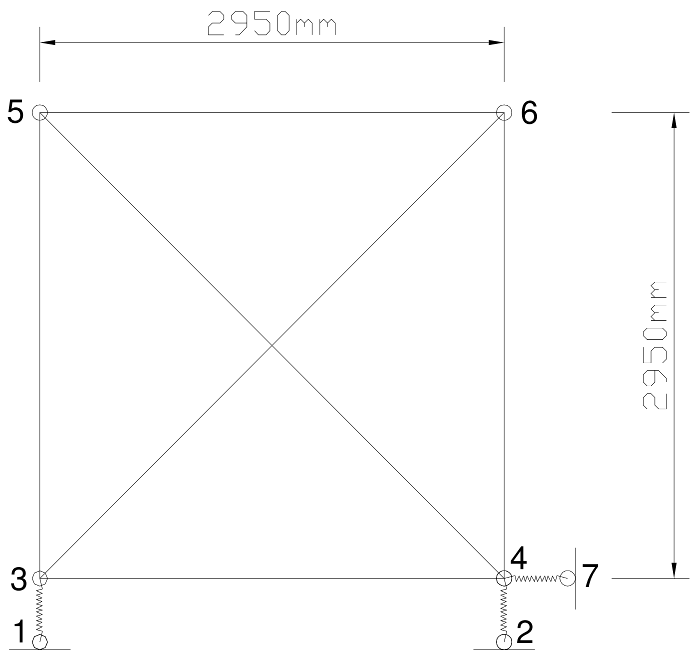

Figure 6-13, model for calibration of the spring elements

In Figure 6-14 and Figure 6-14, the results of the modelling are shown. Figure 6-14 shows the overlap for the vertical springs. Here, the difference in terms of energy dissipation is 8.4%. Figure 6-15 shows the results for the horizontal spring – the difference in terms of energy dissipation between DRAIN3DX-model and cyclic test is 4.6%.

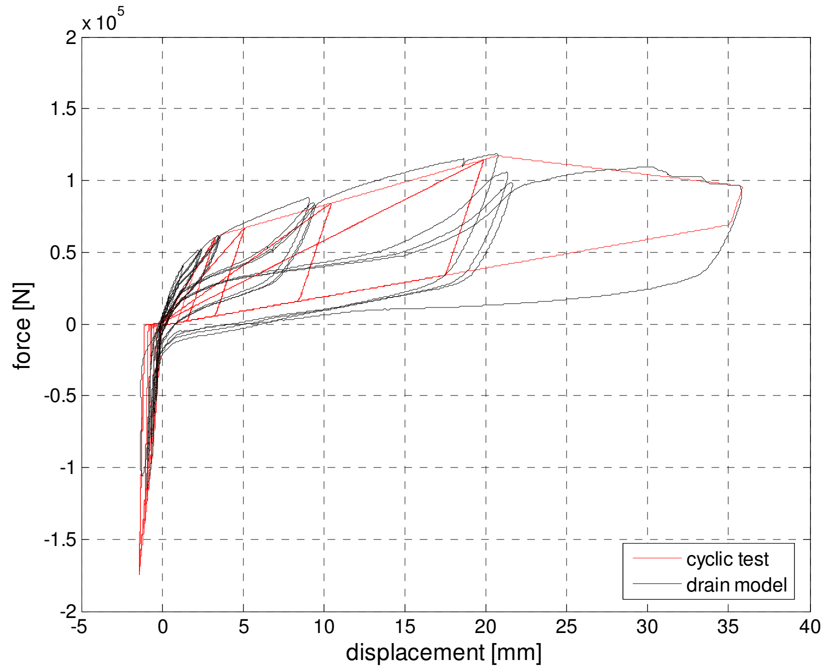

Figure 6-14, model and experiment output for the vertical springs

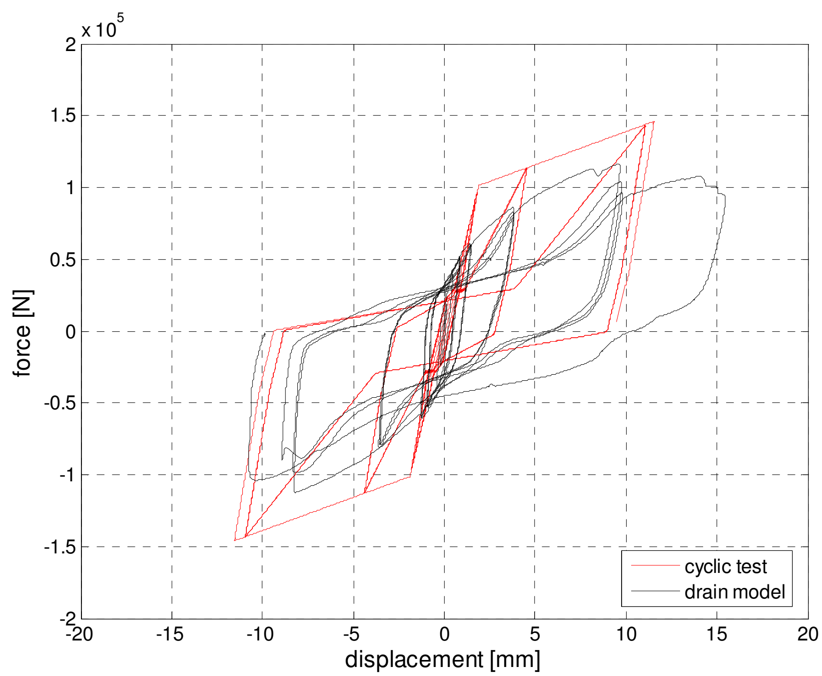

Figure 6-15, model and experiment output for the horizontal springs

6.7.2 Fitting of special holddown

In the SOFIE seven storey building, large uplift forces are expected. Therefore, special holddowns are designed for the seven storey building. For the specifications of the special holddown, it is referred to Appendix A.

A ramp test result is available for the special holddown. In a ramp test, a comparison of the ultimate displacement and maximum force is possible. The same model in DRAIN is used as for the calibration of the normal holddowns and shear connectors (Figure 6-13). Calibration is done for stiffness k1 and k2, yield displacement and ultimate displacement. For the other variables (k3-k6 and F0) the values from the normal holddown are taken. The output of the ramp test together with an overlapping model result is given in Figure 6-16.

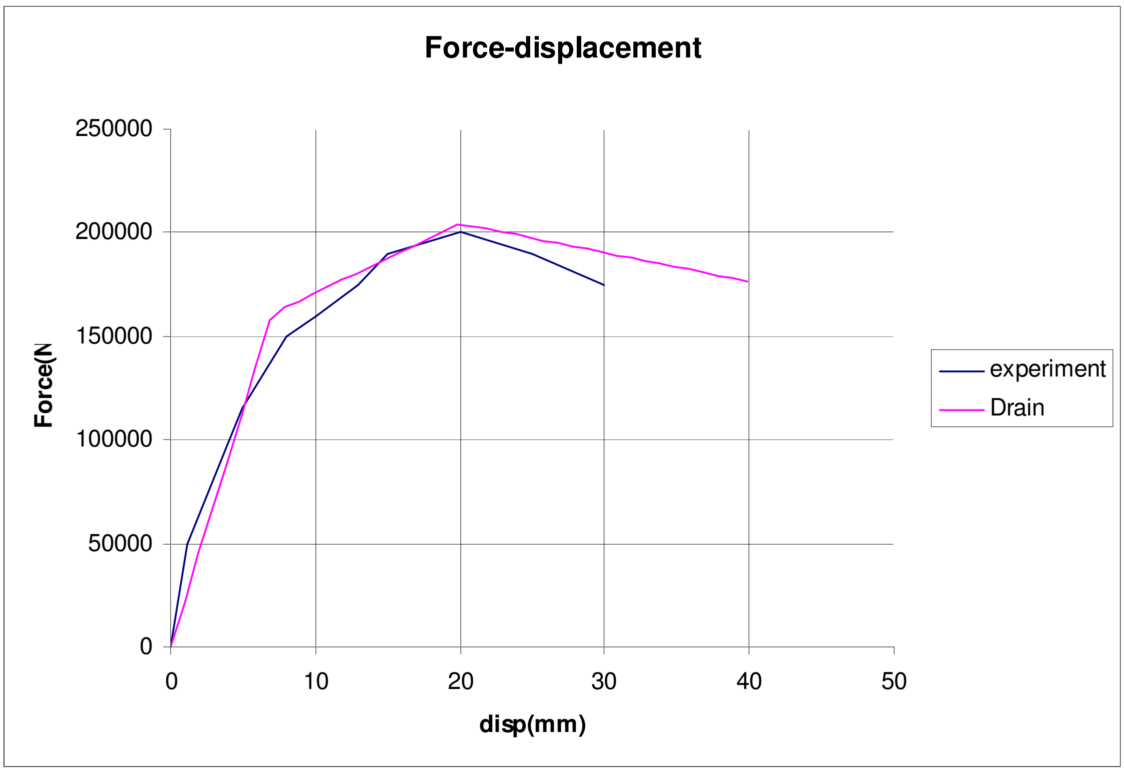

Figure 6-16, model and experiment output for the calibration of the special holddown

The value for k1 and k2 are graphically determined from the output in the ramp test.

The model produces good fitting results with variables given as in Table 6-1. It is mentioned that research is done on fitting the model for the ramp test results. The rest of the parameters are reproduced in proportion from the Simpson HTT22 holddown (section 6.7.1). DRAIN input variables for both holddowns are found in Table 6-1.

DRAIN 3D Input variable	Special holddown	Simspon HTT22
K1 (N/mm)	23000	18200
K2 (N/mm)	4107	3250
K3 (N/mm)	-1769	1400
K4 (N/mm)	6216	4919
K5 (N/mm)	46000	36400
K6 (N/mm)	1474	1167
Yield displacement (mm)	7	3.3
Ultimate displacement (mm)	20	20
Residual force (N)	1271	1006

Table 6-1, values for a good fitting model

6.7.3 Calibration of wall to wall connection

The parameters for the wall-to-wall connection are determined in an experiment within the scope of the thesis. The connection can be modelled with a hysteretic model with six different inclinations. A graphical presentation of the element is given in Figure 6-1 .
The wall-to-wall connection is tested and modelled for the first time in this document. Therefore, the calibration description is more detailed as for the other connections.

<u>Geometry of the model</u>

The setup of the test is modelled in DRAIN 3D as is given in Figure 6-17

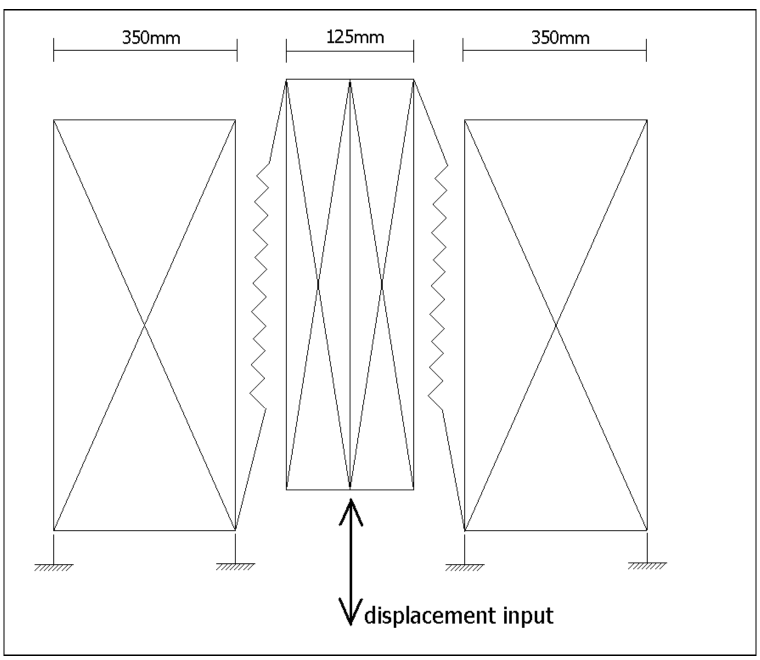

Figure 6-17, model for the calibration of the wall-to-wall connection

The displacement input of the model is in accordance with the input file of the experiment. The model can be calibrated with the experimental results. The element to be calibrated is the spring connection.

Spring element

The (hysteretic) spring connection is modeled with the six inclination diagram. The variables that are used for calibration are: k1, k2, k3, k4, k5, k6, the yield displacement, the ultimate displacement and the residual force F0 (see Figure 6-18).

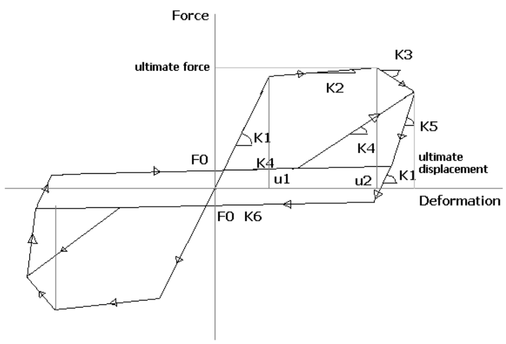

Figure 6-18, the six inclination diagram used for calibration of the connection

The calibration is completed when the ultimate displacement, ultimate force and the dissipated energy are almost equal to the values found in the experiment.

Ultimate force and ultimate displacement can be read directly from the diagram from the experiment (Figure 5-19). The amount of dissipated energy requires some calculation. The dissipated energy is found by taking the surface under the force-displacement curve as explained in Figure 6-19.

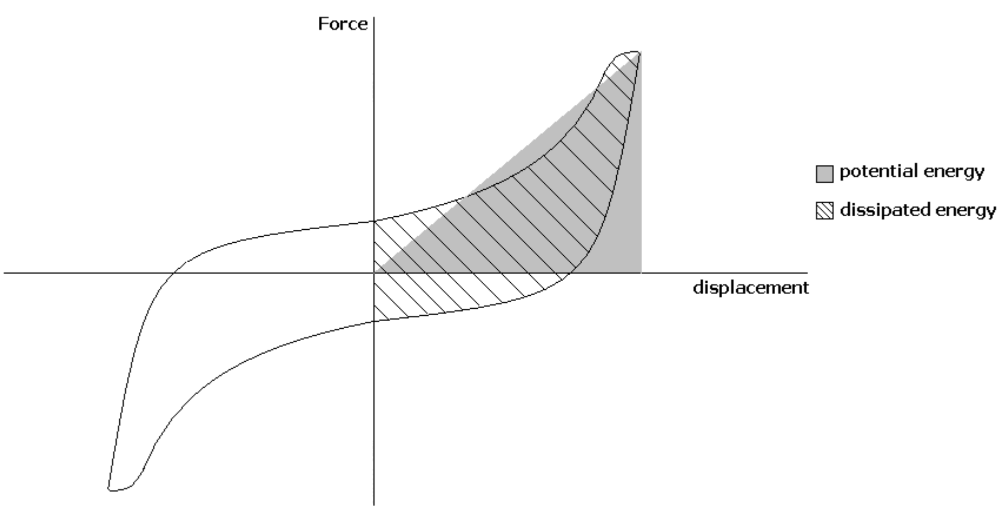

Figure 6-19, amount of dissipated energy

Results

With trial-and-error, the variables are defined till a good fitting model output is available. The diagram of the final model and from the experiment number two (see also Figure 5-19) are given in Figure 6-20.

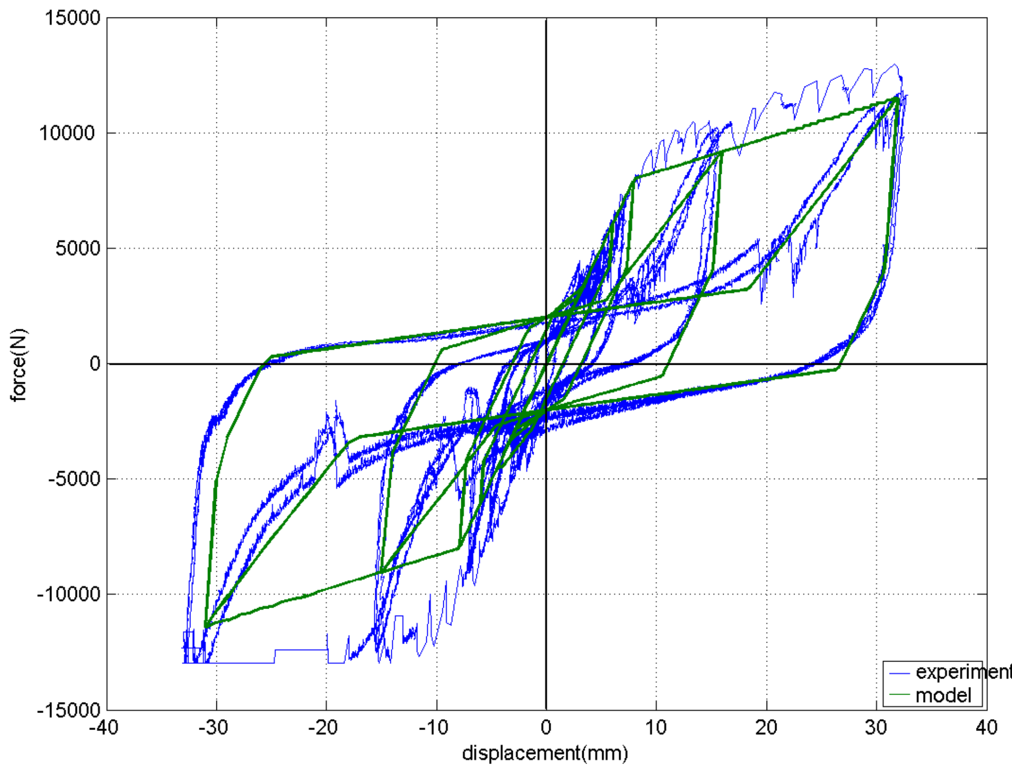

Figure 6-20, output of the model and the experiment

The model produces good fitting results with variables given as in Table 6-2

DRAIN 3D Input variable	Wall-to-wall connection
K1 (N/mm)	1000
K2 (N/mm)	147
K3 (N/mm)	-561
K4 (N/mm)	613
K5 (N/mm)	6400
K6 (N/mm)	-147
Yield displacement (mm)	8
Ultimate displacement (mm)	50
Residual force (N)	2000

Table 6-2, values for a good fitting model

Ultimate displacement and force are approximated by the model with an accuracy of 11%. The dissipated energy from the experiment (1.9*10^6 Nmm) and from the model (1.84*10^6 Nmm) differs by 4%.

6.7.4 Number of springs in the model

In section 6.6 it is described that the number and the location of vertical springs in the model is not corresponding to the number and location of holddowns in the building. Within the current version of DRAIN 3D it is not possible to define a 'holddown-spring' when a 'wall-to-wall-spring' is already defined. With this restriction, the number of springs in the model is already reduced. Further on in the building there are corners where multiple holddowns are present.
In the model these corners are defined by one node. In this way, there are nodes in the model that are connected with one spring connection defined representing multiple holddowns. This results in stiffer spring properties for the vertical springs at these locations. In total a number of 5 different vertical springs are defined in the model for which the stiffness calculation can be found in Appendix D. Horizontal springs are defined at the location of every separate wall section. Spring stiffness is defined with regard to the number of shear connectors designed in each wall section. The calculation of the properties of the horizontal springs in the model is found in Appendix D.

6.7.5 Damping in the springs

The equivalent damping in the springs is determined from modal analysis. The relationship between the stiffness matrix K and the damping matrix C is described as C = β * K with β a coefficient equal to:

$$\beta = \frac{T\xi}{\pi}$$

The damping ratio for timber structures with dowel type fasteners generally is around 10%. This damping ratio can be entered in the equation for β. The fundamental period T is obtained by the modal analysis function of the DRAIN 3D software. As presented in chapter 7, the fundamental period of the model is 0.41 seconds. The coefficient $\beta = 0.01$.

6.7.6 Input of other parameters in DRAIN 3D

In this section, the parameter and type of analysis are described. Within the software, a lot of options are available. Also the input of the parameters requires some choices. These options and choices are done for the model of the SOFIE building, but will not be described in this report. For information on the way of definition and the options please refer to the program manual.

Earthquake input

The input of the earthquake loading used in the model is the acceleration versus time format. The model is subjected to a time history analysis of the 1995/01/17 JMA Kobe earthquake (Figure 6-21). The N-S component of the earthquake in N-S direction is used for all three directions (E-W, N-S, up-down) with different scale factors. With these scale factors the earthquake accelerations are scaled to the real earthquake.

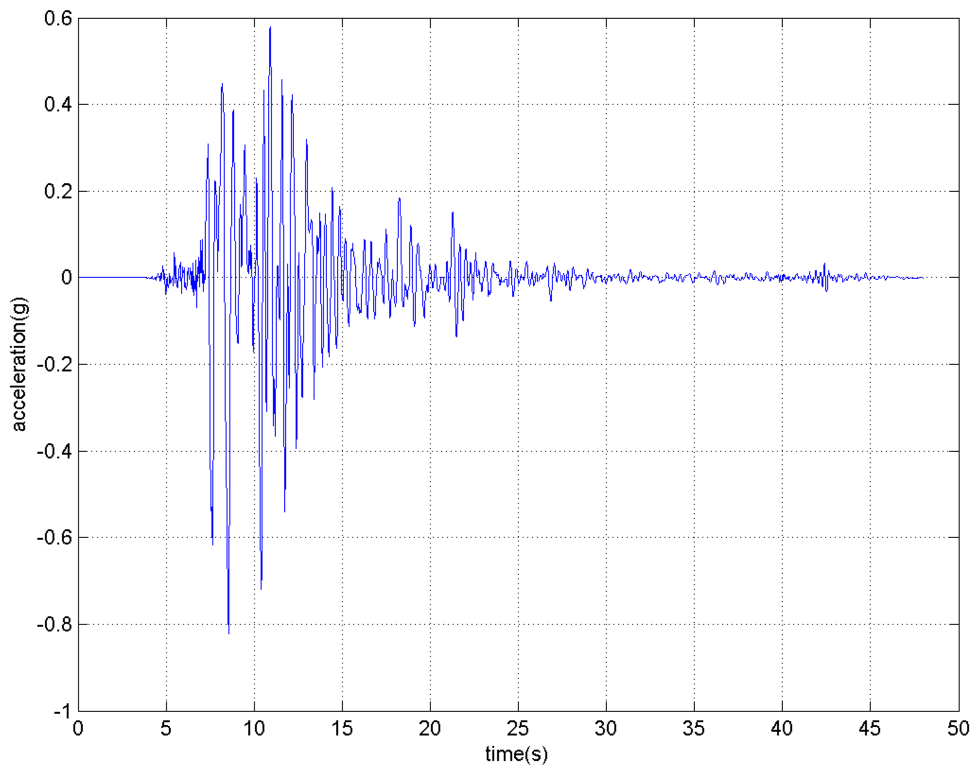

Figure 6-21, accelerogram of the applied JMA Kobe earthquake (N-S)

Types of analysis

Three types of analysis are carried out; modal analysis, static analysis and dynamic analysis. The modal analysis is done first. Modal analysis is not an analysis segment, but it is used to check the damping coefficients that are used by the program to fulfil the damping determined in section.
The static analysis is done to check whether the model is stable. The dynamic analysis is calculated directly after the static analysis. It consists of acceleration analysis. In the acceleration analysis, an input of the total time of the calculation, time-step and maximum number of steps is needed. The total time equals the total duration of the earthquake (approximately 48 seconds, see figure Figure 6-21).The time step is chosen 0.01 and the maximum number of steps is defined 99999.

7 Results of Drain model

7.1 Results

The results of the DRAIN 3D model are discussed in this chapter. First the plain results of the model are presented in this section. The displaced model during the JMA Kobe earthquake at a time of 860 seconds is presented in Figure 7-1. At the time of 860 seconds the maximum displacement in the model occurs. In Figure 7-1 a west view on the left and south view on the right is given.

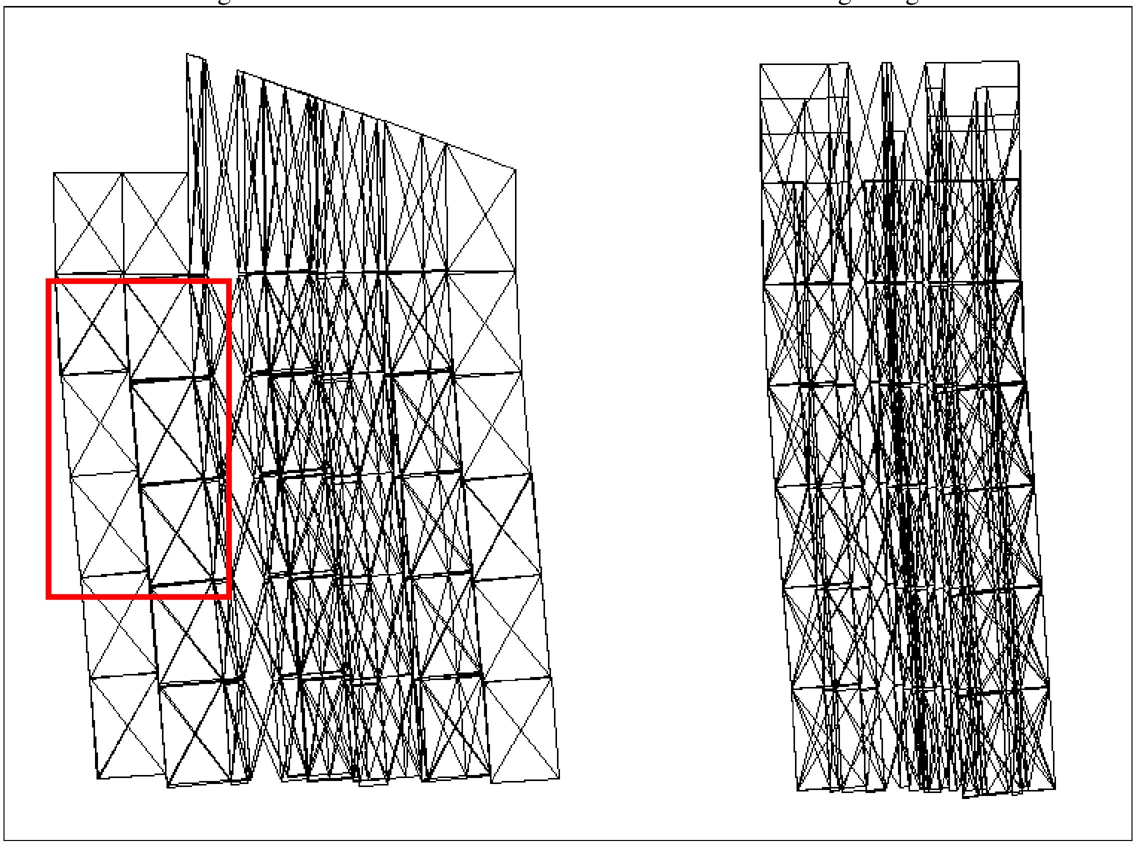

Figure 7-1, 2D presentation of the model results (west view left and south view right)

In Figure 7-2 the deformation of six panels in the west wall is presented. The exact location in the model is indicated in Figure 7-1 with the box.

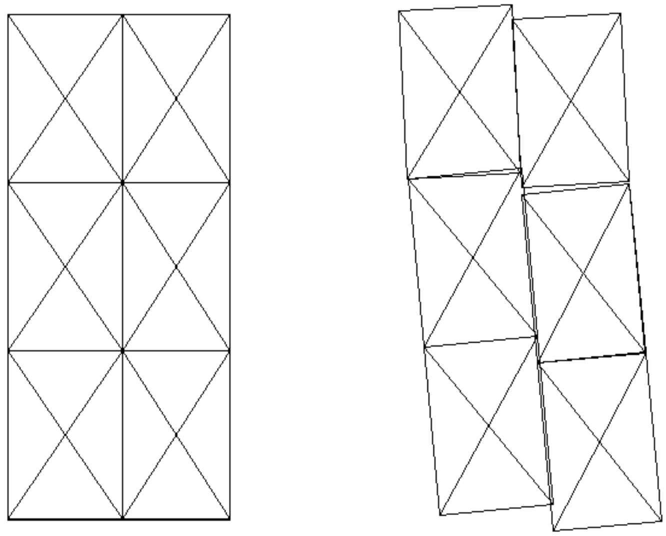

Figure 7-2, detail of six panels in y-wall in start position and deformed position

7.2 Comparison with the 3D experiment

The DRAIN 3D model described in this chapter is checked on its accuracy in two ways. First a comparison on the model results and the output from the full scale experiment is done.

7.2.1 Modal analysis

A modal analysis is carried out in DRAIN 3D to determine the fundamental period of motion of the building in the model. The modal analysis output is compared with the fundamental period that is determined in the full scale test. From the comparison of the periods an indication on the accuracy of the model is available. The error in the model is approximately 5-30%.

	Experiment	Model mode shape 1	Rate of error
X	0.43	0.39	10%
Y	0.29	0.41	30%

Table 7-1, natural frequencies from the experiment and the model

7.2.2 Displacement

The displacement of the model is compared on the maximum displacement of similar points in the full scale building and in the model. In this way another indication on the reliability of the model is available. It is mentioned here that the names of the walls in the experiment are different from the names in the model. The names used in the full scale experiment are given in Figure 7-3. In Figure 7-4 the names in the model are presented. For example the south wall in the experiment is named the east wall in the model.

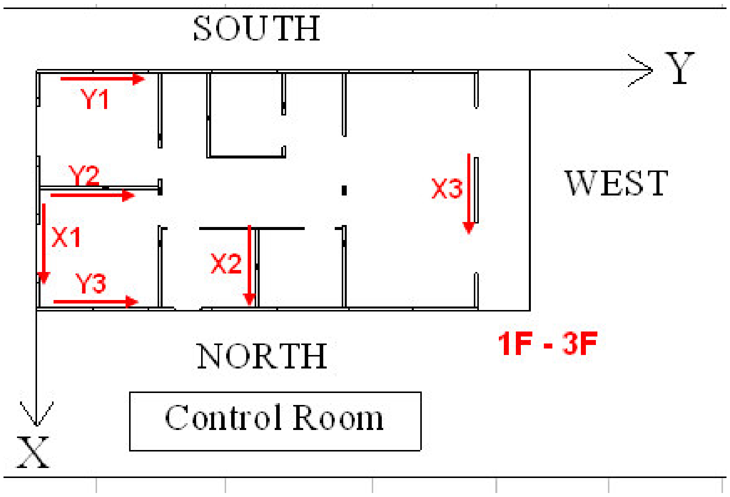

Figure 7-3, use of channels and indications in the full scale test

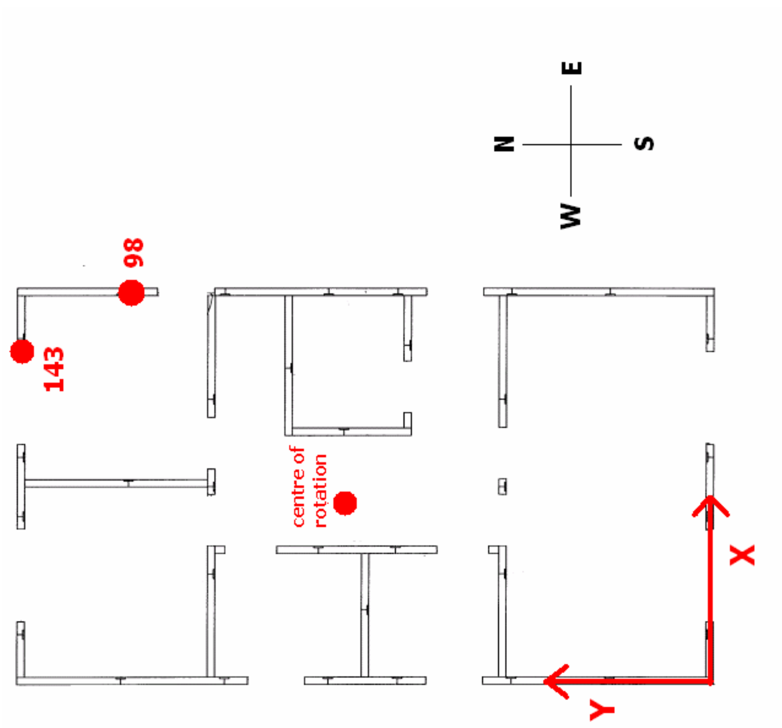

Figure 7-4, use of axis and indications in the model

The maximum displacement for the experiment south wall and the experiment north wall are compared graphically in Figure 7-5 and in Figure 7-6 and numerically in Table 7-2.

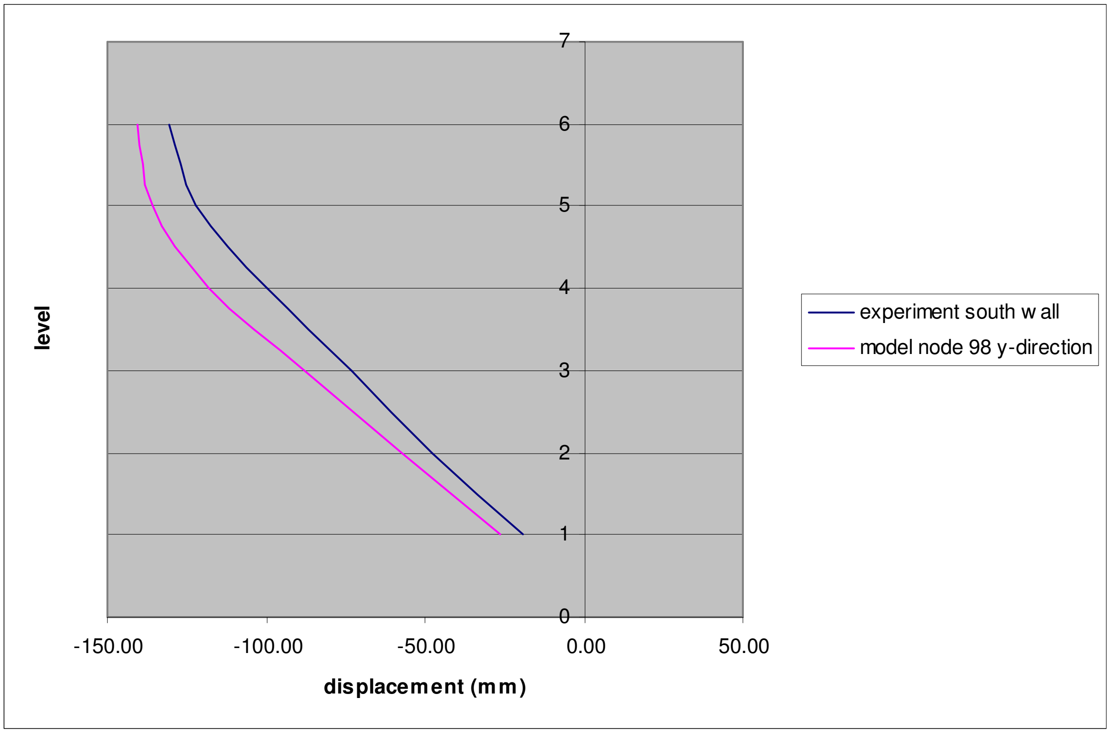

Figure 7-5, the experiment south wall displacement and the displacement of node 98 on each level compared

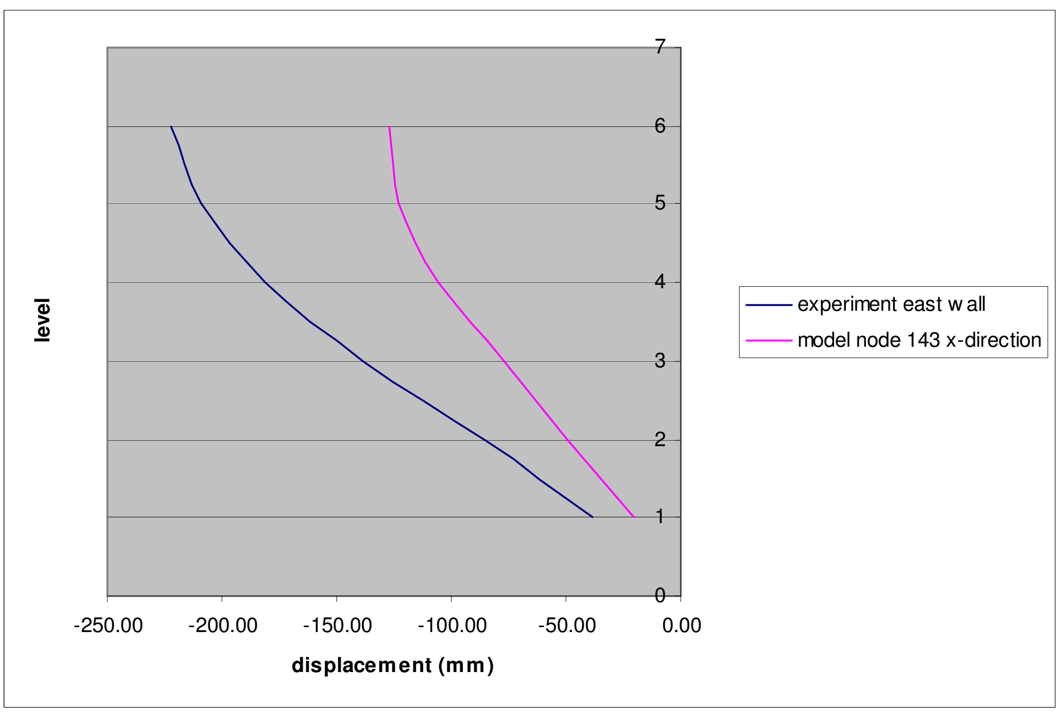

Figure 7-6, the experiment east wall displacement and the displacement of node 143 on each level compared

difference	y1 exp	node98 model	rate of error	x1exp	node 143 model	rate of error
1	-18.97	-26.32	138.75%	-38.52	-20.76	53.90%
2	-47.67	-57.29	120.18%	-85.47	-49.23	57.60%
3	-73.21	-87.62	119.68%	-138.78	-77.43	55.79%
4	-99.74	-118.32	118.63%	-181.36	-105.74	58.30%
5	-122.16	-135.74	111.12%	-209.01	-122.80	58.75%
6	-130.47	-140.36	107.58%	-222.34	-127.38	57.29%

Table 7-2, numerical comparison of experiment and model

It is concluded the model in x and y direction has an accuracy varying from 53% until 138%.

7.3 Comparison with time-step

By comparing the results of the model with a time-step of 0.1 with the calculation with time-step 0.05 an indication on the error in the model is obtained. This method is used more often in numerical calculations to get a indication on the error. A comparison is made for the displacement of node 98 with the different time-steps for the calculation. The comparison is done numerically in Table 7-3. The rate of error in the model is approximately 30%. It can be concluded that the displacements in the model increase with a decreasing time-step.

Level	y(0.1)	y(0.05)	Rate of error y negative
1	-11.77	-7.32	62.24%
2	-20.97	-14.95	71.28%
3	-29.58	-22.14	74.85%
4	-38.45	-29.40	76.47%
5	-43.51	-33.40	76.78%
6	-44.34	-33.74	76.09%

Table 7-3, node 98 comparison

7.4 Influence of the experimented connection

In this section the influence of the experimented wall-to-wall connection on the total building behaviour is investigated. This is done by running the model twice with time-step 0.1. The properties of the wall-to-wall spring in the first running are given the parameters obtained from the experiment. In the second running the parameters of the spring are doubled in stiffness and strength. A comparison of node 98 on each level gives an indication on the influence of the connection in the model (Figure 7-7). The maximum displacement of the building changes approximately with 50 to 70% after doubling spring properties.

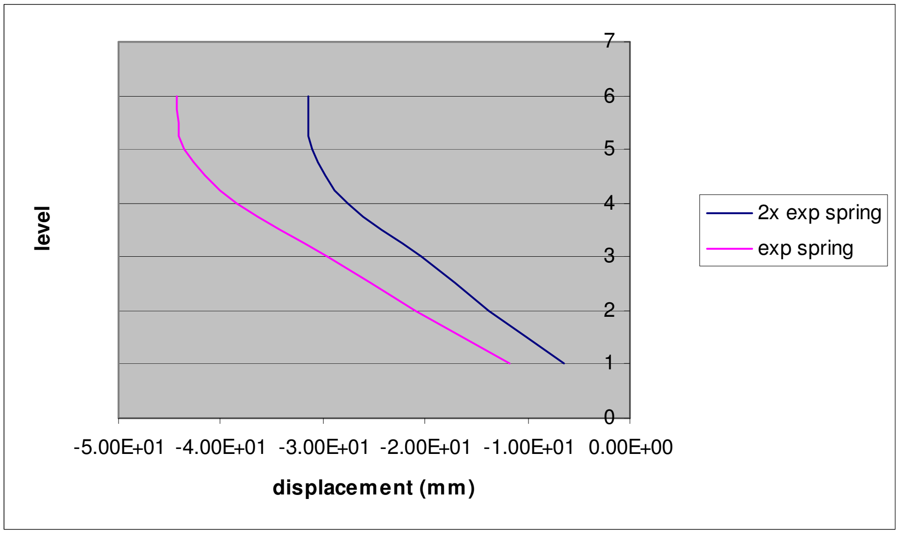

Figure 7-7, influence of the wall-to-wall connection on the building behaviour in y-direction

8 Conclusions

8.1 Experiment

The symmetrical setup of the test, presented in Figure 5-5, with a connecting element between the two side panels is a good way of testing the connection without large rotations occurring.

In the experiment three and five layered specimens are tested within the same test setup. Results indicate a negligible difference in the specimen response to cyclic loading, so three or five layered specimens have equal mechanical properties in this configuration.

The important property in earthquake loading is the energy dissipation. The amount of energy dissipated in the connection with a total of 12 screws lies between 3 and 4 kNm. A double connection is tested, so between 1.5 and 2 kNm per joint tested, with 3 fasteners per shear plane and 6 fasteners per wall-to-wall connection.

The failure of the wall-to-wall connection can be explained by plastic deformation of the screws. The properties of the screw and the timber allow very large embedment displacement and the formation of plastic hinges in the fasteners. Fastener bending angles are around 25°.

8.2 3D model

The DRAIN 3D version that was used for modelling of the three storey building is, after some adjustments suitable for modelling the SOFIE seven level building. These changes dealt with extension of the internal memory and the maximum number of elements that can be defined. With the new compiled DRAIN 3D version the analysis for the seven storeys is done.

It is important to model the panels with openings for doors or windows as completely rigid panels. Without these rigid modelling the output is not consistent with the output from the experiment. This is because a ‘soft-storey’ is created in this case which was not found in the experiment.

The seven storey model is capable of resisting JMA Kobe 1995 with its current configuration and gives reasonable and acceptable results. The deformation shape of the model and the experiment are similar and the ultimate displacements in both directions are in the same order.

The properties found from the experiment on the wall-to-wall connection have been defined within the DRAIN 3D software. The connection is best approximated with element 6 in the program, a hysteresis model with six different inclinations.

In the full scale test on the SOFIE structure, a step loading is applied for determining the natural frequency of the building. With the modal analysis option in DRAIN 3D the natural frequency of the model is calculated. The output of the model can be compared with the frequency determined in the test. There is a difference of approximately 5-30% which is an indication on the accuracy of the model.

	Experiment	Model mode shape 1	Rate of error
X	0.43	0.39	10%
Y	0.29	0.41	30%

Table 8-1, comparison of the natural periods from the experiment and the model

The same error of approximately 30% is found by halving the time-step in the calculation. This method is used more often in numerical applications to estimate the error of a computer model.

A comparison is done of the displacements within the model and the displacements from the experiment. It can be concluded that the results for the y-direction have a rate of error of 7 to 38%, which is satisfying. For the x-direction a difference of 42 to 47% is found. See also table 8.2.

difference	**y1 exp**	**node98 model**	**rate of error**	**x1exp**	**node 143 model**	**rate of error**
1	-18.97	-26.32	138.75%	-38.52	-20.76	53.90%
2	-47.67	-57.29	120.18%	-85.47	-49.23	57.60%
3	-73.21	-87.62	119.68%	-138.78	-77.43	55.79%
4	-99.74	-118.32	118.63%	-181.36	-105.74	58.30%
5	-122.16	-135.74	111.12%	-209.01	-122.80	58.75%
6	-130.47	-140.36	107.58%	-222.34	-127.38	57.29%

Table 8-2, comparison of the horizontal displacements from the experiment and the model

The influence of the wall-to-wall connection on the total behaviour of the building is significant. With a time-step of 0.1, this influence can be stated as 50% until 70%.

9 Recommendations

9.1 Experiment

The experiment is done on a small symmetrical connection. A total of six screws are tested. The real SOFIE connection has larger dimensions and more screws are applied with larger panels. For the experiment in the scope of this thesis, it has been assumed that the real connection can be approximated with the specimen used in the tests. A full scale test could give additional information on the actual behaviour. However, it is felt that the tests performed give a good representation of the behaviour in a full scale wall.

The calibrated results of the experimented connection are multiplied on the number of screws present in the real connection. Research is needed if this simple multiplication is justified.

The X-lam panels are available in different number of layers (from 3 to 18). In the experiment is demonstrated that the difference between a three and a five layered panel is negligible.
The deformation in the connection is dependent on the fastener deformation to a high degree. From the experiments on the three and five-layered panels, it is stated that the thickness of the panels and the number of layers has no influence on the connection behaviour. This must be checked by doing the same experiment on panels with a significant higher thickness.

9.2 3D Model

The 3D model is simplified for numerical reasons. With a more detailed model of the building a more detailed analysis of the structural behaviour is possible. But when all holddowns and shear connectors are defined as they are present in the building there are numerical problems. The reason of this numerical failure is still unclear and more research is needed to avoid these problems.

The influence of the properties of the wall-to-wall connection on the earthquake response of the building is significant. Therefore it is advised to do more experiments on the full-scale connection. In this way accurate properties can be obtained and a better modelling of the structure is possible.

The calculations are done with the JMA KOBE 1995 NS accelerations. These accelerations are applied in x, y and z direction. In the real earthquake different accelerations are occurring in the three directions. These accelerations must be applied to the model for a better calculation.

As presented in the results section, the results for the y-direction are satisfying, but the results for the x-direction need more research.
Bibliography

- Brunious, C., Warner, A. Earthquakes and Society. [http://www.umich.edu/~gs265/society/earthquakes.htm]
- Tarbuck, Edward J and Frederick K. Lutgens. Earth: An Introduction to Physical Geology. Prentice Hall: New Jersey, 1996.
- Shodek, D.L. Structures (2004) fourth edition. New Delhi, Prentice hall of India
- Clough, R.W., Penzien, J. Dynamics of structures (1993) 2nd edition. Singapore, McGraw-Hill Book Co.
- Sandhaas, C. .Seismic behaviour of historic timber-frame buildings in the Italian Dolomites (March 2004), Florence

- Thelandersson, Larsen, Timber Engineering (2003) . John Wiley & Sons
- Hu, Liu and Dong, Earthquake Engineering (1996), E&FN Spon
- Manolis & Koliopoulos. Stochastic Structural Dynamics in Earthquake Engineering (2001). Wit Press
- Japanese society of Civil Engineers. Dynamic analysis and earthquake resistant design (1997). A.A.Balkema/Rotterdam/Brookfield
- Metrikine & Vrouwenvelder . Dynamics of structures-Vibration of structures (2006) , Delft University of Technology
- Metrikine. Dynamics, Slender structures and an introduction to Continuum Mechanics. Delft University of Technology
- Eurocode 8: Design of structures for earthquake resistance - Part 1: General rules, seismic actions and rules for buildings
- KLH kreuzlagenholz, www.klh.at, loaded December 2008
- Finnforest, www.finnforest.com, loaded December 2008
- SOFIE project – shaking table test on a 7-storey full-scale X-lam building, 2007
- Blass, Aune, Choo, Görlacher, Griffiths,Hilson, Racher, Steck. STEP 1,timber engineering, basis of design, material properties, structural components and joints (1995) First edition. Centrum hout, The Netherlands
- National Earthquake information center. www.neic.usgs.gov, loaded December 2008
- IVALSA, Lauriola, Sandhaas. Quasi-static and pseudo-dynamic tests on XLAM walls and buildings
- Cecotti, Follesa, IVALSA. Seismic behaviour of multi-storey Xlam buildings.
- Paz,Leigh. Structural Dynamics, theory and computation (1997), New York, Chapman and Hall
- Cecotti, Follesa, Lauriola, Sandhaas.Which behaviour factor formulti-stroey buildings made of cross-laminated wooden panels?
- Follesa, Lauriola. Preliminar modeling on 7 storey cross laminated building

Appendix A
Building properties

- Centre of rotation
- Determination of masses
- Lumped masses
- AutoCAD drawing of special holddown

Appendix B
Calculations

- Hand calculations
- Rayleigh method
- Shear forces

Appendix C
Wall-to-wall experiment

- Wall-to-wall connection model
- Calibration of the wall-to-wall connection
- Graphs of experiment
- Pictures experiment

Appendix D
Model

- Mass distribution in model
- DRAIN 3D model
- Stiffness of springs
- Results DRAIN 3D model
- Software code

Appendix E, software code